Spectral CT

Marc Kachelrieß

German Cancer Research Center (DKFZ)
Heidelberg, Germany
www.dkfz.de/ct

DEUTSCHES
KREBSFORSCHUNGSZENTRUM
IN DER HELMHOLTZ-GEMEINSCHAFT

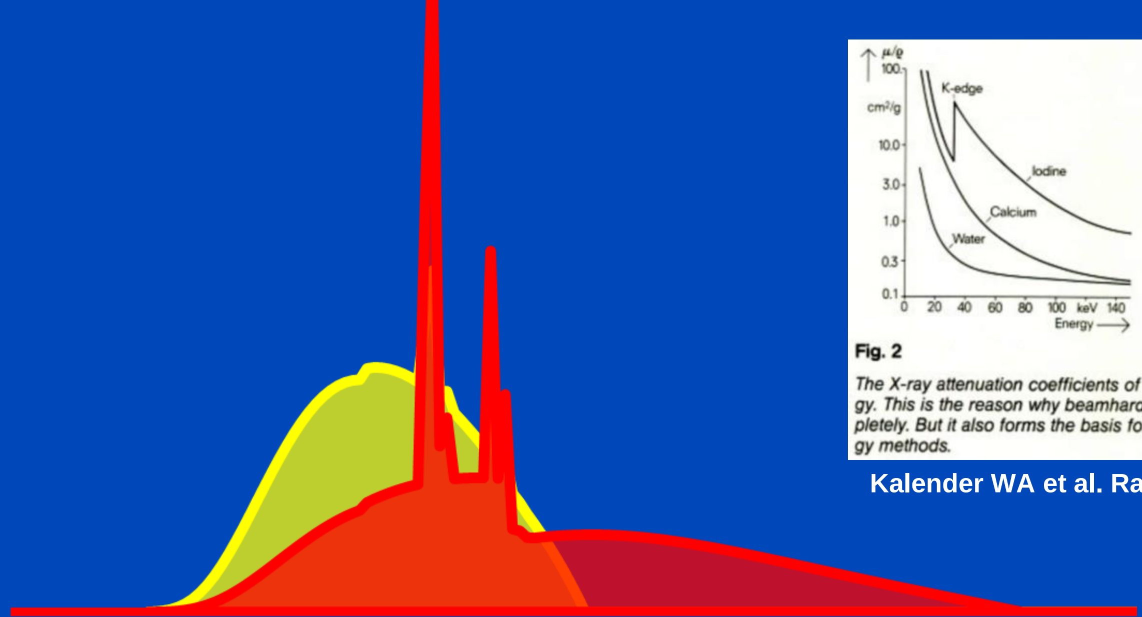

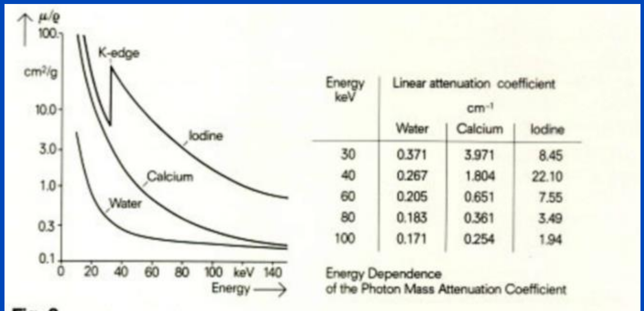

Energy keV	Linear attenuation coefficient cm^{-1}		
	Water	Calcium	Iodine
30	0.371	3.971	8.45
40	0.267	1.804	22.10
60	0.205	0.651	7.55
80	0.183	0.361	3.49
100	0.171	0.254	1.94

Energy Dependence of the Photon Mass Attenuation Coefficient

Fig. 2

The X-ray attenuation coefficients of different materials vary widely with energy. This is the reason why beamhardening effects cannot be controlled completely. But it also forms the basis for material-selective imaging by dual energy methods.

Kalender WA et al. Radiology 164:419-423, 1987

80 kV

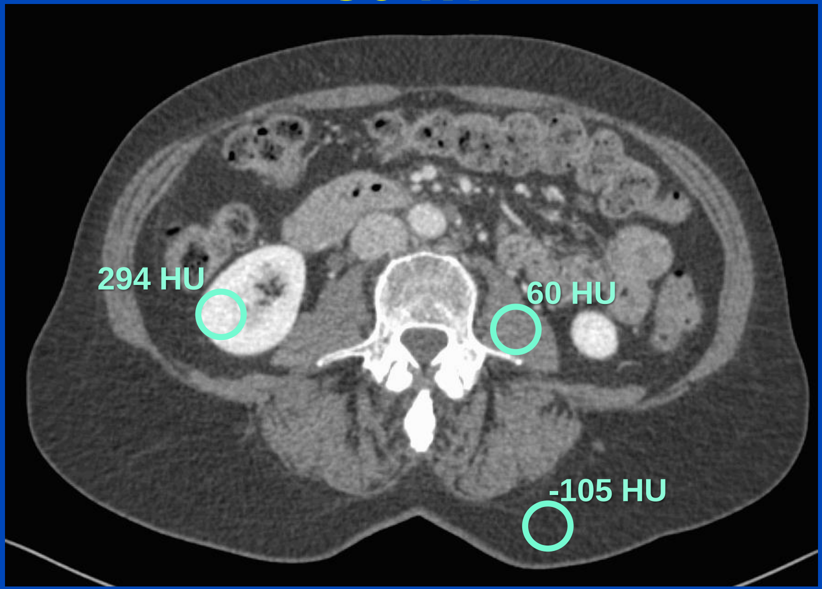

140 kV Sn

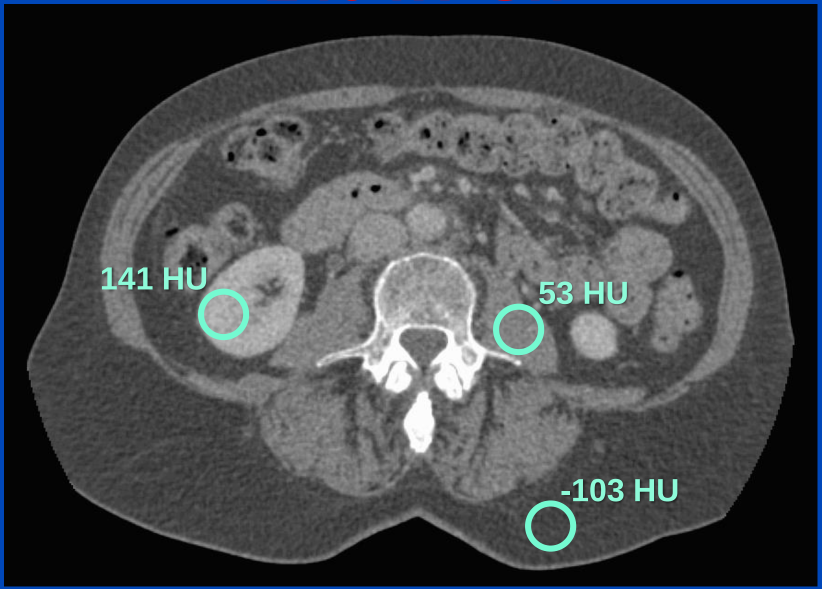

***C* = 50 HU, *W* = 600 HU**

Dual-Source-CT (since 2005)

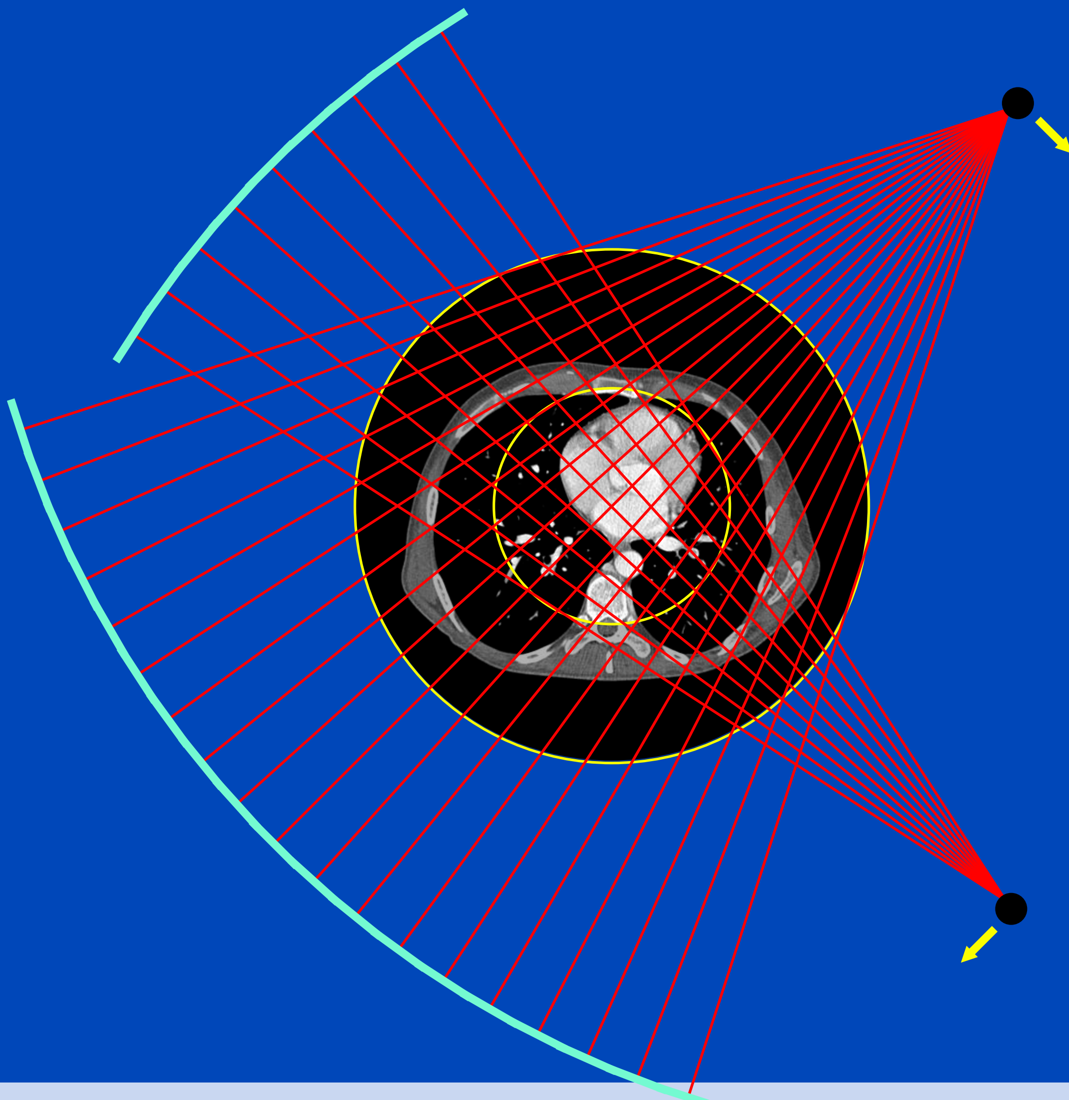

Siemens SOMATOM Force
3rd generation
dual source cone-beam spiral CT

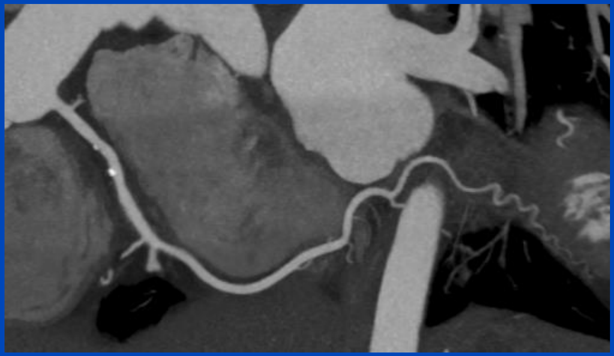

Turbo Flash, 70 kV, 0.55 mSv
63 ms temporal resolution
143 ms scan time

1980ies: The First Clinical DECT Product Implementation

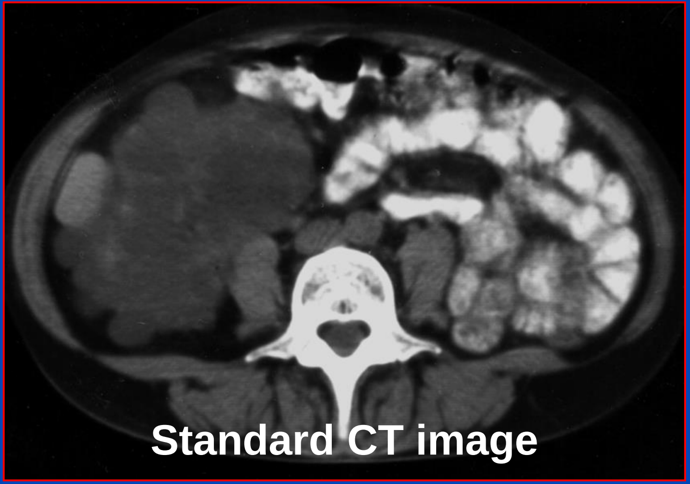
Standard CT image

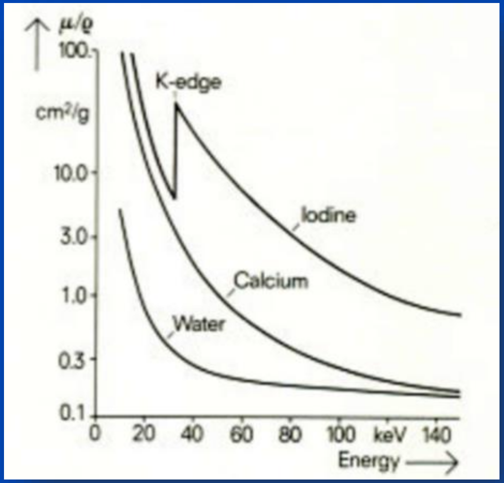

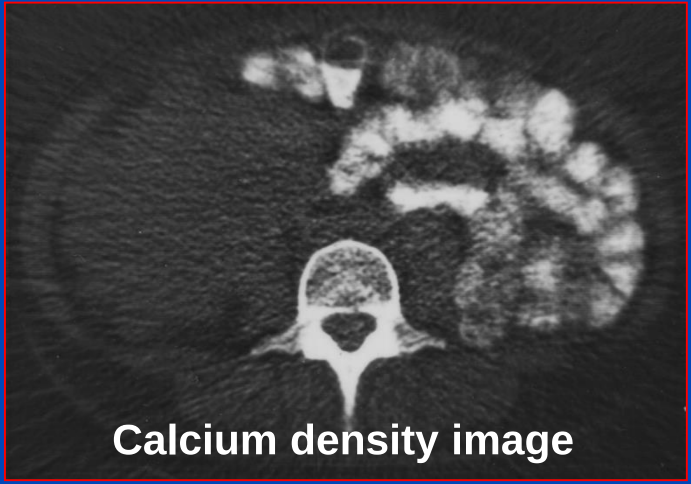
Calcium density image

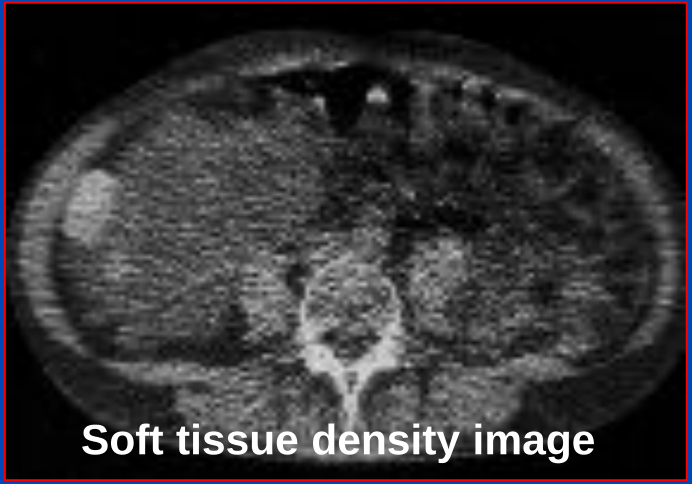
Soft tissue density image

Examples

(Slide Courtesy of Siemens Healthcare)

DE bone removal

Single DECT scan

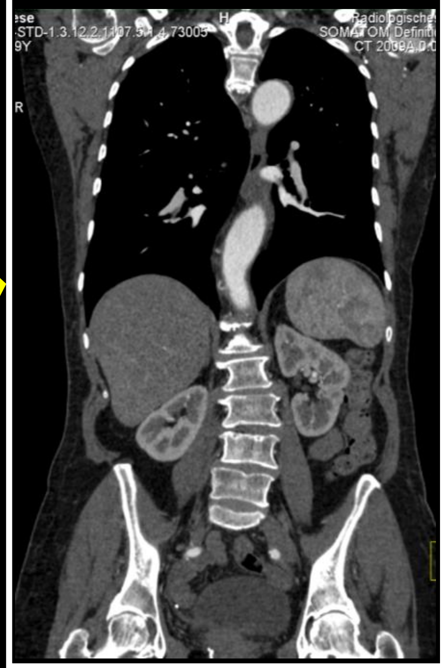

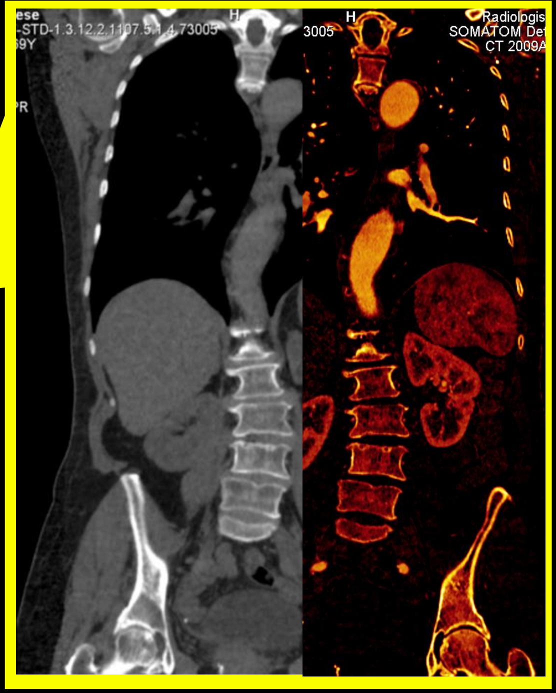

Virtual non-contrast and iodine image

Dual Energy whole body CTA: 100/140 Sn kV @ 0.6 mm

Courtesy of Friedrich-Alexander University Erlangen-Nürnberg

Monoenergetic Imaging

(mono+ = noise reduction with frequency split)

Courtesy of Prof. Michael Lell, Friedrich-Alexander University Erlangen-Nürnberg

DECT
and Pseudo Monochromatic Imaging

Pseudo monochromatic imaging is a linear combination of DECT f_L and f_H: $f_\alpha = (1-\alpha)\, f_\mathrm{L} + \alpha\, f_\mathrm{H}$

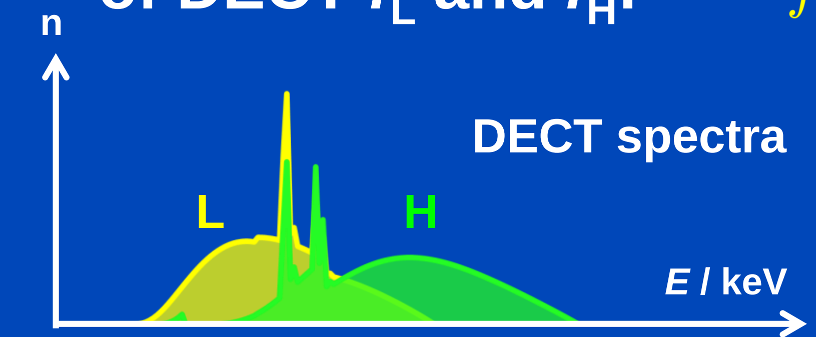

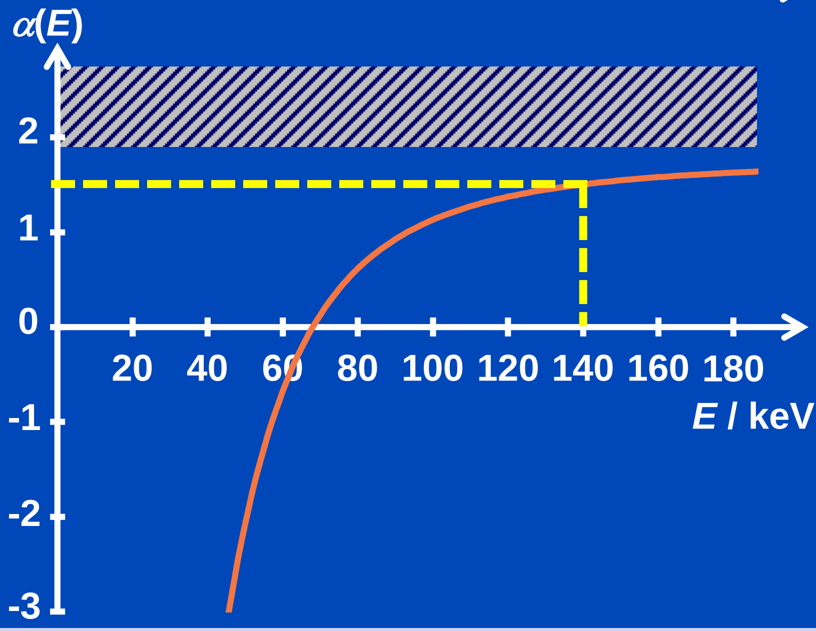

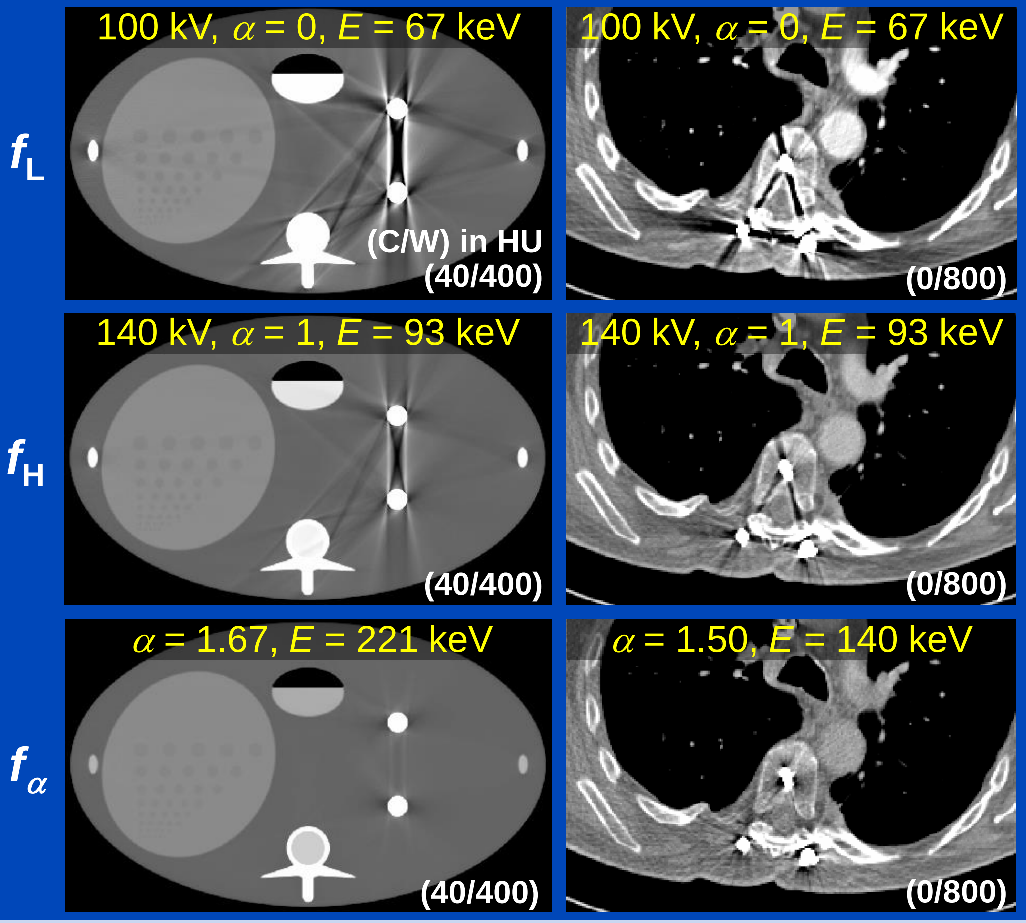

Kuchenbecker, Faby, Sawall, Lell, Kachelrieß. Dual energy CT: How well can pseudo-monochromatic imaging reduce metal artifacts? Med. Phys. 42(2), 2015

Dual Energy Metal Artifact Reduction
(linear combination plus noise reduction with mono+)

50 keV **80 keV** **160 keV**

Courtesy of Prof. Michael Lell, Friedrich-Alexander University Erlangen-Nürnberg

Patient Data Set – Pseudo Monochromatic Imaging

z = -723 mm | z = -792 mm

$f_L = f_0$ (E = 67 keV)

$f_H = f_1$ (E = 93 keV)

$f_{1.55}$ (E = 154 keV)

$f_{2.00}$ (E = --- keV)

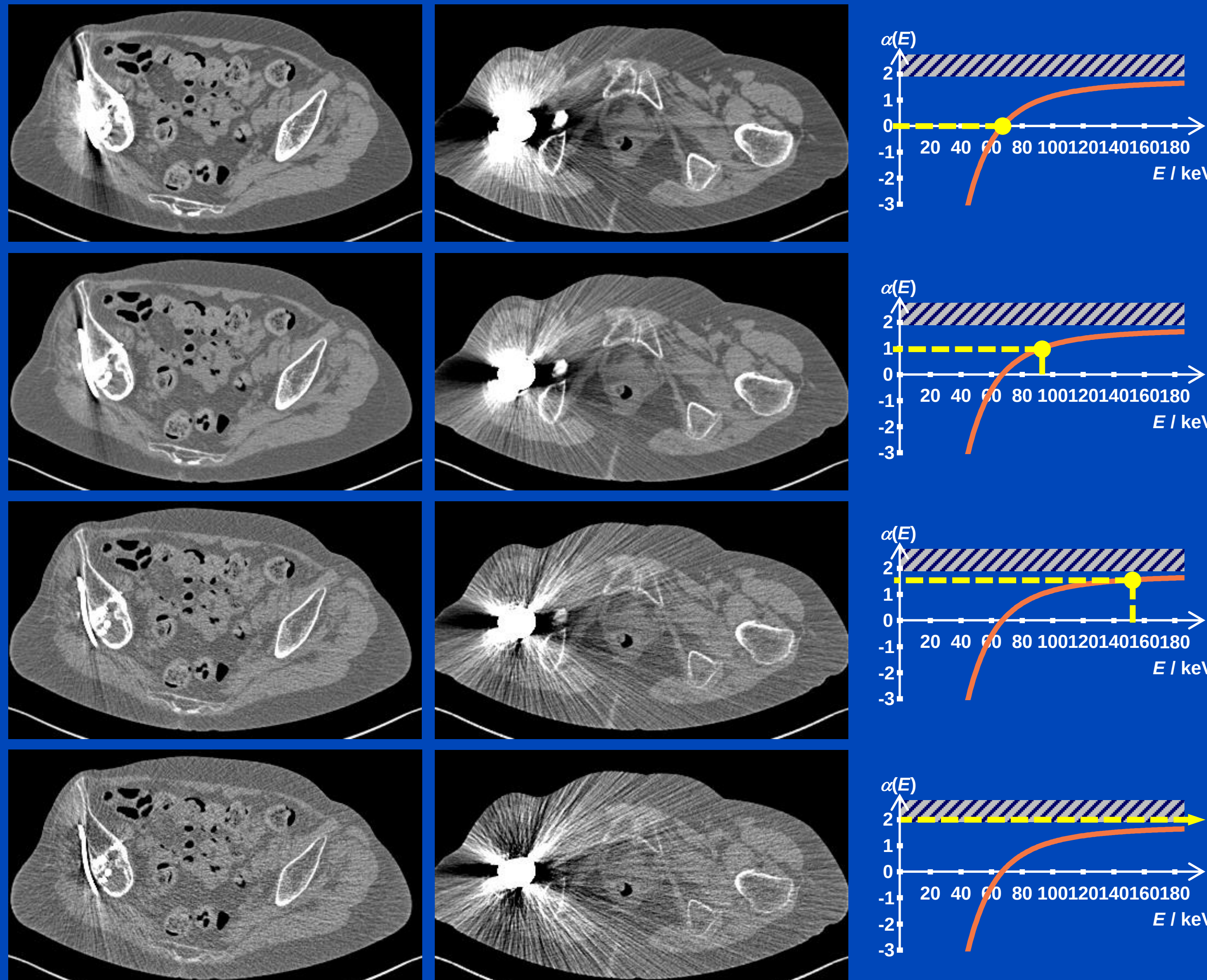

C = 0 HU, W = 800 HU

dkfz.

	Original	DEMAR	iMAR[1] (FSNMAR[2])
Patient 1 100 kV 140 kV Sn			
Patient 2 100 kV 140 kV Sn			
Patient 3 100 kV			

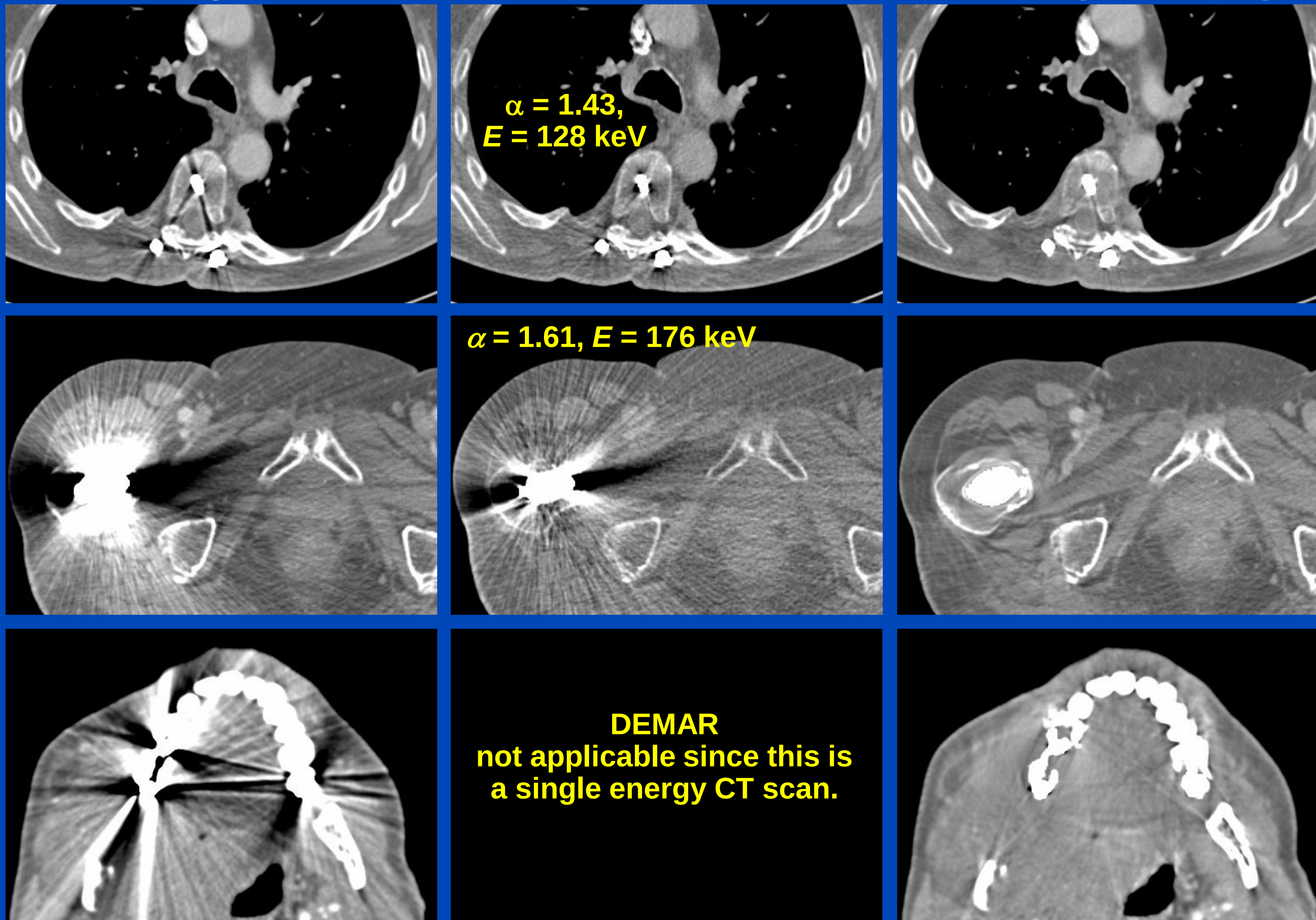

[1]Iterative metal artifact reduction (iMAR) is the Siemens product implementation of FSNMAR.
[2]Frequency split normalized metal artifact reduction: Meyer, Kachelrieß. MedPhys 39(4), 2012.

dkfz.

DECT Technology

- **In the clinic:**

– Multiple scans at different spectra	mid-range
– Dual source CT (DSCT), generations 2, and 3	high-end
– Fast tube voltage switching	high-end
– Dual layer sandwich detectors	high-end
– Split filter	mid-range
– Photon-counting CT	high-end

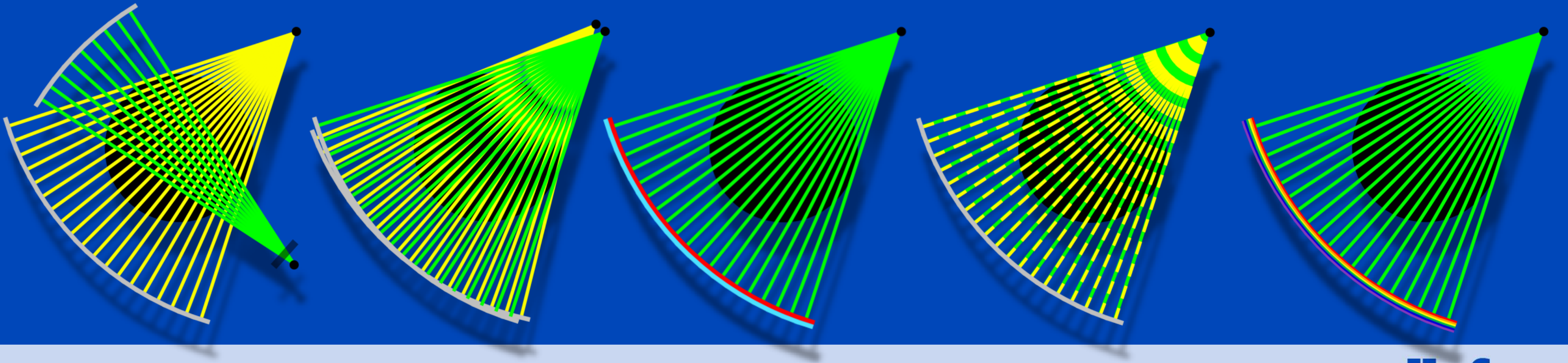

DECT Technology

- DECT approaches in the clinic:
  - Dual source DECT (Siemens)

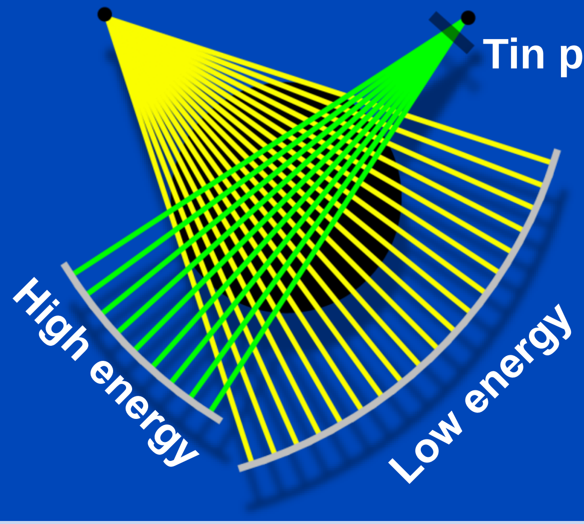

Siemens Somatom Force

Effect of the Prefilter: Without Sn

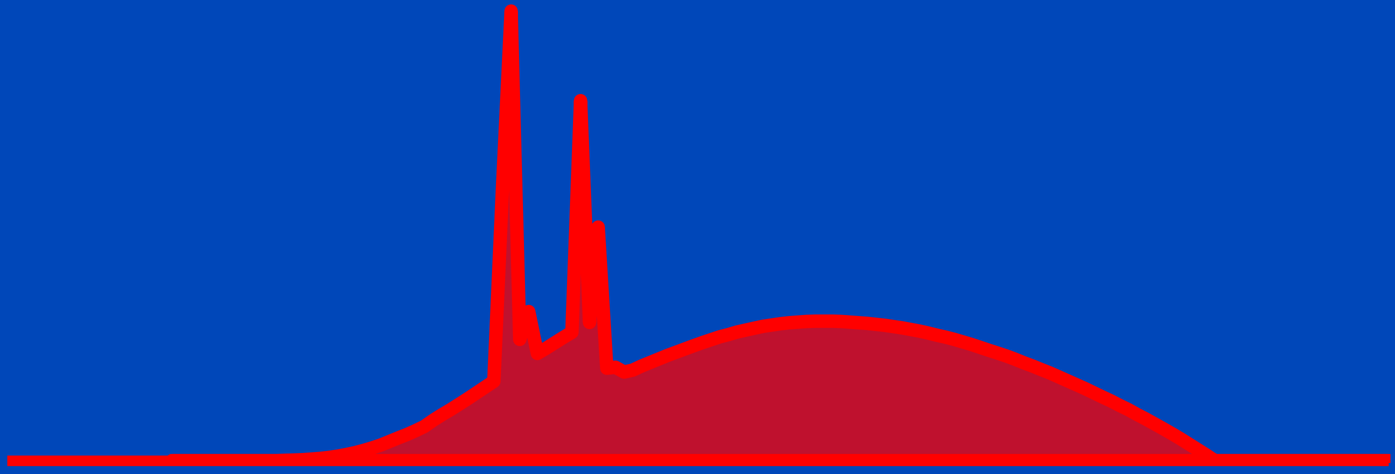

Spectra as seen after having passed a 32 cm water layer.

Effect of the Prefilter: With 0.4 mm Sn

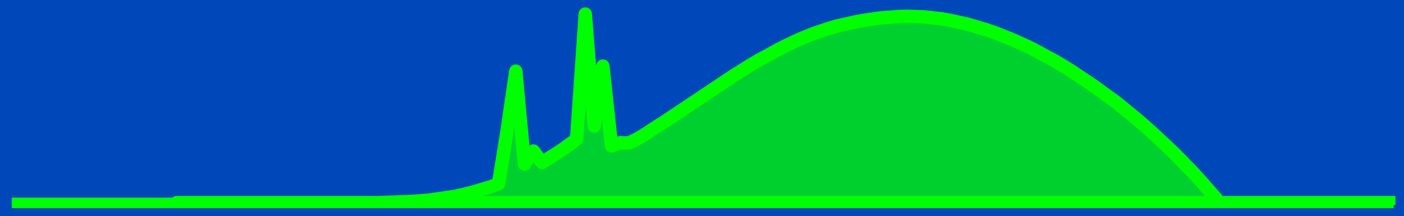

Spectra as seen after having passed a 32 cm water layer.

DECT Technology

- DECT approaches in the clinic:
  - Dual source DECT (Siemens)
  - Fast tube voltage switching (Canon, GE)

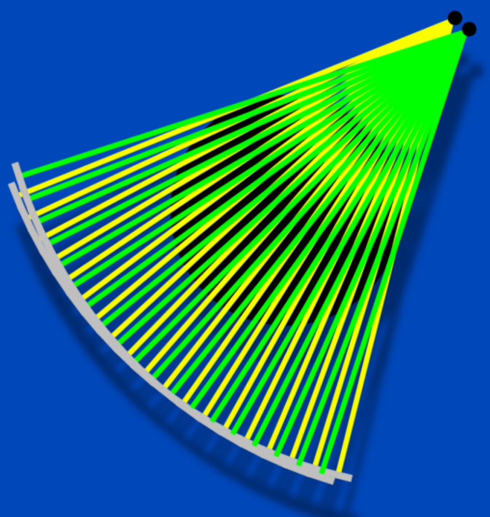

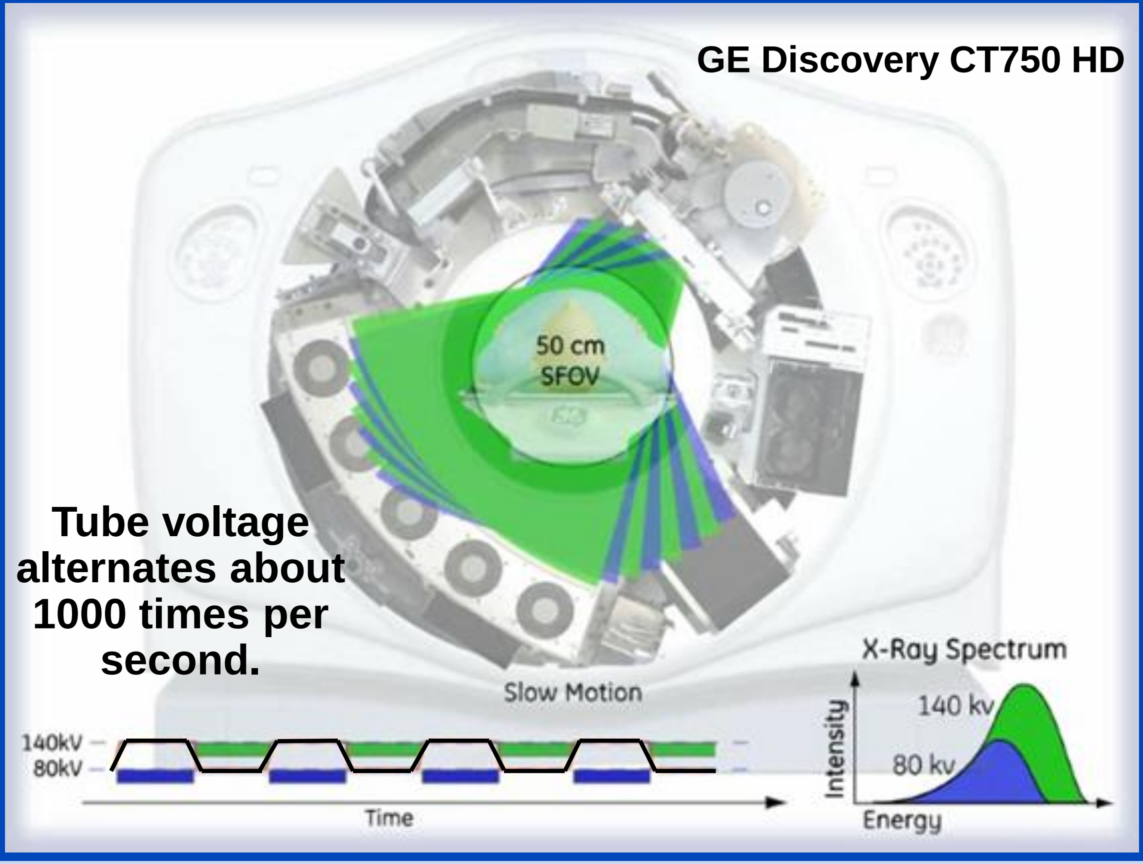

GE Discovery CT750 HD

Tube voltage alternates about 1000 times per second.

With the introduction of the GE Quantix 160 tube (around 2018), that includes microsecond tube current control by an electron extracting dual flat emitter, that is free of the traditional constraints of thermionic emission, the TVS can be regarded of being as almost rectangular shape.

DECT Technology

- DECT approaches in the clinic:
  - Dual source DECT (Siemens)
  - Fast tube voltage switching (Canon, GE)

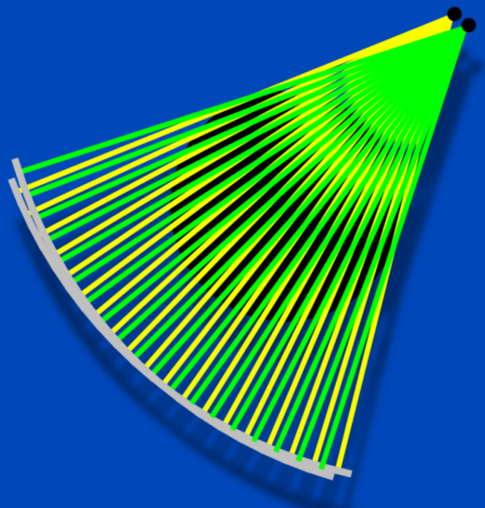

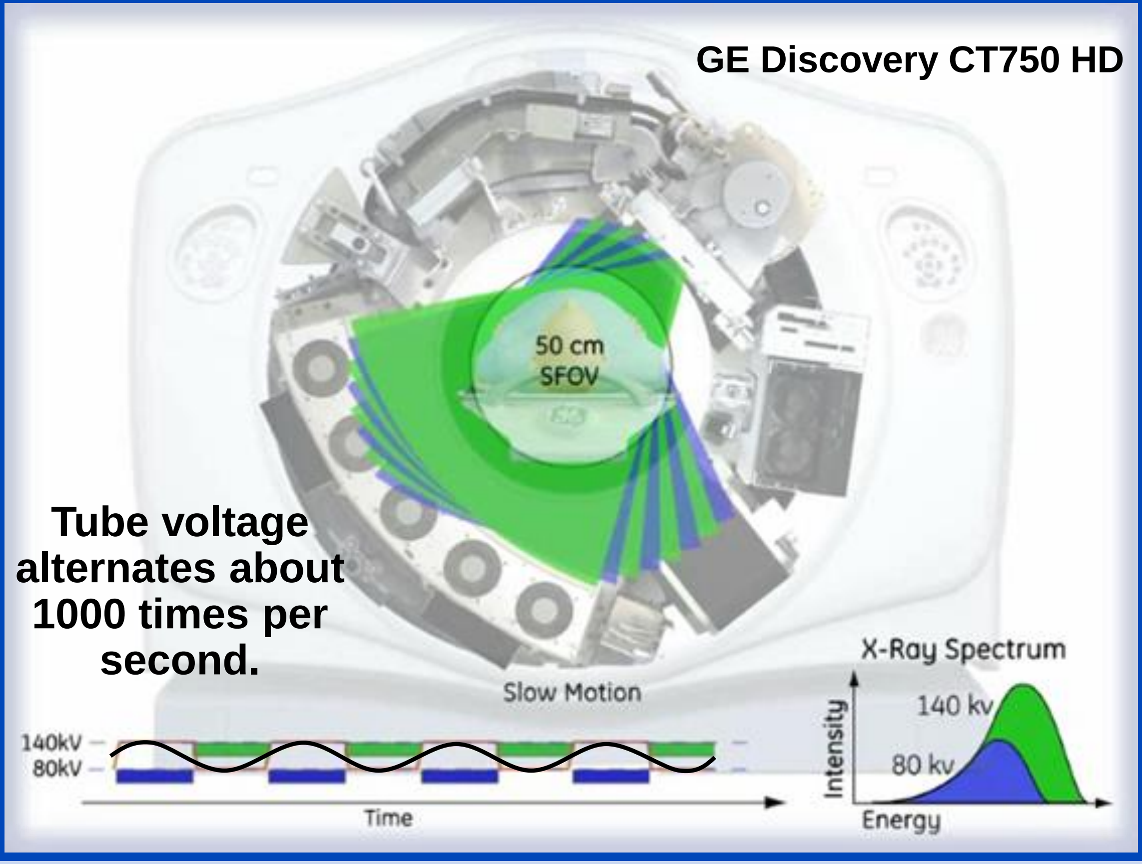

With the introduction of the GE Quantix 160 tube (around 2018), that includes microsecond tube current control by an electron extracting dual flat emitter, that is free of the traditional constraints of thermionic emission, the TVS can be regarded of being as almost rectangular shape.

DECT Technology

- **DECT approaches in the clinic:**
  - **Dual source DECT (Siemens)**
  - **Fast tube voltage switching (Canon, GE)**

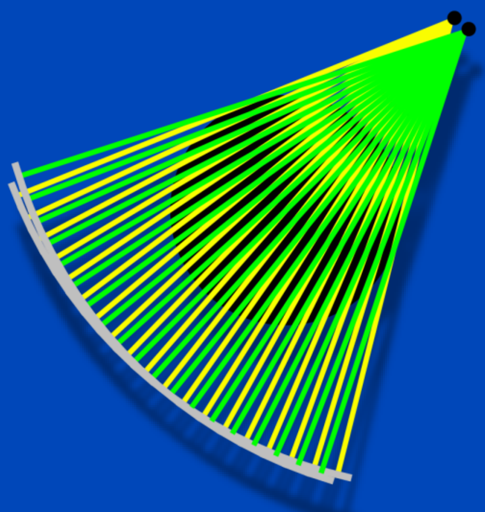

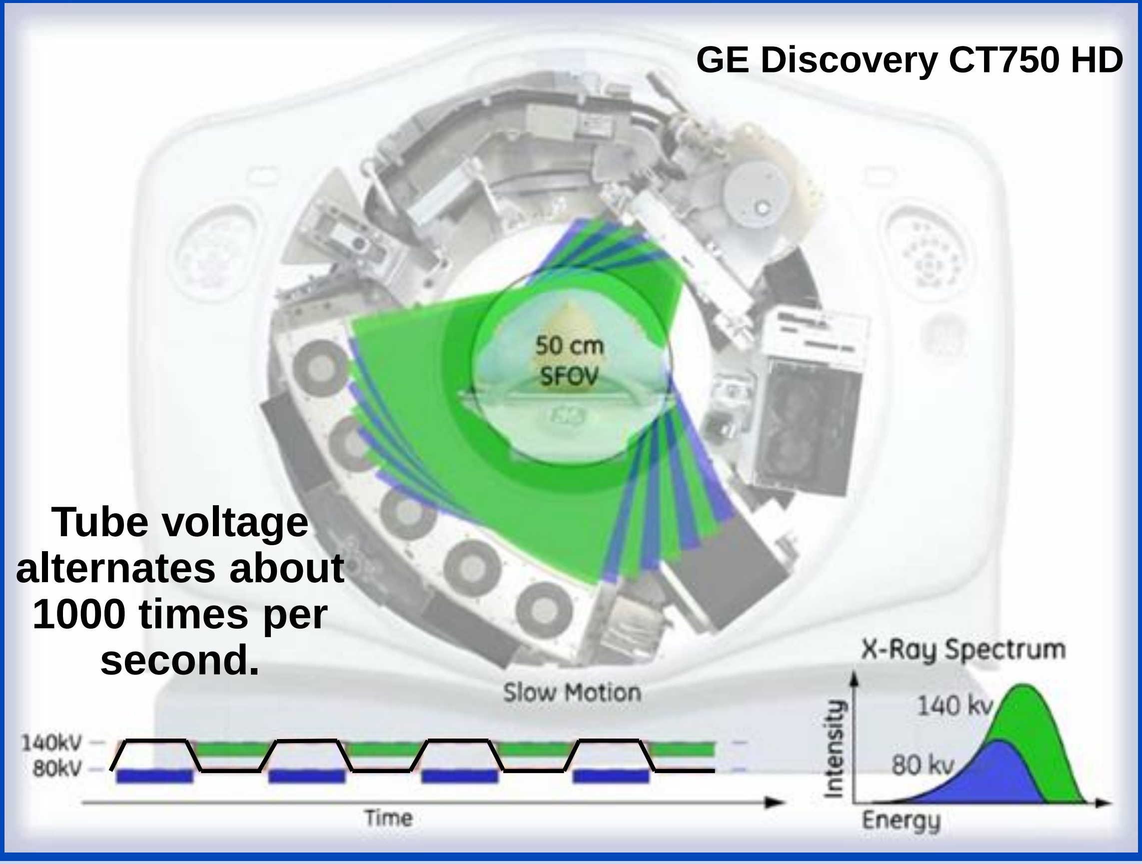

With the introduction of the GE Quantix 160 tube (around 2018), that includes microsecond tube current control by an electron extracting dual flat emitter, that is free of the traditional constraints of thermionic emission, the TVS can be regarded of being as almost rectangular shape.

DECT Technology

- DECT approaches in the clinic:
  - Dual source DECT (Siemens)
  - Fast tube voltage switching (Canon, GE)

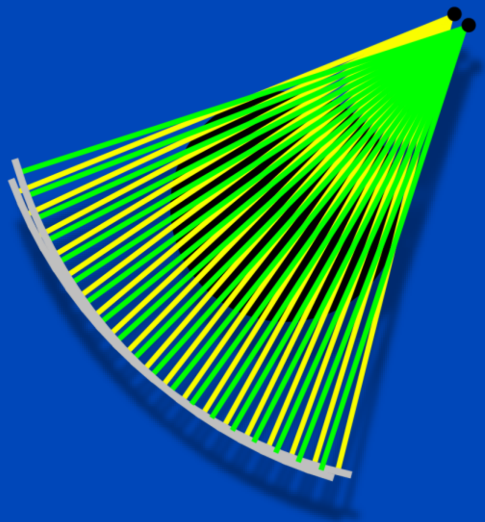

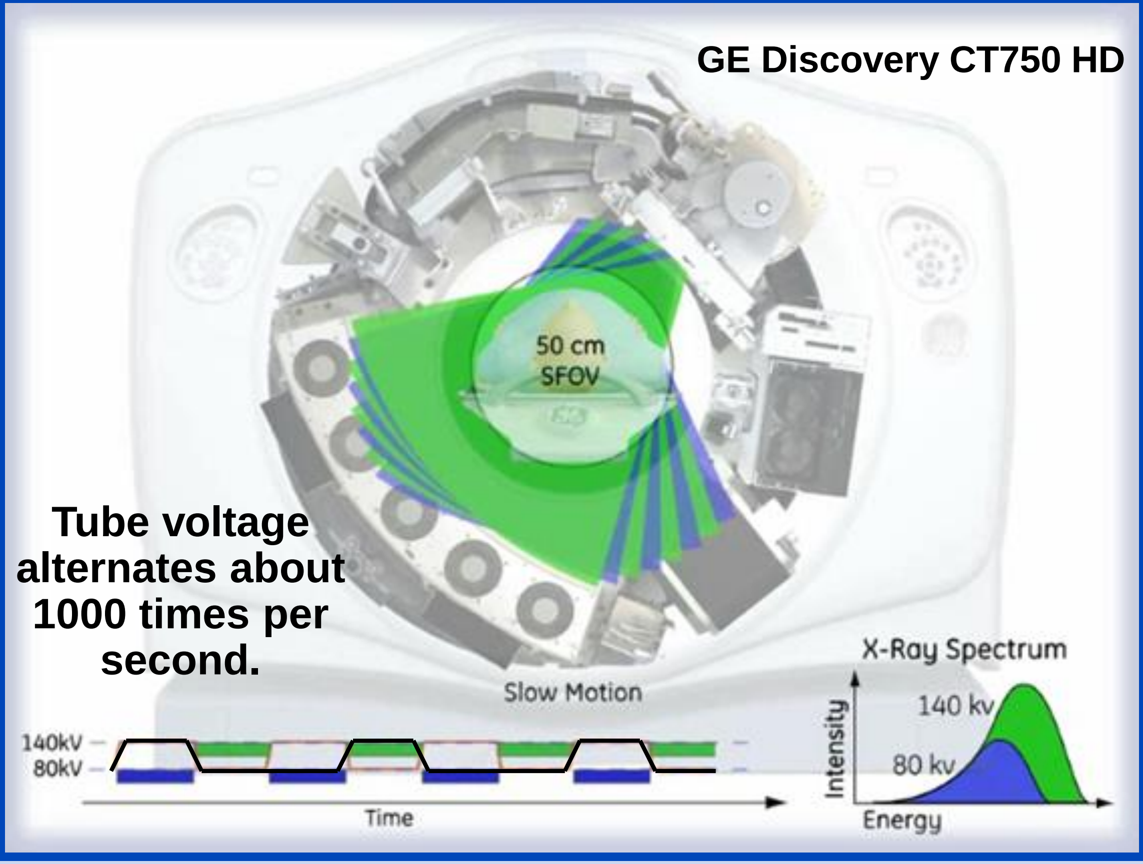

With the introduction of the GE Quantix 160 tube (around 2018), that includes microsecond tube current control by an electron extracting dual flat emitter, that is free of the traditional constraints of thermionic emission, the TVS can be regarded of being as almost rectangular shape.

DECT Technology

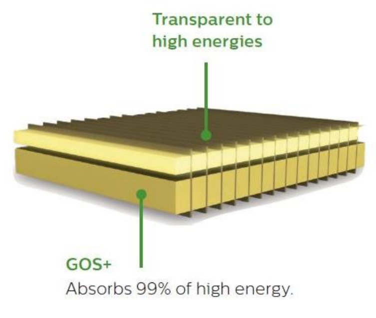

- DECT approaches in the clinic:
  - Dual source DECT (Siemens)
  - Fast tube voltage switching (Canon, GE)
  - Dual layer (sandwich) detector (Philips)

Philips IQon

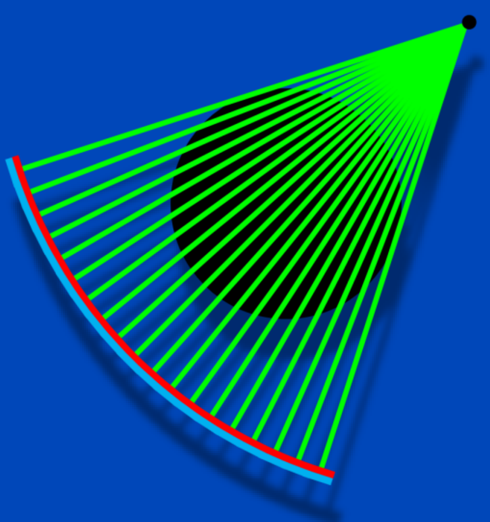

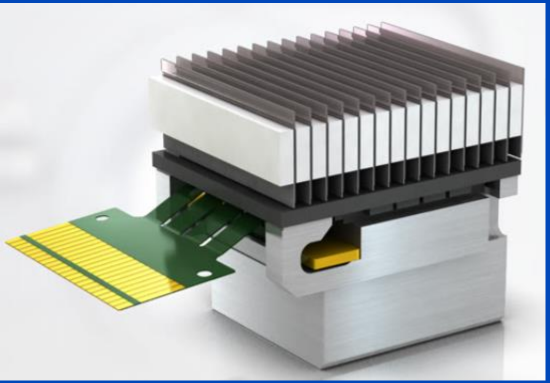

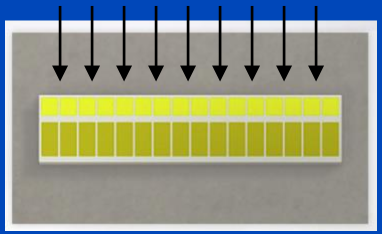

Top layer acts as a prefilter
for the bottom layer.

Siemens X.Cite: 0.7 mm Sn and 0.07 mm Au

K-edges: Sn = 29 keV, Au = 81 keV

DECT Technology

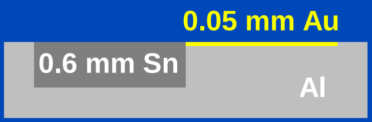

- DECT approaches in the clinic:
  - Dual source DECT (Siemens)
  - Fast tube voltage switching (Canon, GE)
  - Dual layer (sandwich) detector (Philips)
  - Split filter (Siemens)

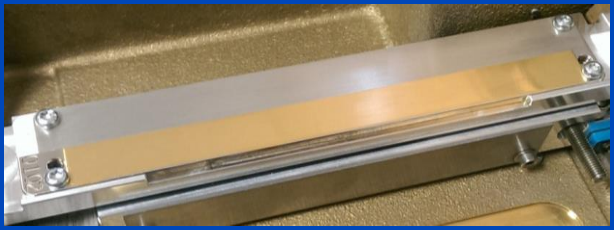

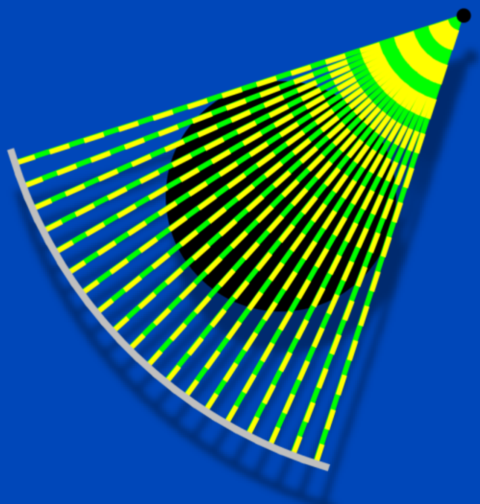

Siemens Definition Edge TwinBeam

DECT Technology

- DECT approaches in the clinic:
  - Dual source DECT (Siemens)
  - Fast tube voltage switching (Canon, GE)
  - Dual layer (sandwich) detector (Philips)
  - Split filter (Siemens)
  - Photon counting detector, multiple energy bins

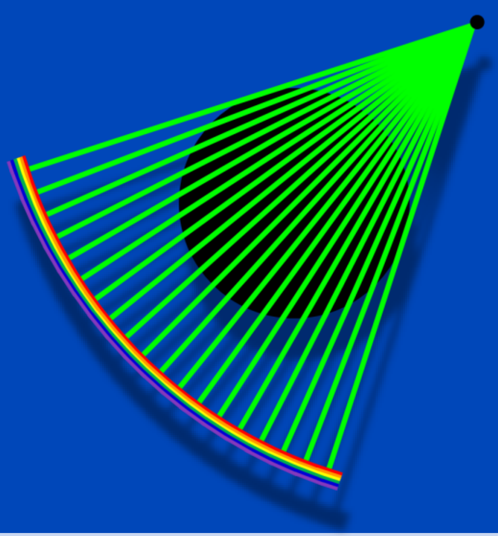

Siemens Naeotom Alpha

80 kV / 140 kV

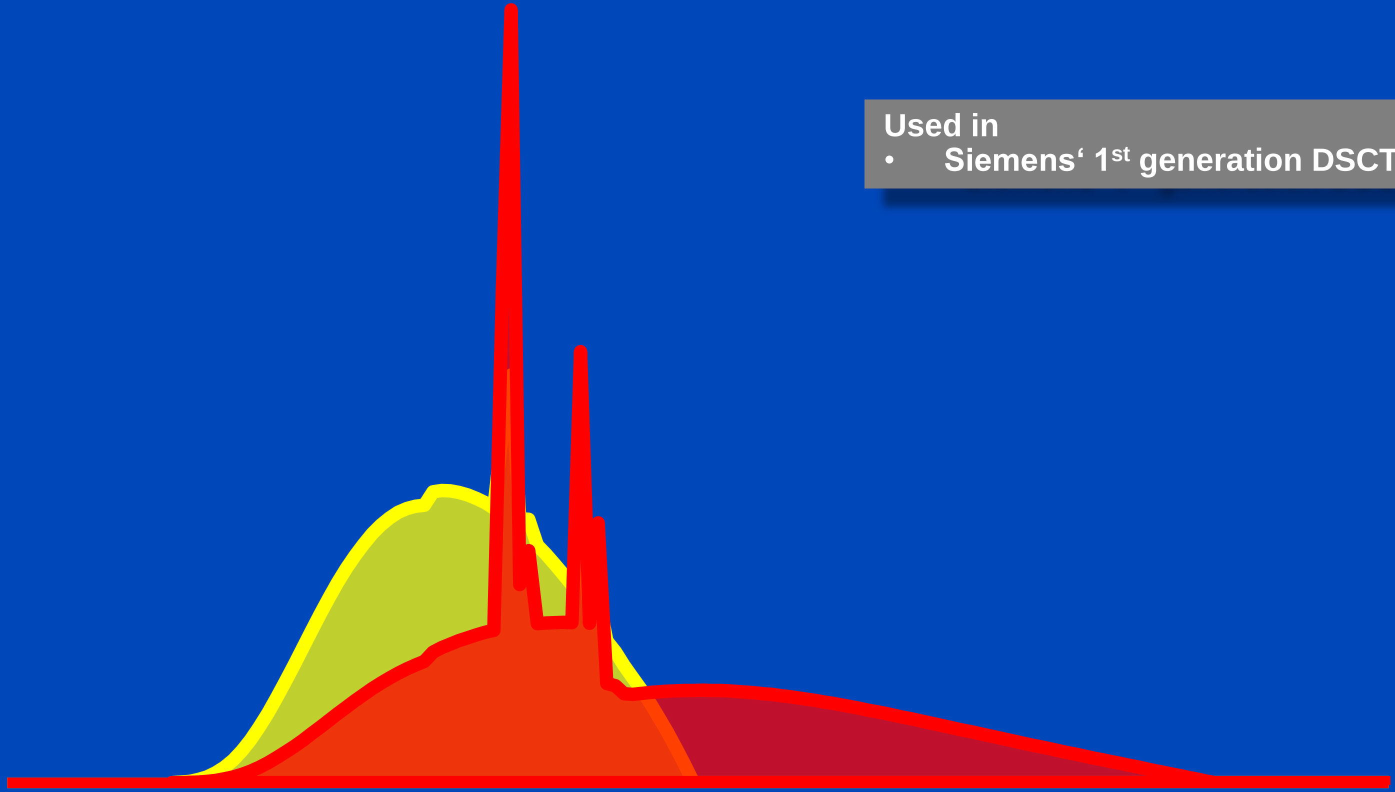

Used in
- Siemens' 1st generation DSCT

80 kV / 140 kV

Used in
- Siemens‘ 1st generation DSCT

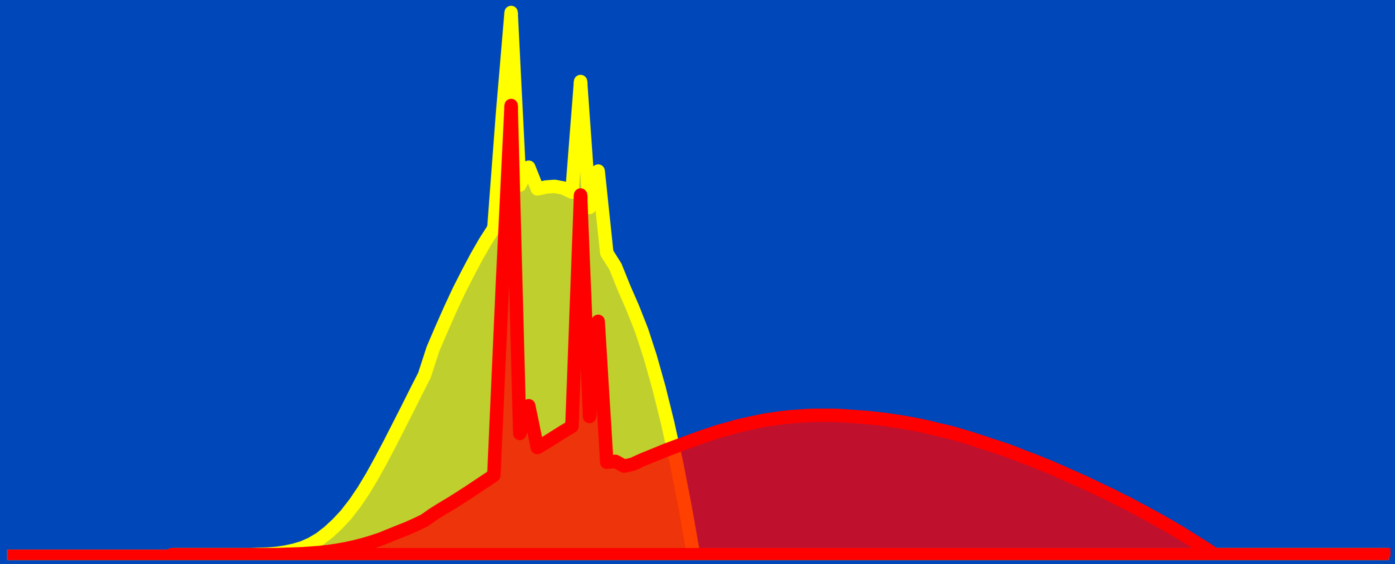

Spectra as seen after having passed a 32 cm water layer.

dkfz.

80 kV / 140 kV Sinrect kV-Switching

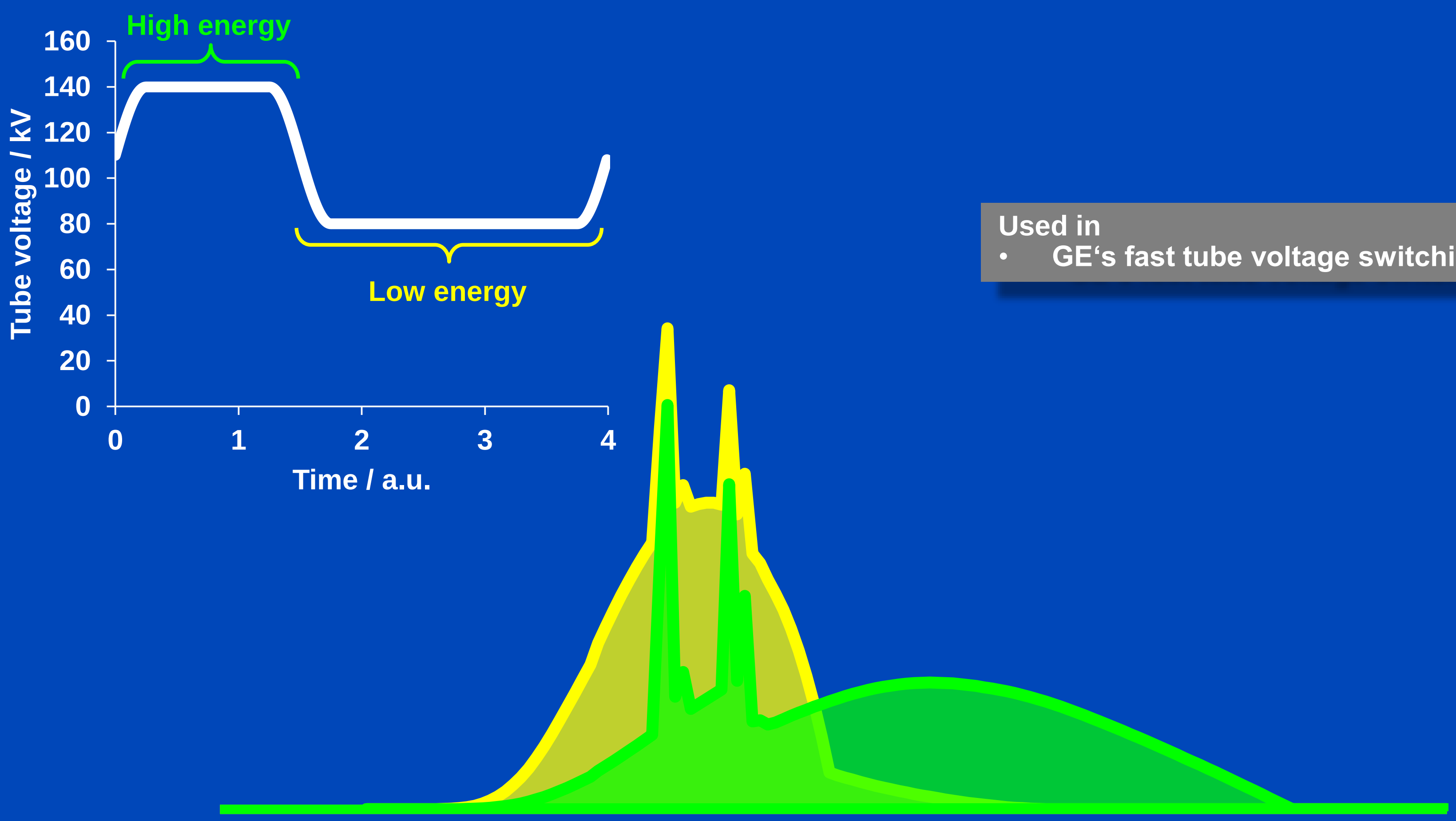

Used in
- GE's fast tube voltage switching CT

Spectra as seen after having passed a 32 cm water layer.

80 kV / 140 kV $Sn_{0.4\ mm}$

Used in
- Siemens' 2nd generation DSCT

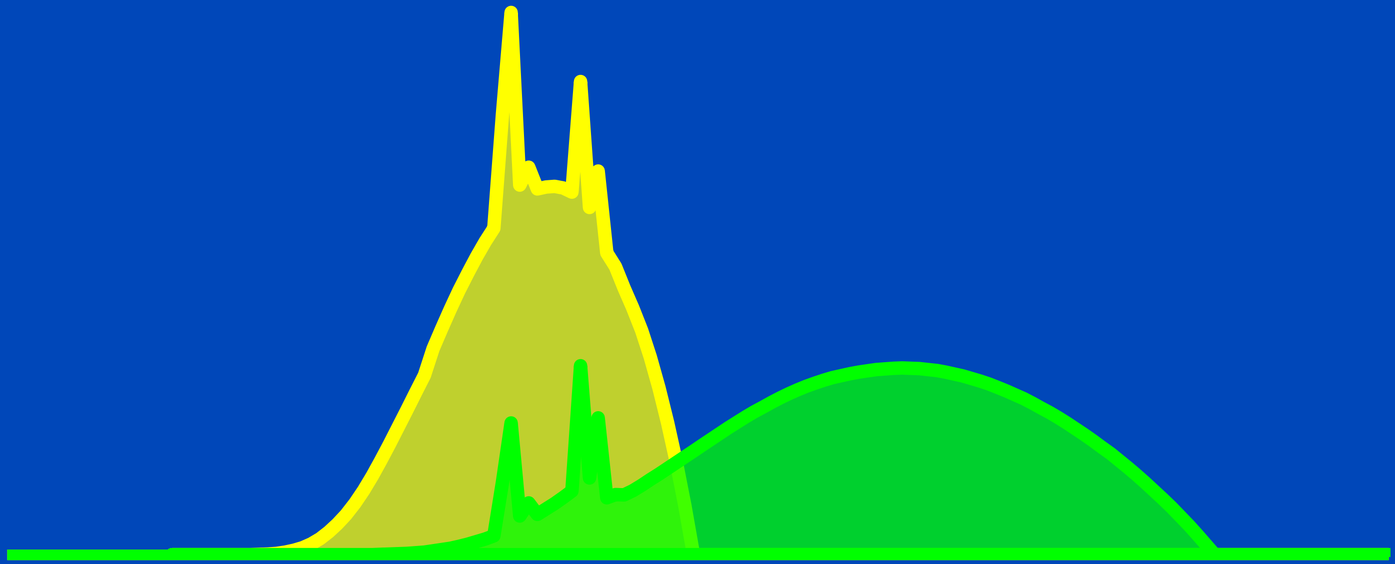

Spectra as seen after having passed a 32 cm water layer.

100 kV / 140 kV $Sn_{0.4\ mm}$

Used in
- Siemens‘ 2nd generation DSCT

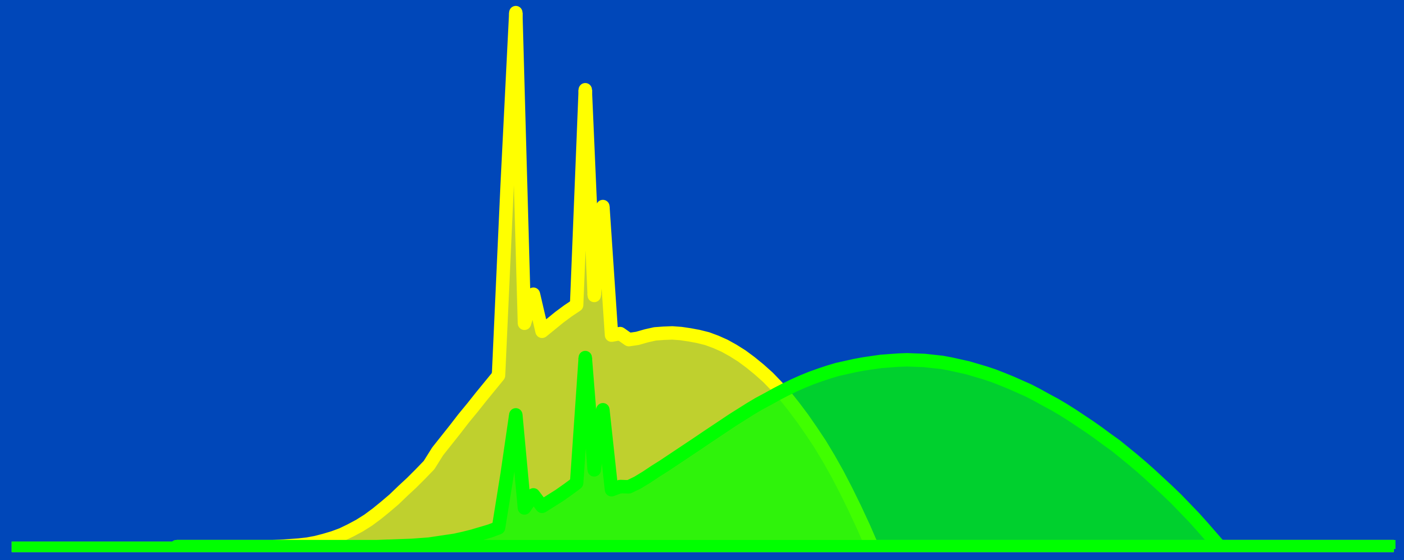

Spectra as seen after having passed a 32 cm water layer.

90 kV / 150 kV $Sn_{0.6\ mm}$

Used in
- Siemens‘ 3rd generation DSCT

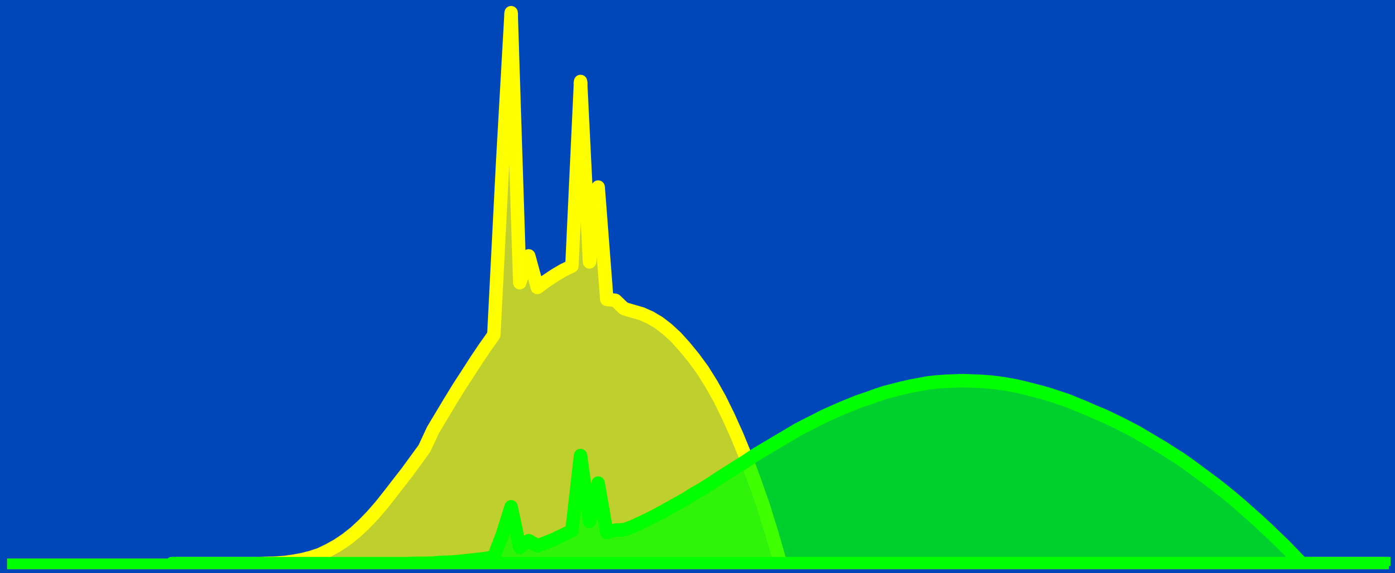

Spectra as seen after having passed a 32 cm water layer.

140 kV YAG / GOS

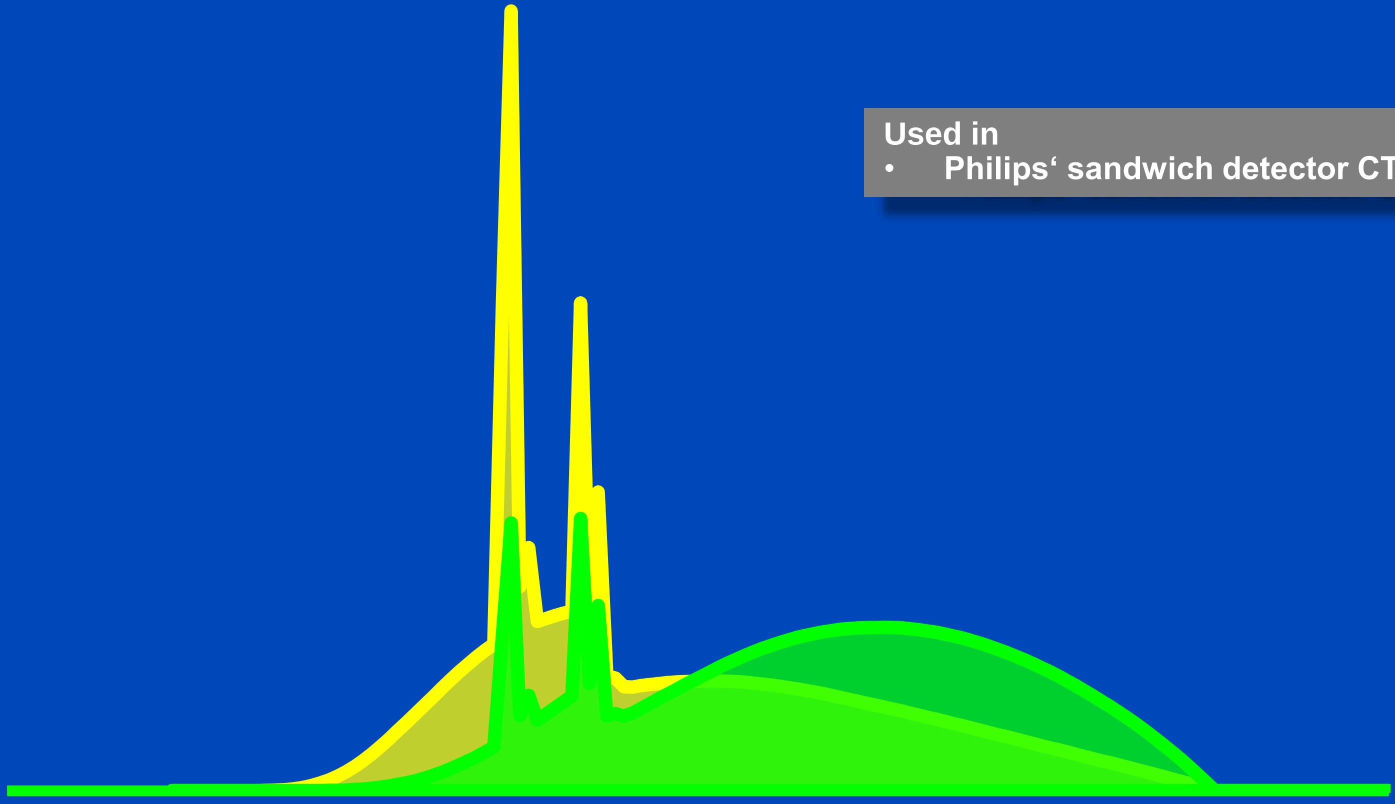

Used in
- Philips‘ sandwich detector CT

Spectra as seen after having passed a 32 cm water layer.

Split filter 120 kV (Au+Sn)

Used in
- Siemens‘ split filter DSCT

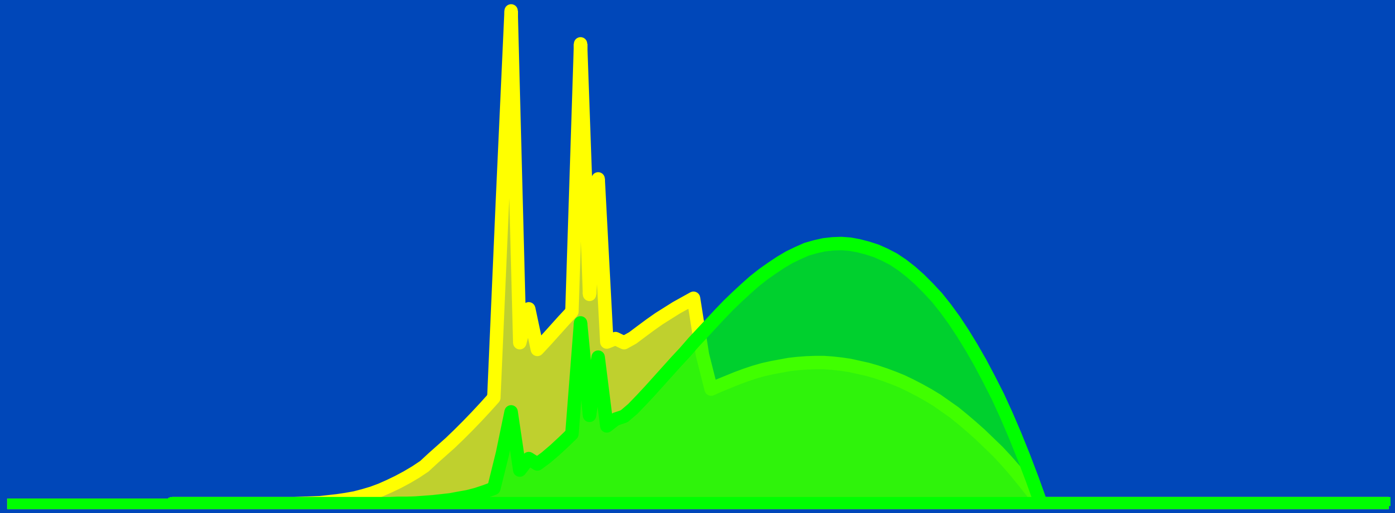

Spectra as seen after having passed a 32 cm water layer.

Photon Counting 140 kV
2 Bins Perfect

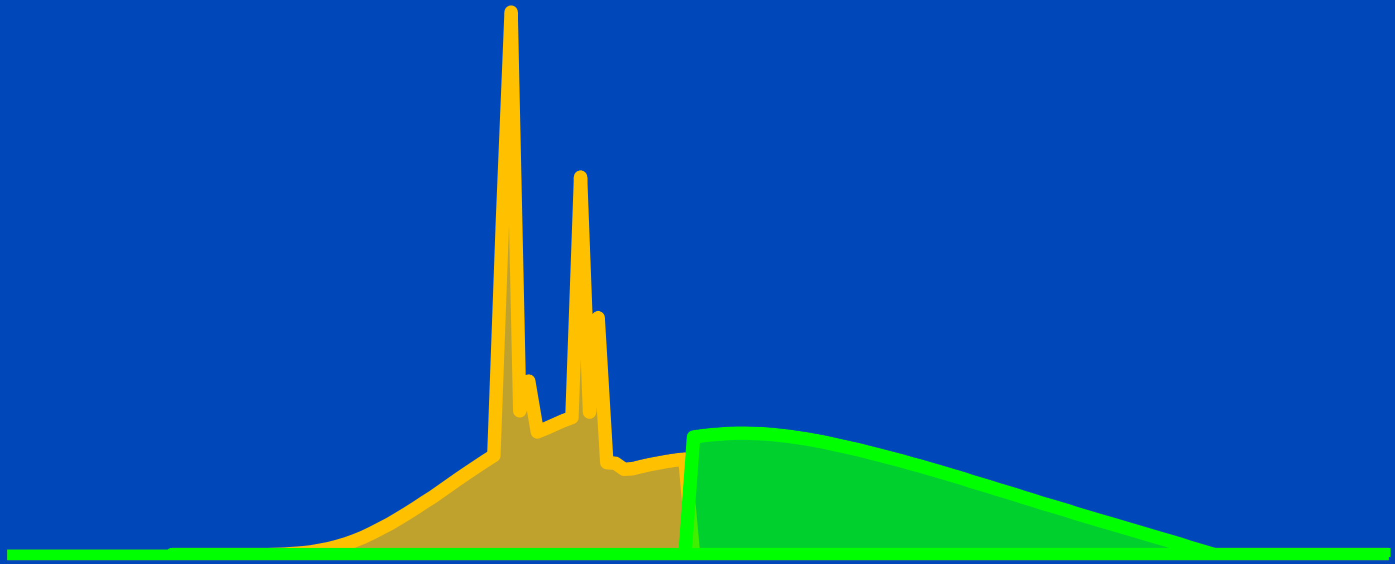

Spectra as seen after having passed a 32 cm water layer.

Photon Counting 140 kV
2 Bins Realistic

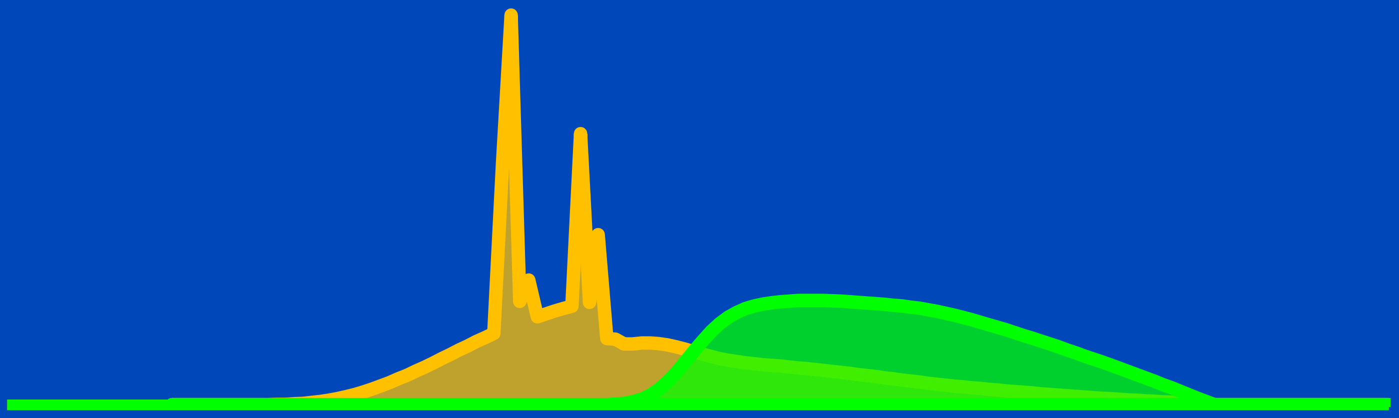

Photon Counting 140 kV
4 Bins Realistic

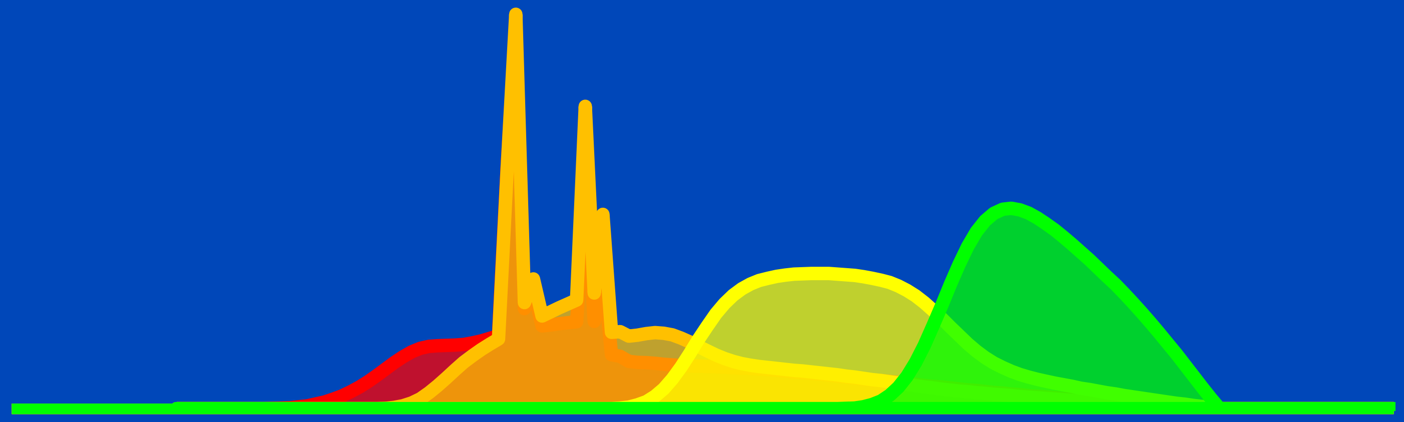

Spectra as seen after having passed a 32 cm water layer.

Material Mixtures

- **In volumetric mixtures the linear attenuation coefficient mixes linearly with the volumetric fraction**

$$\mu = \mu_1 \frac{V_1}{V_1 + V_2} + \mu_2 \frac{V_2}{V_1 + V_2}.$$

- **Since the sum of the weighting factors equals one the CT-value mixes accordingly:**

$$CT = CT_1 \frac{V_1}{V_1 + V_2} + CT_2 \frac{V_2}{V_1 + V_2}.$$

Image-Based Classification of Materials

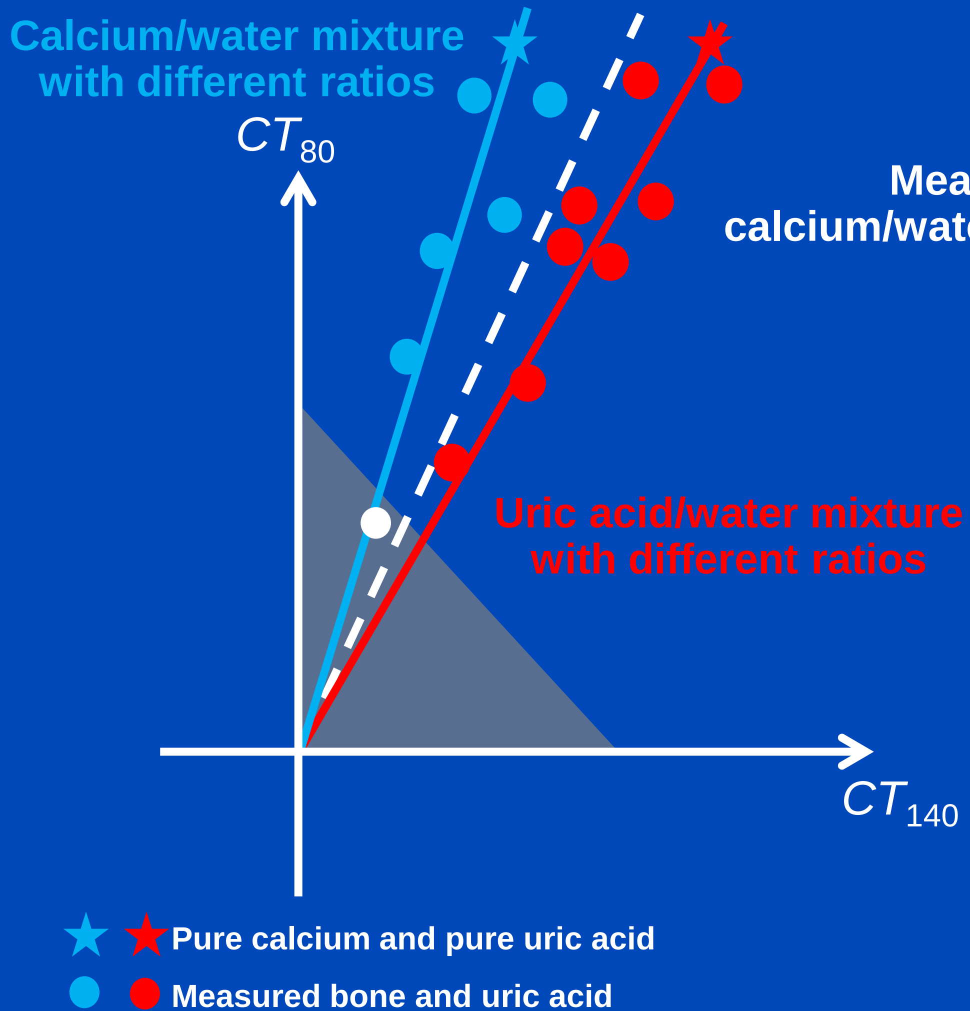

Measured data can be classified into calcium/water mixtures and uric acid/water mixtures.

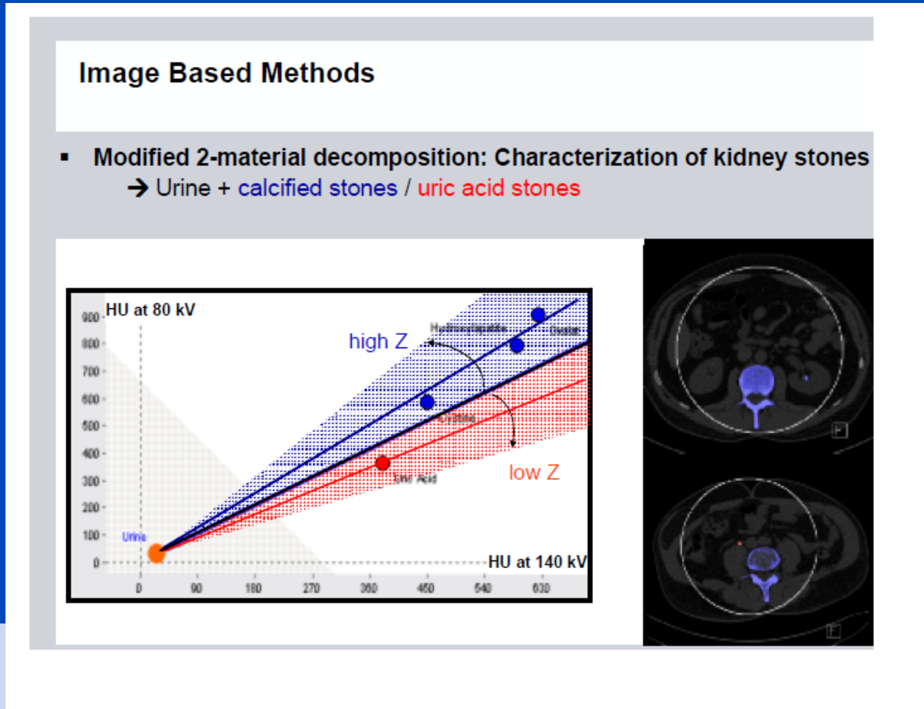

Image-Based Decomposition (Three Materials)

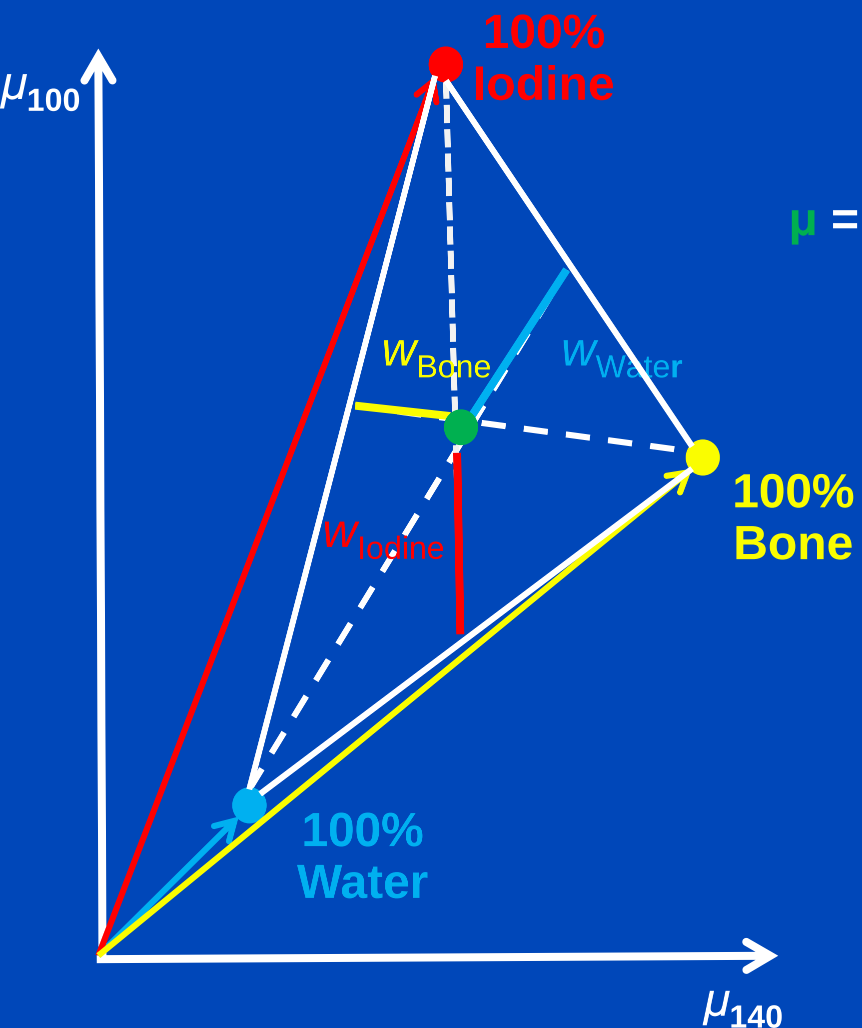

$$\mu = w_{Water} \bullet \mu_{Water} + w_{Bone} \bullet \mu_{Bone} + w_{Iodine} \bullet \mu_{Iodine}$$

$$w_{Water} + w_{Bone} + w_{Iodine} = 1$$

$$w_{Water}, w_{Bone}, w_{Iodine} \geq 0$$

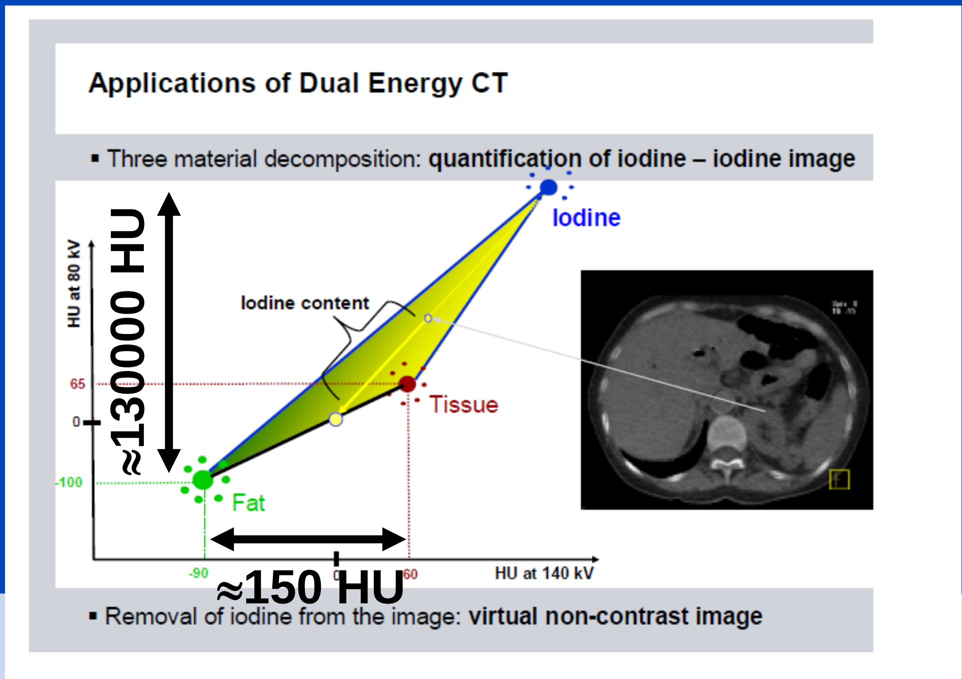

Material Mixtures

- Two water-iodine mixtures

$$CT_1(E) = (1 - w_1)CT_\mathrm{W}(E)$$

$$CT_2(E) = (1 - w_2)CT_\mathrm{W}(E)$$

- Their relative contrast is in ratio

$$\frac{CT_1(E_{100\,\mathrm{kV}}) - CT_2(E_{1}}{CT_1(E_{150\,\mathrm{kV}}) - CT_2(E_{1}}$$

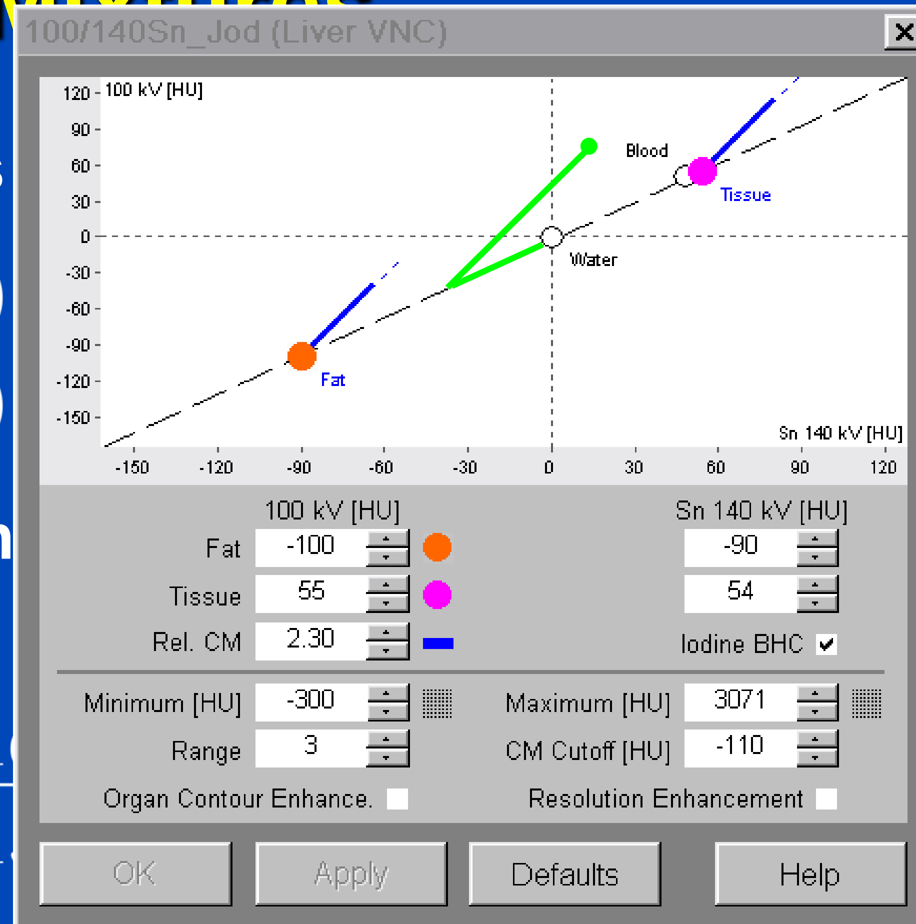

- Hence, it can be used to calibrate DECT

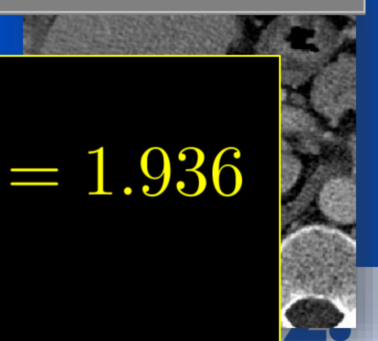

$$\frac{CT_\mathrm{I}(60\ \mathrm{keV})}{CT_\mathrm{I}(80\ \mathrm{keV})} = \frac{\mu_\mathrm{I}(60\ \mathrm{keV})/\mu_\mathrm{W}(60\ \mathrm{keV}) - 1}{\mu_\mathrm{I}(80\ \mathrm{keV})/\mu_\mathrm{W}(80\ \mathrm{keV}) - 1} = 1.936$$

In monochromatic scans or in rawdata-based preprocessed DECT data!

Decomposition Increases Noise

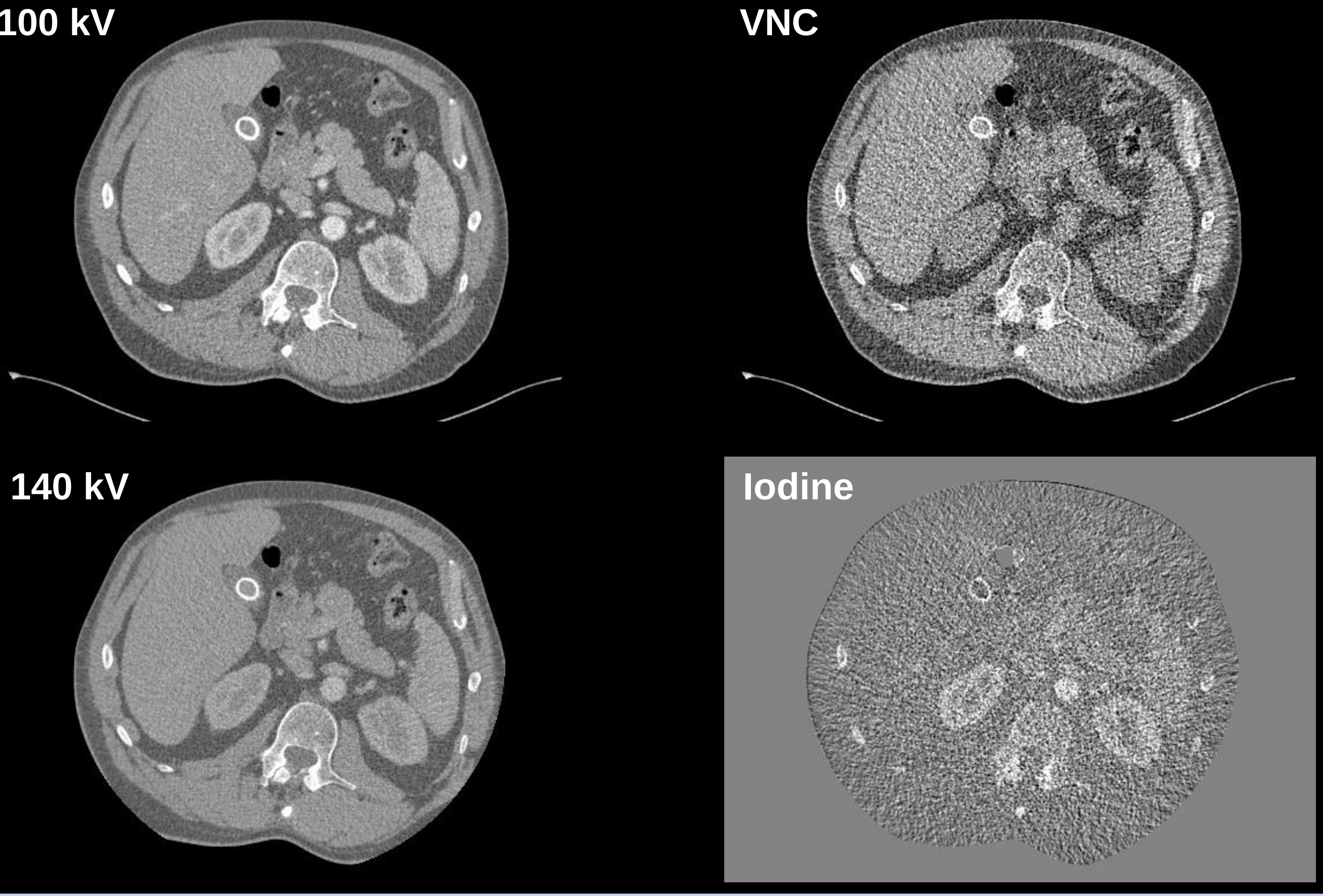

C = 0 HU, W = 700 HU

Denoising is Mandatory!

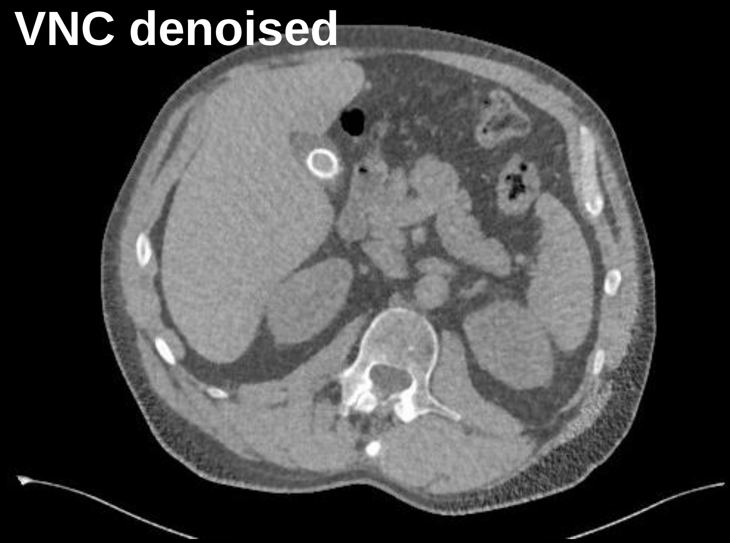

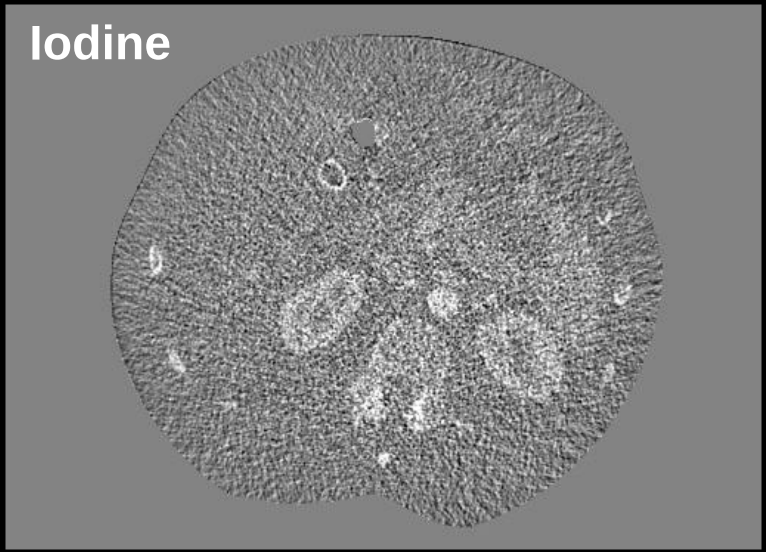

Simple Denoising Example

- **Assume CT images with air = 0 and water = 1**
- **Mix image:** $f_\alpha = (1-\alpha) f_{\mathrm{L}} + \alpha f_{\mathrm{H}}$ $\quad \alpha$ to minimize noise
- **Water image:** $f_{\mathrm{W}} = (1-\beta) f_{\mathrm{L}} + \beta f_{\mathrm{H}}$ $\quad \beta = \frac{\mathrm{RelCM}}{\mathrm{RelCM}-1} > 1$
- **Iodine overlay:** $f_{\mathrm{I}} = \gamma (f_{\mathrm{L}} - f_{\mathrm{H}})$ $\quad \gamma$ such that $f_{\mathrm{W}} + f_{\mathrm{I}} = f_\alpha$

- **Denoised images:**

$$\hat{f}_{\mathrm{I}} = \mathrm{LP}(f_{\mathrm{I}}) + 0.5\,\mathrm{HP}(f_\alpha)$$

$$\hat{f}_{\mathrm{W}} = f_\alpha - \hat{f}_{\mathrm{I}}$$

  - **Low pass LP = (1 2 2 2 2 2 1) / 12, for example (pixel size dependent)**
  - **High pass HP = 1- LP**

Macovski et al. “Measurement-Dependent Filtering: A Novel Approach to Improved SNR” IEEE TMI MI-2(3): 122-127, 1983

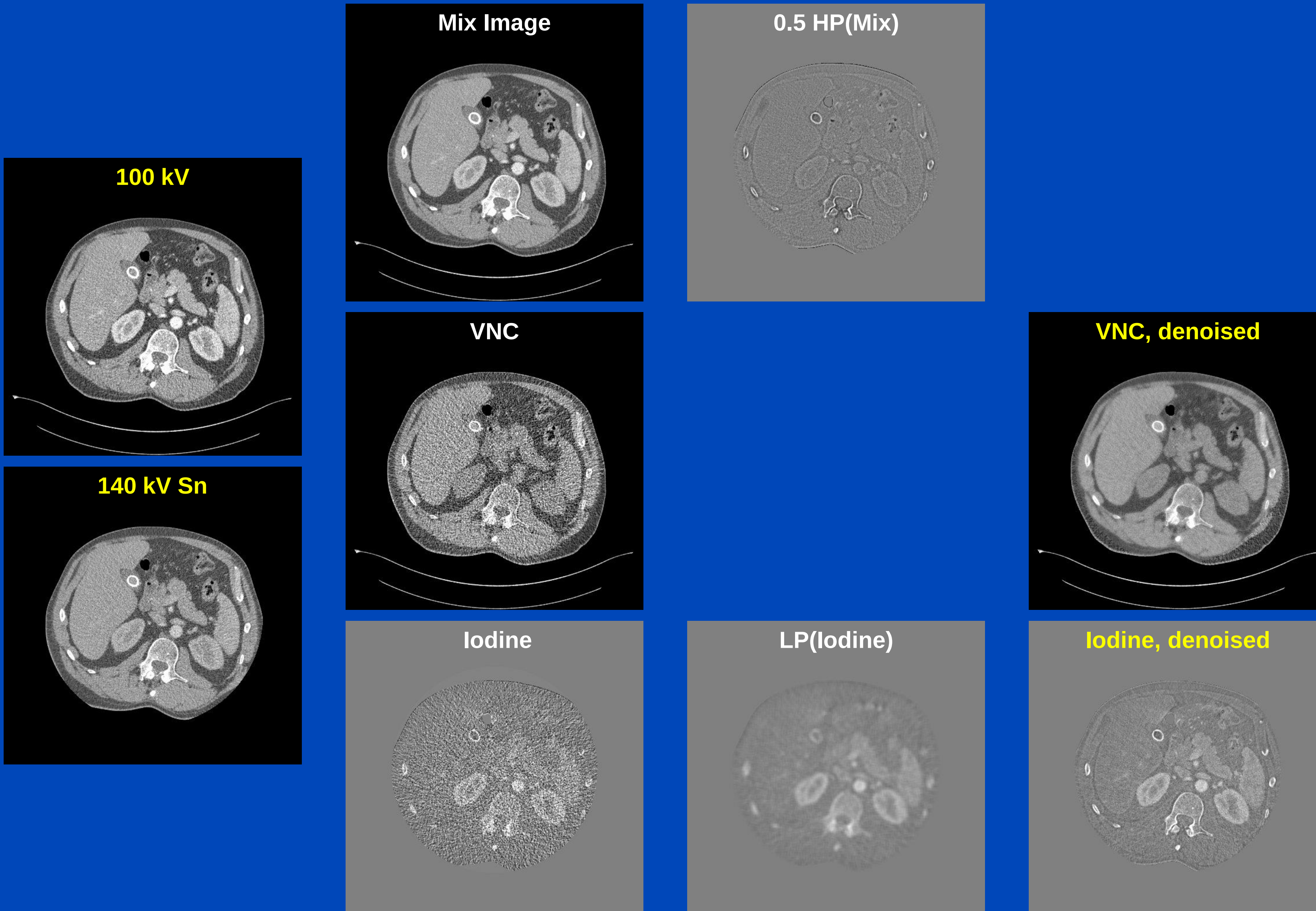

C **= 0 HU,** ***W*** **= 500 HU for the low, high and VNC images.** ***C*** **= 0 mg/mL,** ***W*** **= 27.6 mg/mL for the iodine images.**

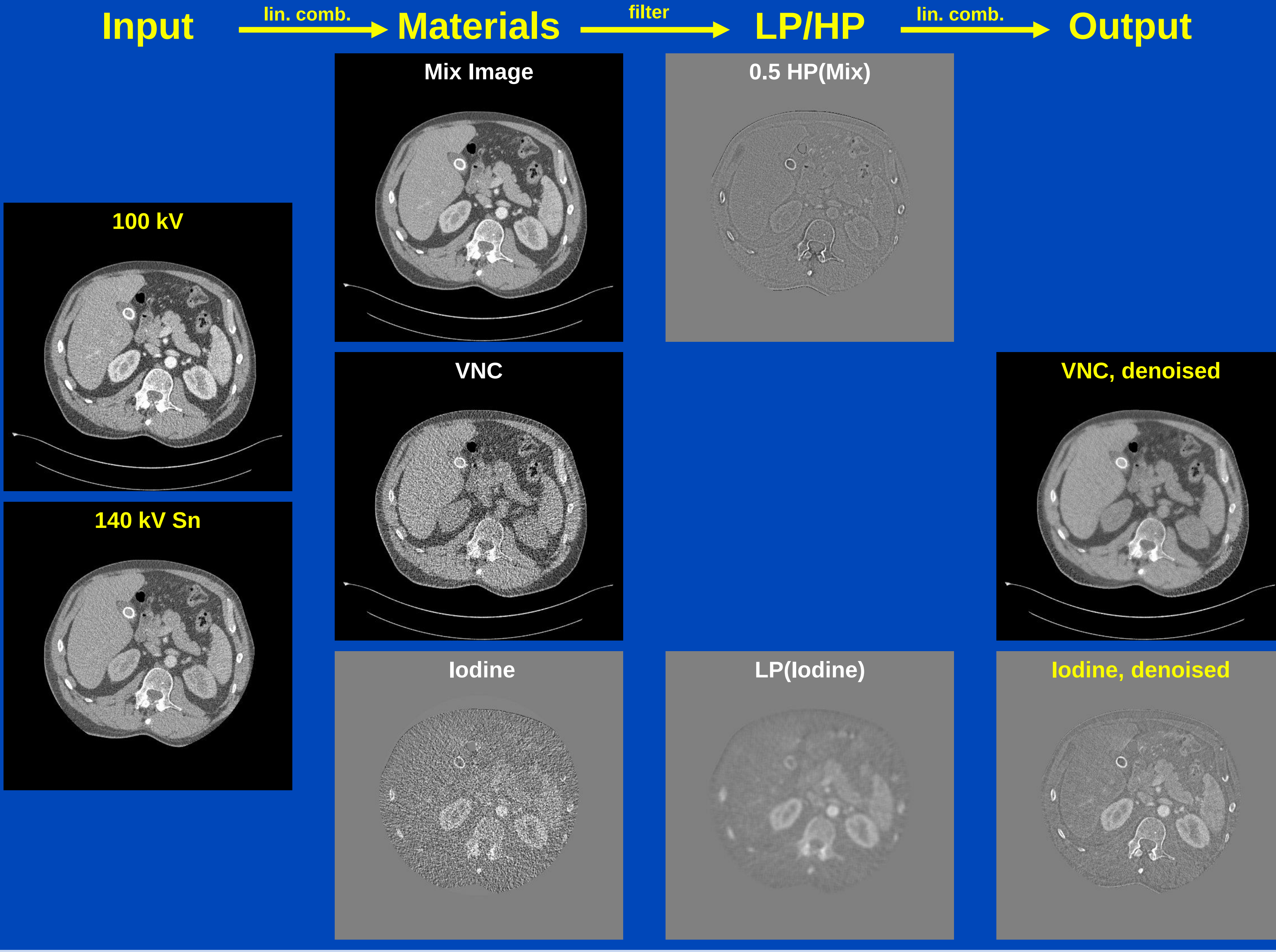

C = 0 HU, *W* = 500 HU for the low, high and VNC images. *C* = 0 mg/mL, *W* = 27.6 mg/mL for the iodine images.

Why is Subtraction Potentially Better?
(in case of no motion)

- W = soft tissue (water) signal, X = iodine signal
- Assume same noise N, e.g. 50 HU, in both measurements M_1 and M_2
  - Var M_1 = Var M_2 = N^2 regardless of whether iodine is present or not
- DECT
  - Measurement 1 (high kV): $M_1 = W + 0.25\,X$
  - Measurement 2 (low kV): $M_2 = W + 0.5\,X$
  - Estimated iodine: $4\,(M_2 - M_1)$ Variance = 16 (Var M_2 + Var M_1) = 32 N^2
  - Estimated soft tissue: $2\,M_1 - M_2$ Variance = 4 Var M_1 + Var M_2 = 5 N^2
- **Subtraction**
  - Measurement 1 (native): $M_1 = W$
  - Measurement 2 (enhanced): $M_2 = W + 0.5\,X$
  - Estimated iodine: $2\,(M_2 - M_1)$ Variance = 4 (Var M_2 + Var M_1) = 8 N^2
  - Estimated soft tissue: M_1 Variance = Var M_1 = N^2

**VNC and iodine noise (standard deviation)
in DECT is about twice as high as in subtraction imaging.**

This simple example assumes iodine to contribute half as much to the gray value for the high kV scan as for the low kV scan. Dose is assumed to be the same in both scenarios.

Optimal Dose Distribution

- A linear combination of a low and a high energy image yields

$$V_\chi = w_L^2 V_L + w_H^2 V_H = w_L^2 \frac{k_L}{D_L} + w_H^2 \frac{k_H}{D_H} = w_L^2 \frac{k_L}{(1-\alpha)D_T} + w_H^2 \frac{k_H}{\alpha\, D_T}$$

  with k relating the variances V to doses D, with $D_T = D_L + D_H$, and with α being the relative dose of the high energy image.

- For the Flash dual source 100 kV / Sn 140 kV we have
  - w_L = -0.943509 and w_H = 1.943850 for χ = VNC
  - w_L = 6.468680 and w_H = -6.466740 for χ = Iodine
  - k_L = 1.087 and k_H = 0.826 (up to an arbitrary factor)

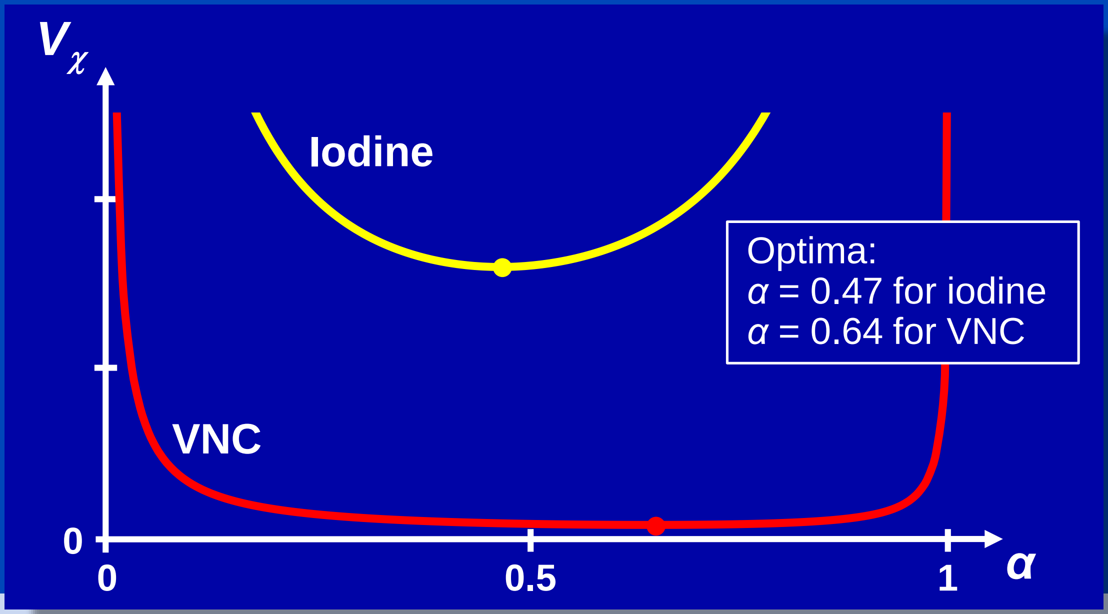

	H_2O	I
Low	1	1+a
High	1	1+b
VNC	1	1

	H_2O	I
Low	1	1+a
High	1	1+b
Iodine	0	(a+b)/2

Here, dose and α refer to the energy absorbed in the patient, and not to mAs or CTDI.

Image-based Techniques
Mixed Image (Linear)

- **Mixed image:**

$$f_\alpha = (1-\alpha)\, f_{\mathrm{L}} + \alpha\, f_{\mathrm{H}}$$

- **Aim of weighting:**
  - Reduce noise
  - Maximize CNR
  - Reduce streak artifacts

Image-based Techniques
Mixed Image (Linear)

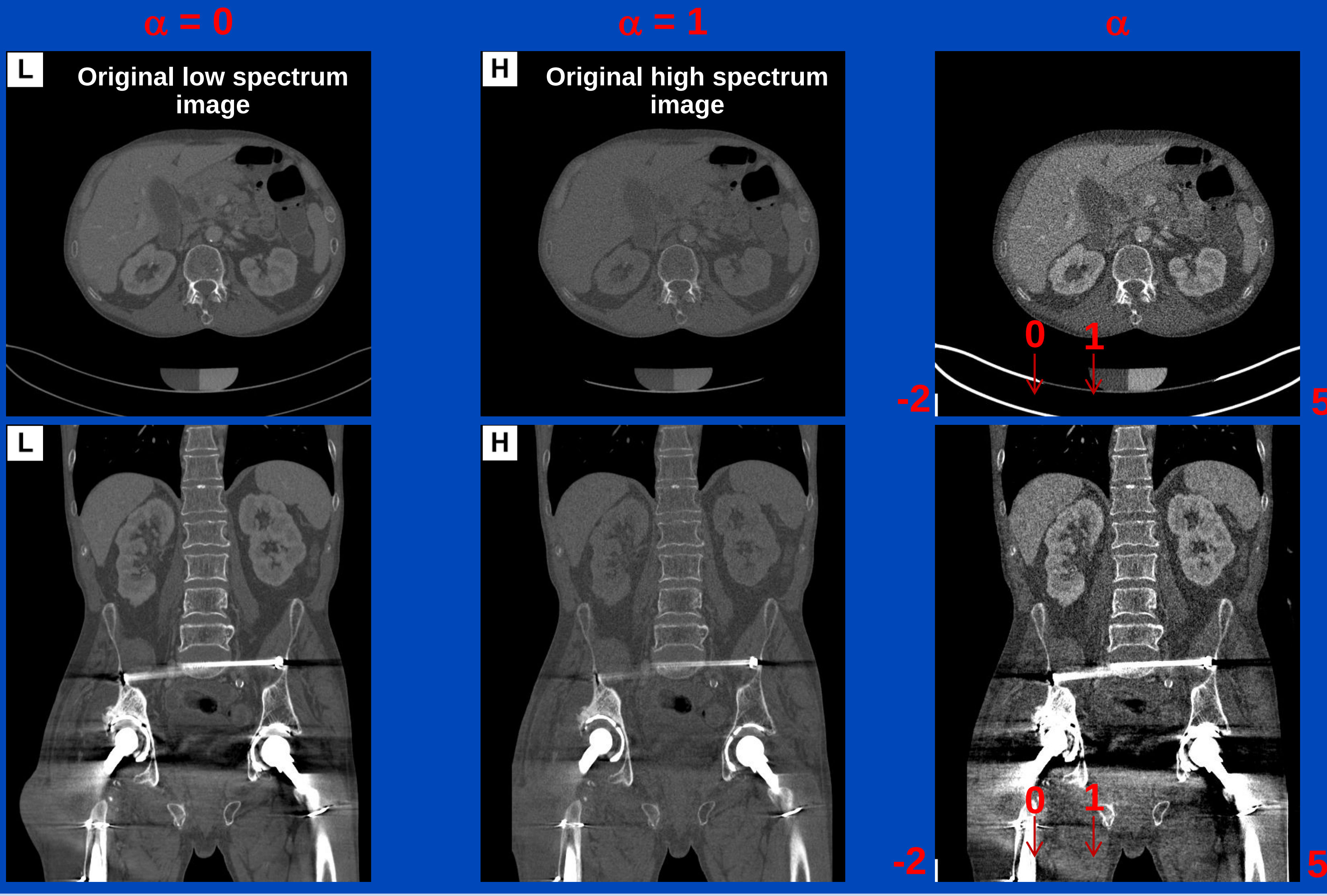

C = 300 HU, *W* = 1400 HU

Photon Counting CT

Photon Counting CT Availability

	Sensor material	Detector pixel size at iso	Pixel binning	FOM	Bins	FDA	Pubs	Installations
Canon	CdZnTe	210 µm	3×3, 1×1	50 cm	5	no	1	1 prototype (Japan)
GE	Si, edge on	400 × 400 µm	?	?	?	no		2 experimental setups (Sweden, USA)
Philips	CdZnTe	274 × 274 µm	?	50 cm	5	no	≈22	1 experimental setup (France)
Siemens CounT	GOS/CdTe dual source	700 × 600 µm / 250 × 250 µm	2×2, 1×1	50 / 28 cm	4	no	≈50	3 experimental systems (Germany, USA)
Siemens CountPlus	CdTe	150 × 176 µm	2×2, 1×1	50 cm	4	no	≈11	3 prototypes (Czech, Sweden, USA)
Siemens Alpha	CdTe/CdTe dual source	2 · 150 × 176 µm	2×2, 1×1	50 / 36 cm	4	yes	≈40	about 100 worldwide

Edge on design (Si only)

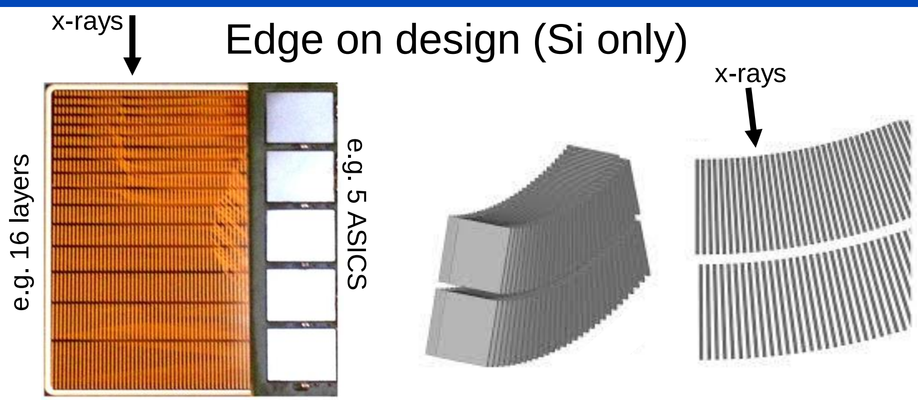

Image courtesy of KTH Royal Institute of Technology

Face on design (all others)

Image courtesy of Siemens Healthineers

The additional factor 2 in the detector pixel size column indicates that some scan modes may use binning.

dkfz.

Face-on Design

- Sensor material: CdTe or CZT
- Sensor thickness as seen by the x-ray: millimeters
- E.g. 64×64 pixels per module and 16 modules to realize a 64-row detector with 1024 channels

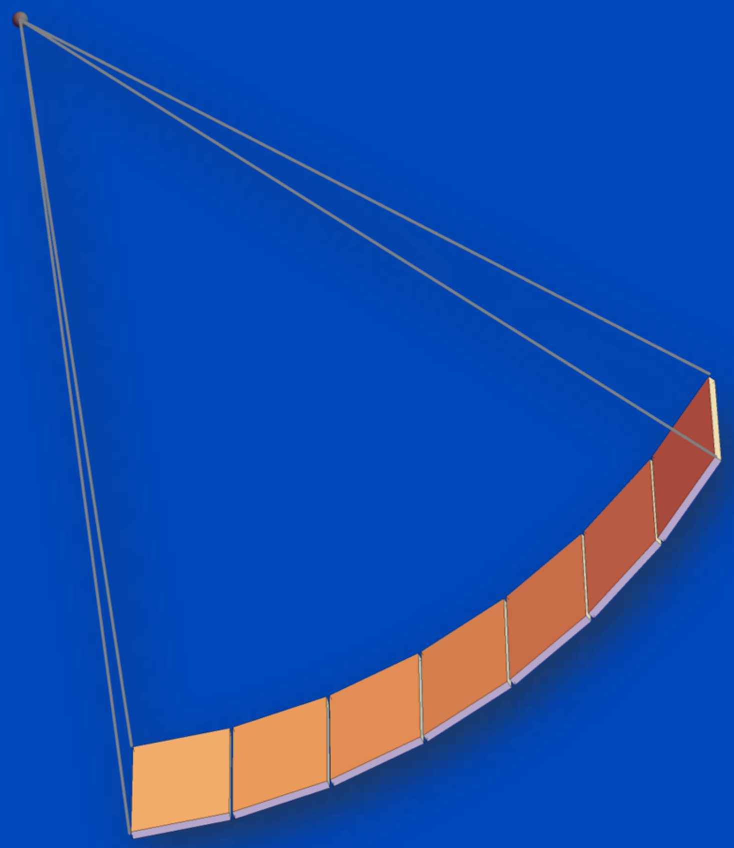

Edge-on Design

- Sensor material: Si
- Sensor thickness as seen by the x-ray: centimeters
- E.g. 64 pixels times 9 in depth per module and 1024 modules to realize a 64-row detector with 1024 channels

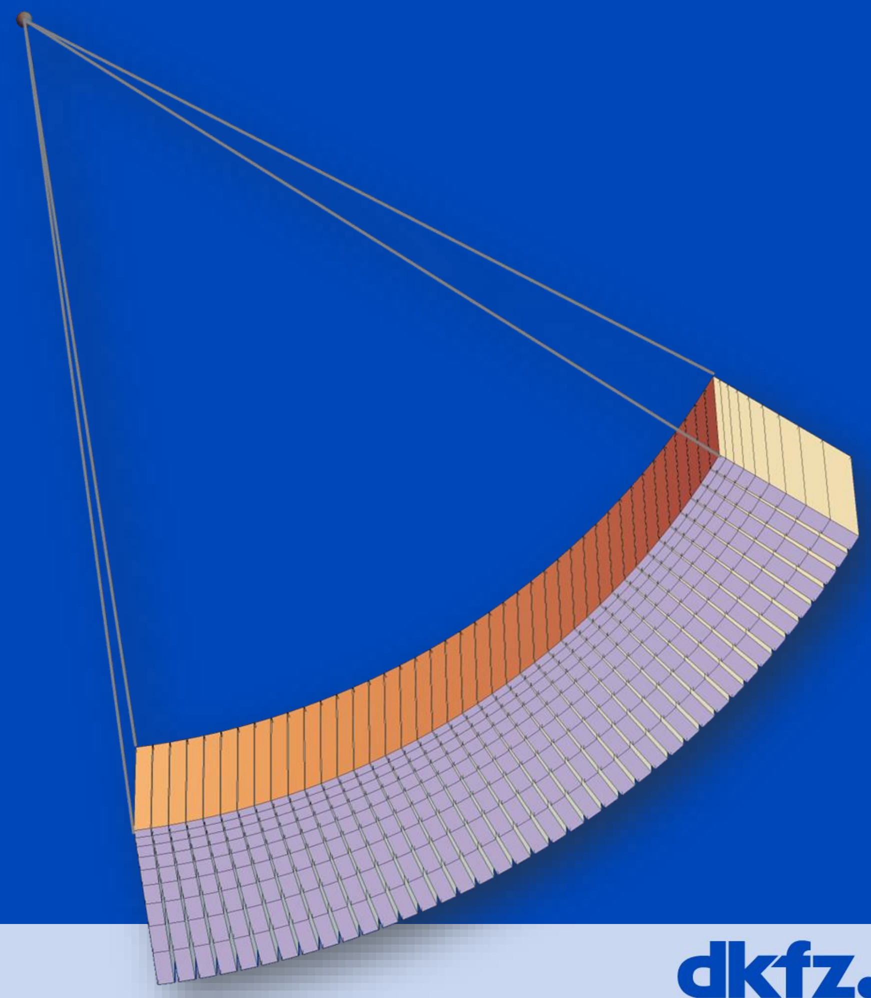

Indirect Conversion | Direct Conversion

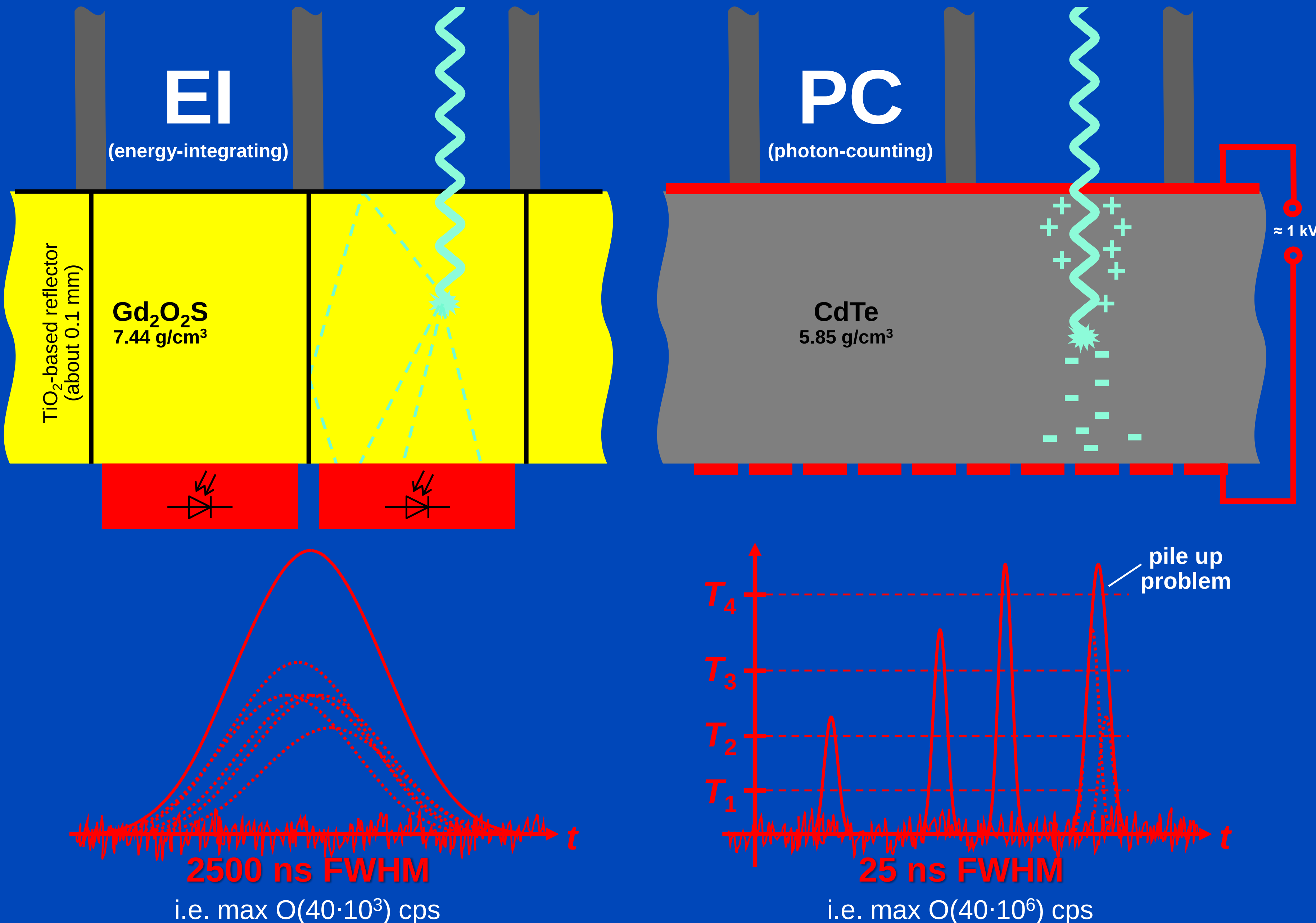

Requirements for CT: up to 10^9 x-ray photon counts per second per mm^2.
Hence, photon counting only achievable for direct converters.

Energy-Selective Detectors: Improved Spectroscopy, Reduced Dose?

Ideally, bin spectra do not overlap, …

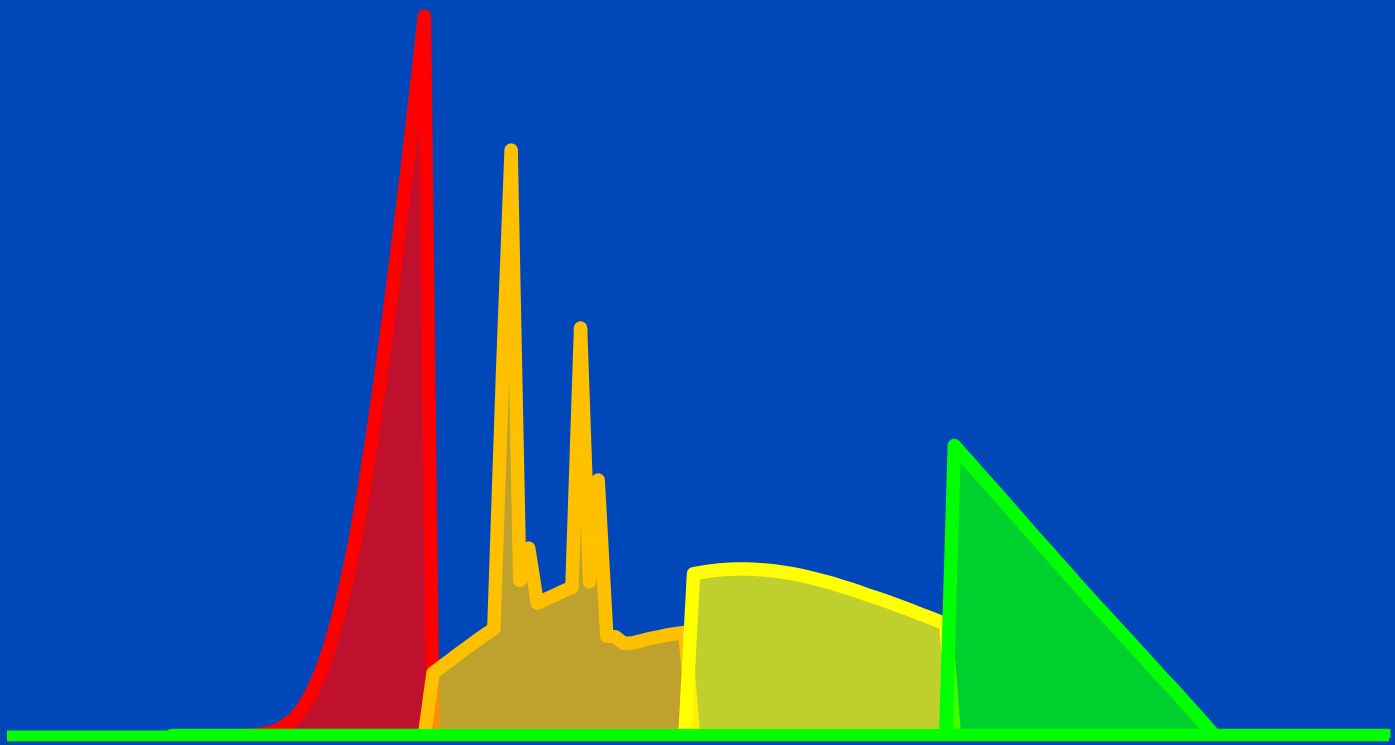

Spectra as seen with 4 bins after having passed a 32 cm water layer.

dkfz.

Energy-Selective Detectors: Improved Spectroscopy, Reduced Dose?

… realistically, however, they do!

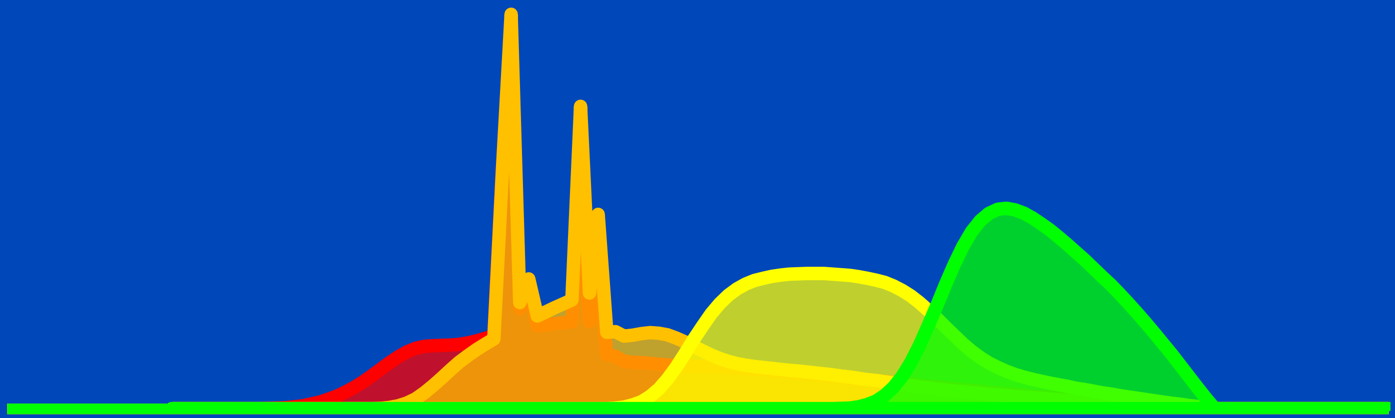

Spectra as seen with 4 bins after having passed a 32 cm water layer.

Photon Events

- Detection process in the sensor
- Photoelectric effect (e.g. 80 keV)

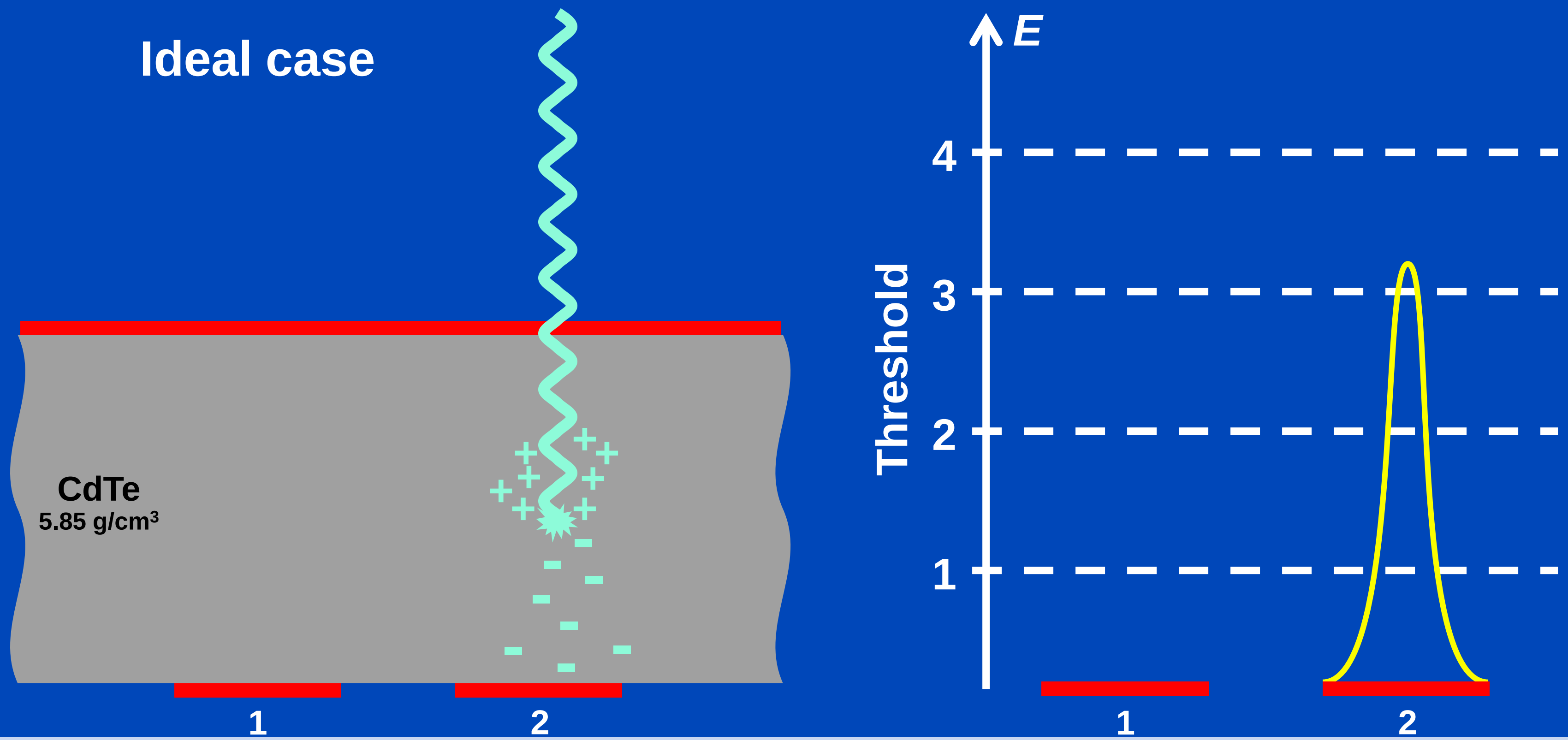

Photon Events

- Detection process in the sensor
- Compton scattering or K-fluorescence (e.g. 80 keV)

Energy dispersion due to secondary photons

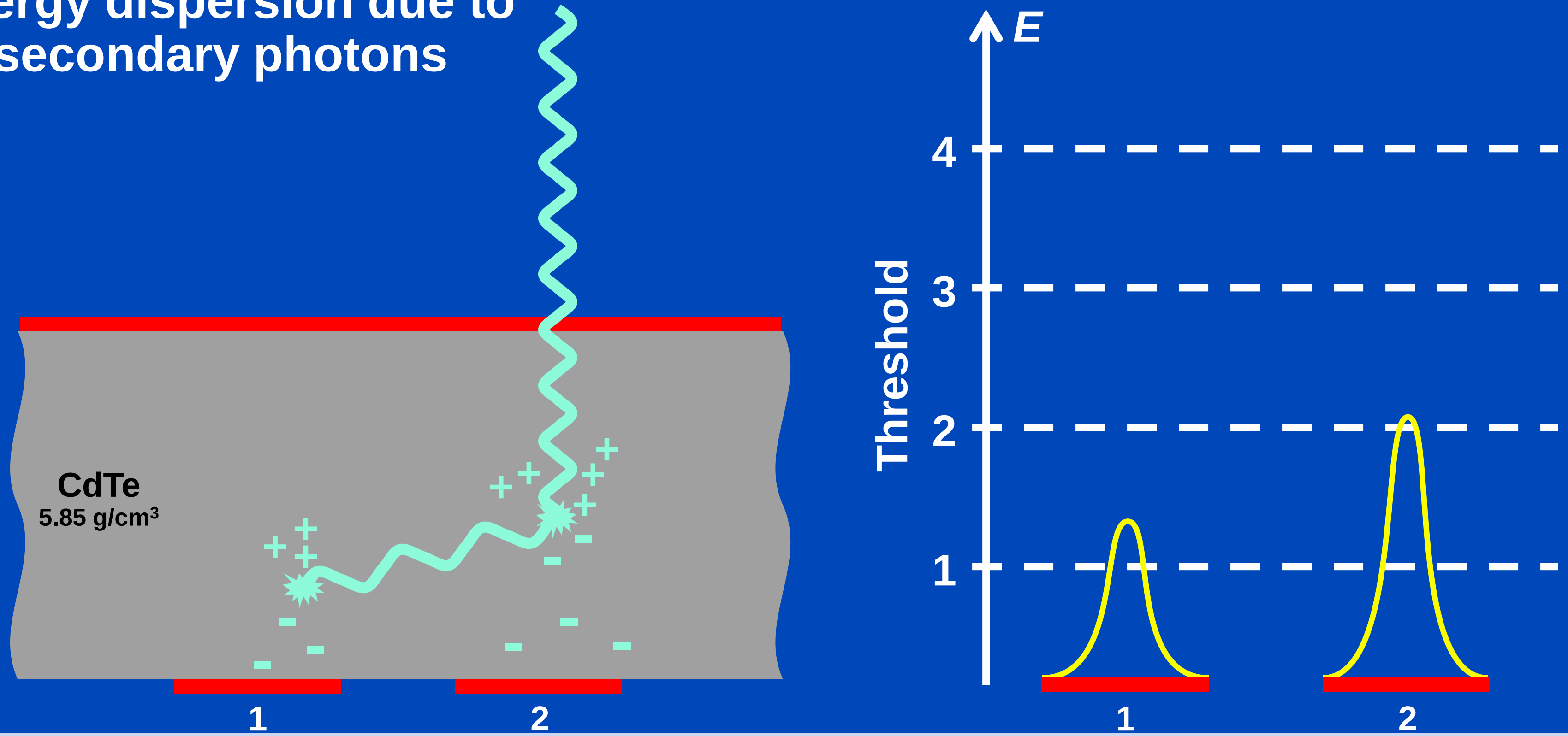

Photon Events

- Detection process in the sensor
- Photoelectric effect (e.g. 80 keV)

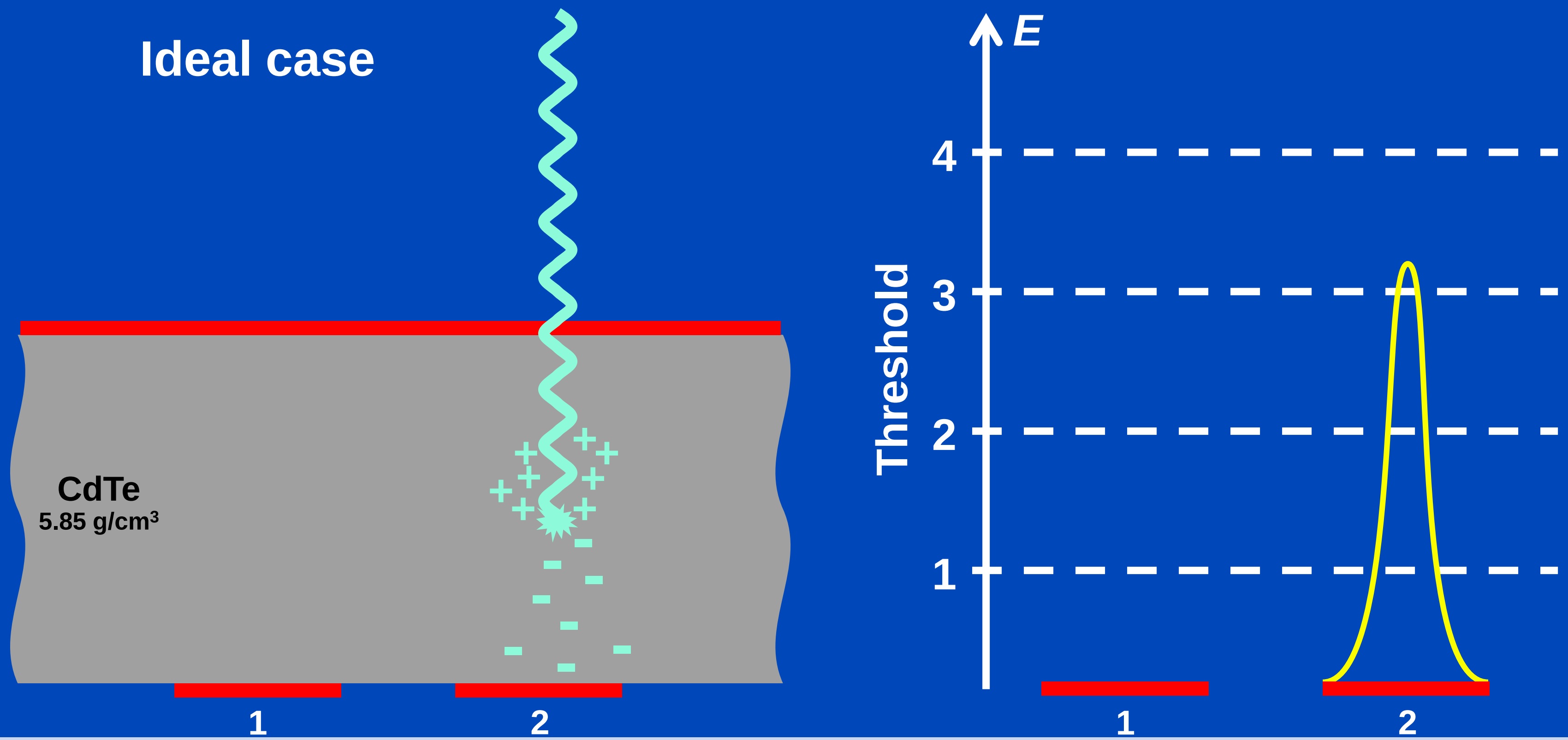

Photon Events

- Detection process in the sensor
- Photoelectric effect (e.g. 30 keV), charge sharing

Energy dispersion due to charge diffusion

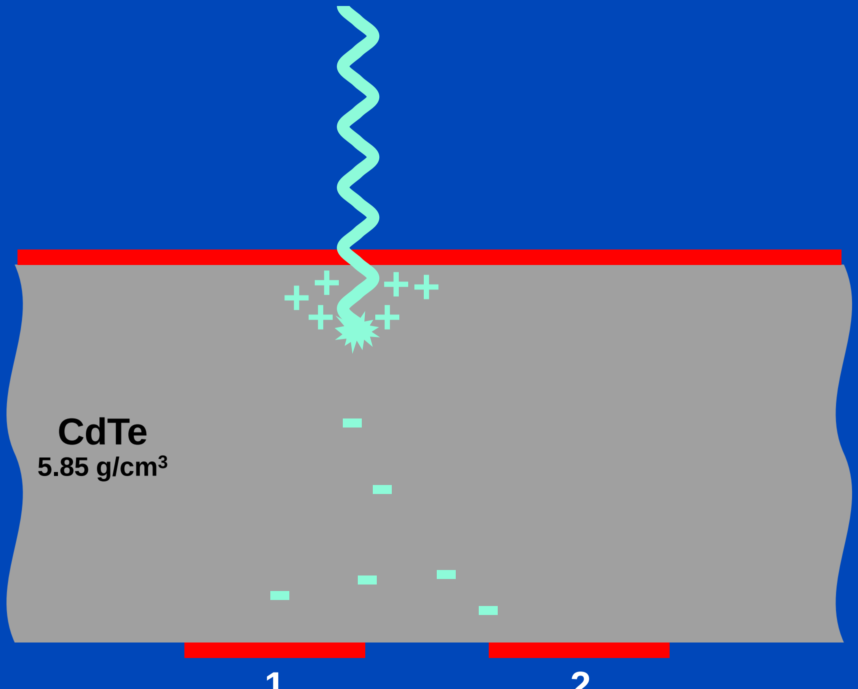

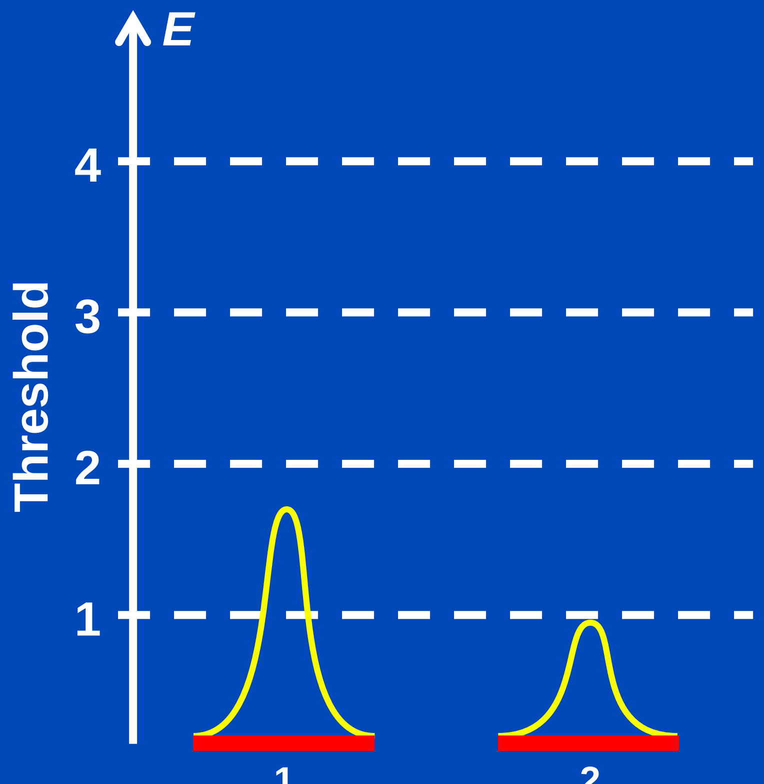

dkfz.


SIEMENS
SOMATOM CounT
@ dkfz.

Siemens CounT
Experimental PCCT System

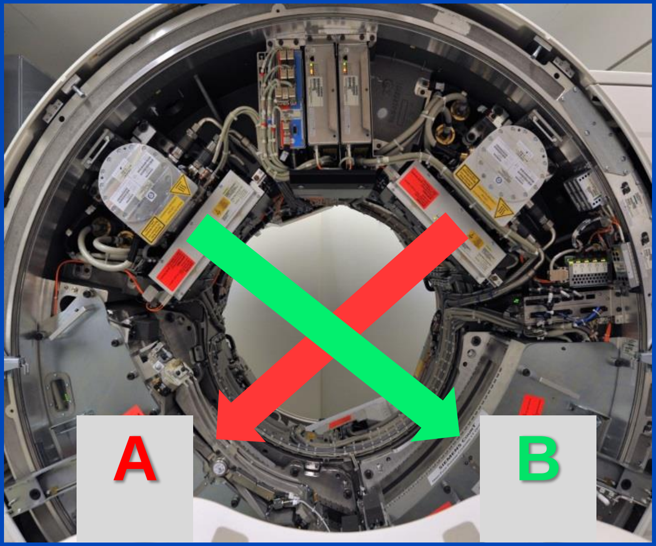

Gantry of a clinical dual source CT scanner

A: conventional CT detector (50.0 cm FOV)

B: Photon counting detector (27.5 cm FOV)

Readout Modes of the CounT

PC-UHR Mode	PC-Macro Mode	EI detector
0.25 mm pixel size	0.50 mm pixel size	0.60 mm pixel size

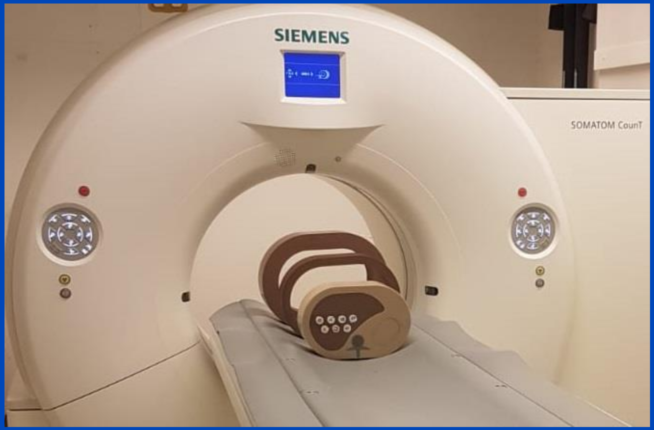

Experimental CT, not commercially available.

Siemens Naeotom Alpha
The World‘s First Photon-Counting CT
is a Dual Source PCCT

Detector Pixel Force vs. Alpha

Force
920 × 96 detector pixels
pixel size 0.52 × 0.56 mm at iso
avg. sampling 0.56 × 0.6 mm at iso
57.6 mm z-coverage

Alpha (Quantum Plus)
1376 × 144 macro pixels
pixel size 0.3 × 0.352 mm at iso
avg. sampling 0.344 × 0.4 mm at iso
57.6 mm z-coverage

Alpha (UHR)
2752 × 120 pixels
pixel size 0.15 × 0.176 mm at iso
avg. sampling 0.172 × 0.2 mm at iso
24 mm z-coverage

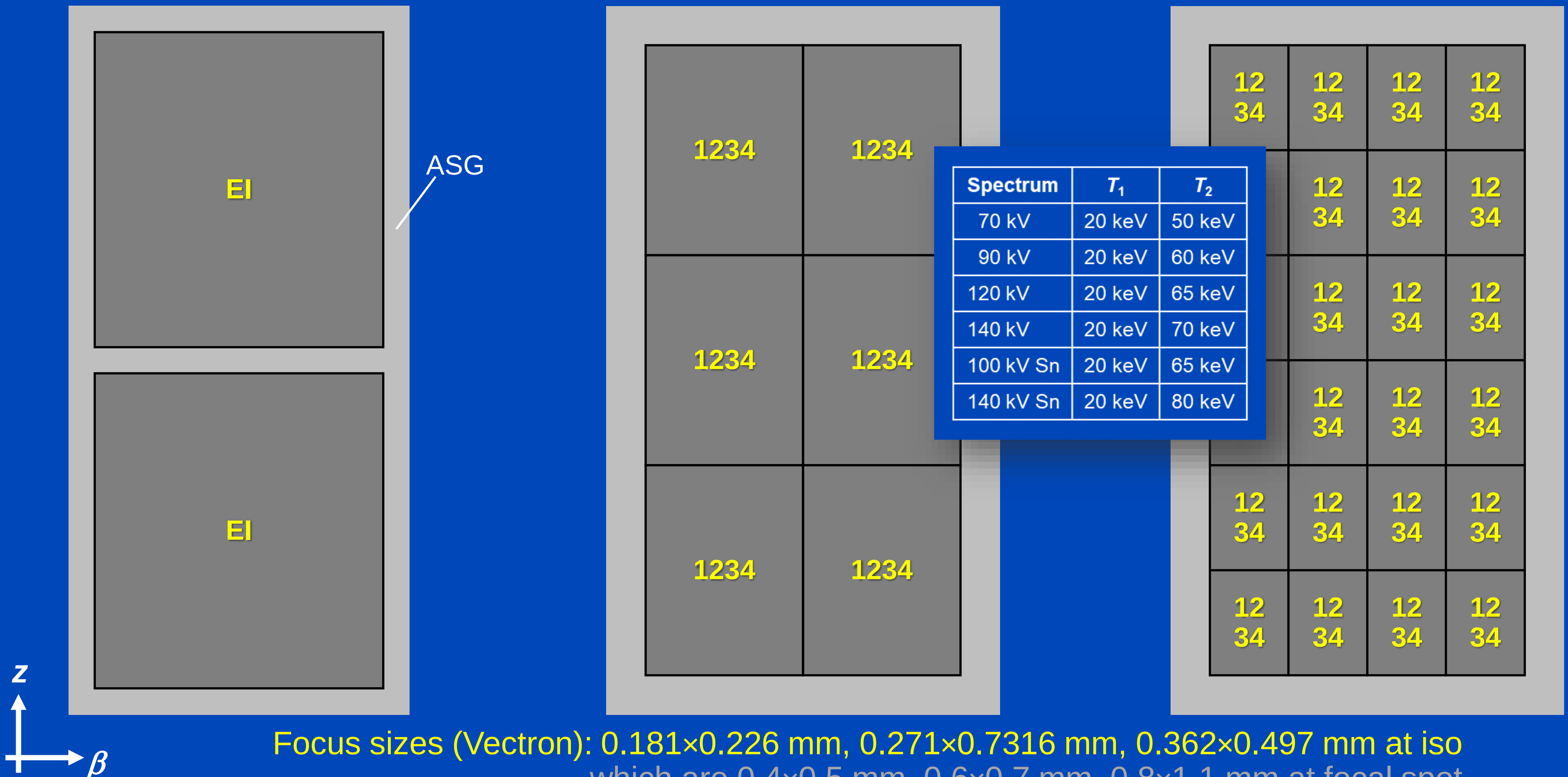

Spectrum	T_1	T_2
70 kV	20 keV	50 keV
90 kV	20 keV	60 keV
120 kV	20 keV	65 keV
140 kV	20 keV	70 keV
100 kV Sn	20 keV	65 keV
140 kV Sn	20 keV	80 keV

Focus sizes (Vectron): 0.181×0.226 mm, 0.271×0.7316 mm, 0.362×0.497 mm at iso
which are 0.4×0.5 mm, 0.6×0.7 mm, 0.8×1.1 mm at focal spot

ASG information taken from [J. Ferda et al. Computed tomography with a full FOV photon-counting detector in a clinical setting, the first experience. European Journal of Radiology 137:109614, 2021]

Evolution of Spatial Resolution

similar to
2005: Somatom Flash (B70)

similar to
2014: Somatom CounT (U70)

scanned at
2021: Naeotom Alpha (Br98u)

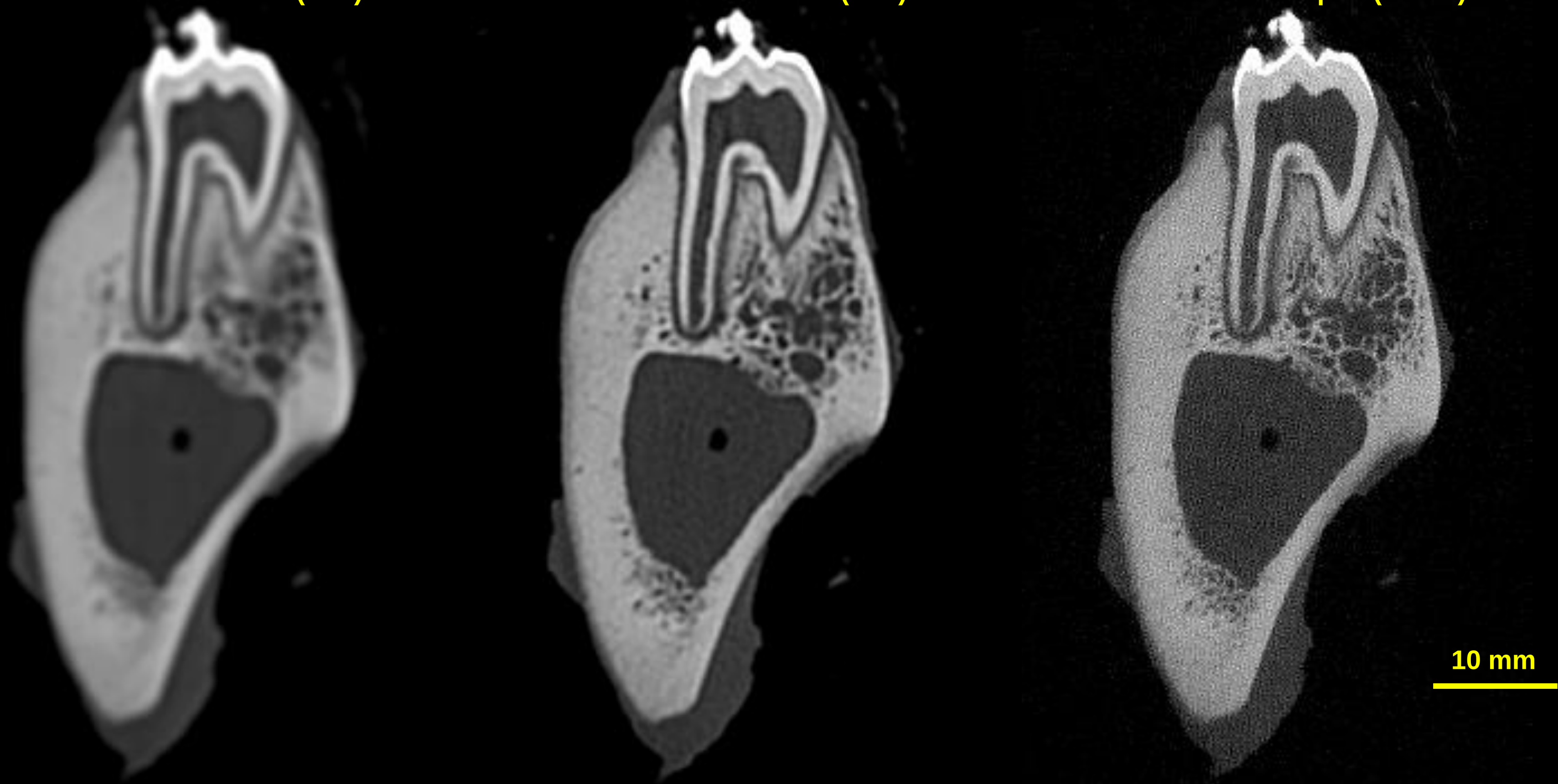

Pixel size 0.181 mm
Slice thickness 0.60 mm
Slice increment 0.30 mm
$MTF_{50\%}$ = 8.0 lp/cm
$MTF_{10\%}$ = 9.2 lp/cm

Pixel size 0.181 mm
Slice thickness 0.20 mm
Slice increment 0.10 mm
$MTF_{50\%}$ = 12.1 lp/cm
$MTF_{10\%}$ = 16.0 lp/cm

Pixel size 0.181 mm
Slice thickness 0.20 mm
Slice increment 0.10 mm
$MTF_{50\%}$ = 39.0 lp/cm
$MTF_{10\%}$ = 42.9 lp/cm

All measurements at Naeotom Alpha, Siemens Healthineers. QIR reconstructions such that the maximum spatial resolution of Flash, CounT and Alpha is demonstrated on the same sample. *C* = 1200 HU, *W* = 4000 HU

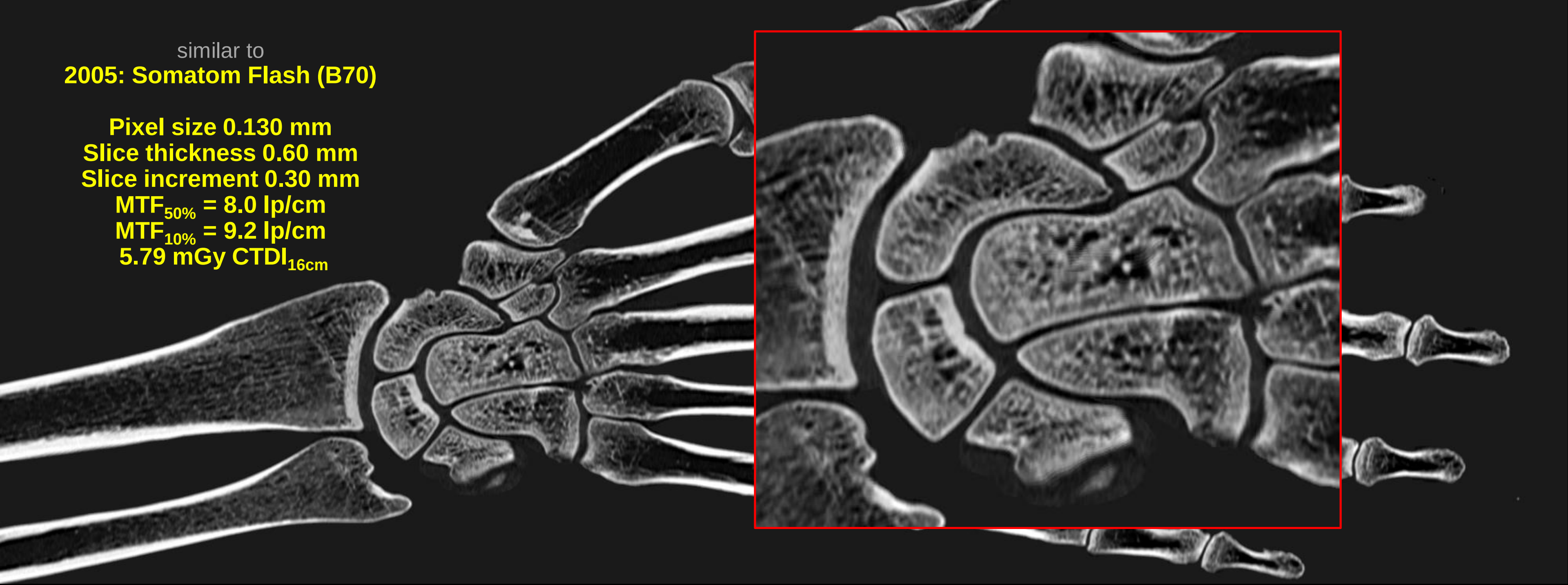
similar to
2005: Somatom Flash (B70)
Pixel size 0.130 mm
Slice thickness 0.60 mm
Slice increment 0.30 mm
$MTF_{50\%}$ = 8.0 lp/cm
$MTF_{10\%}$ = 9.2 lp/cm
5.79 mGy $CTDI_{16cm}$

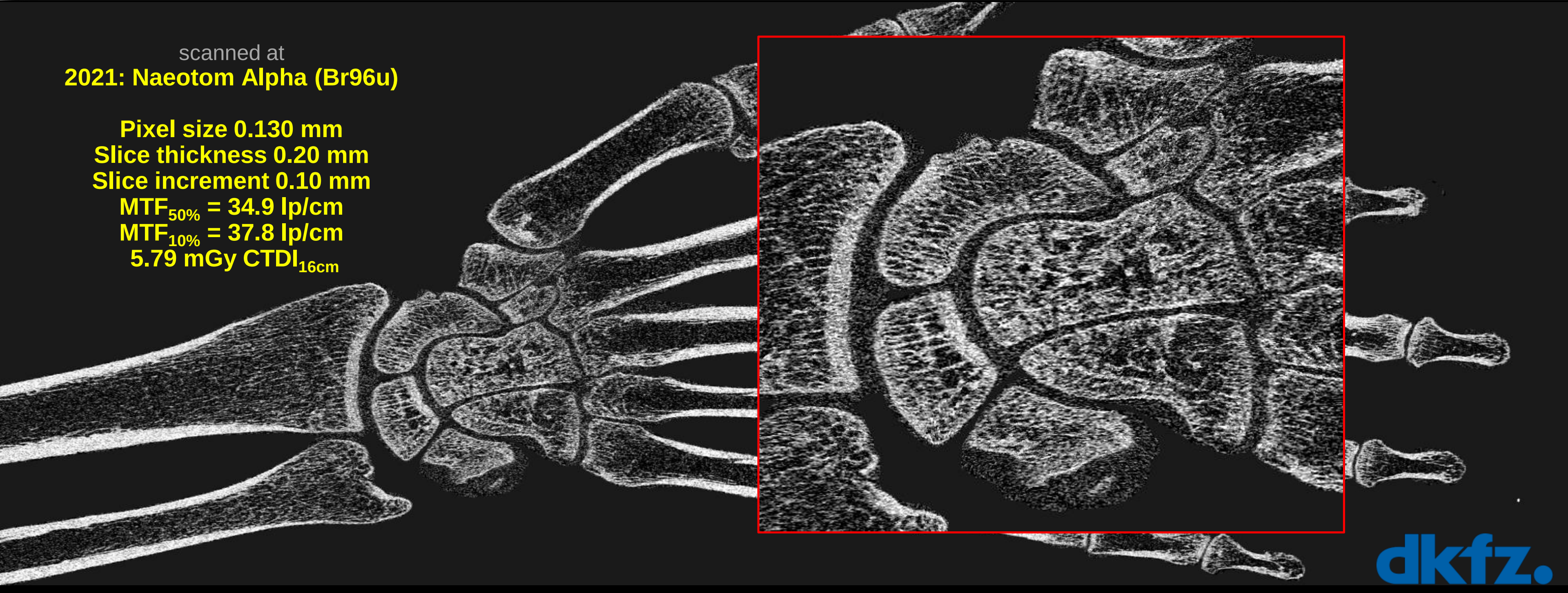
scanned at
2021: Naeotom Alpha (Br96u)
Pixel size 0.130 mm
Slice thickness 0.20 mm
Slice increment 0.10 mm
$MTF_{50\%}$ = 34.9 lp/cm
$MTF_{10\%}$ = 37.8 lp/cm
5.79 mGy $CTDI_{16cm}$
dkfz.

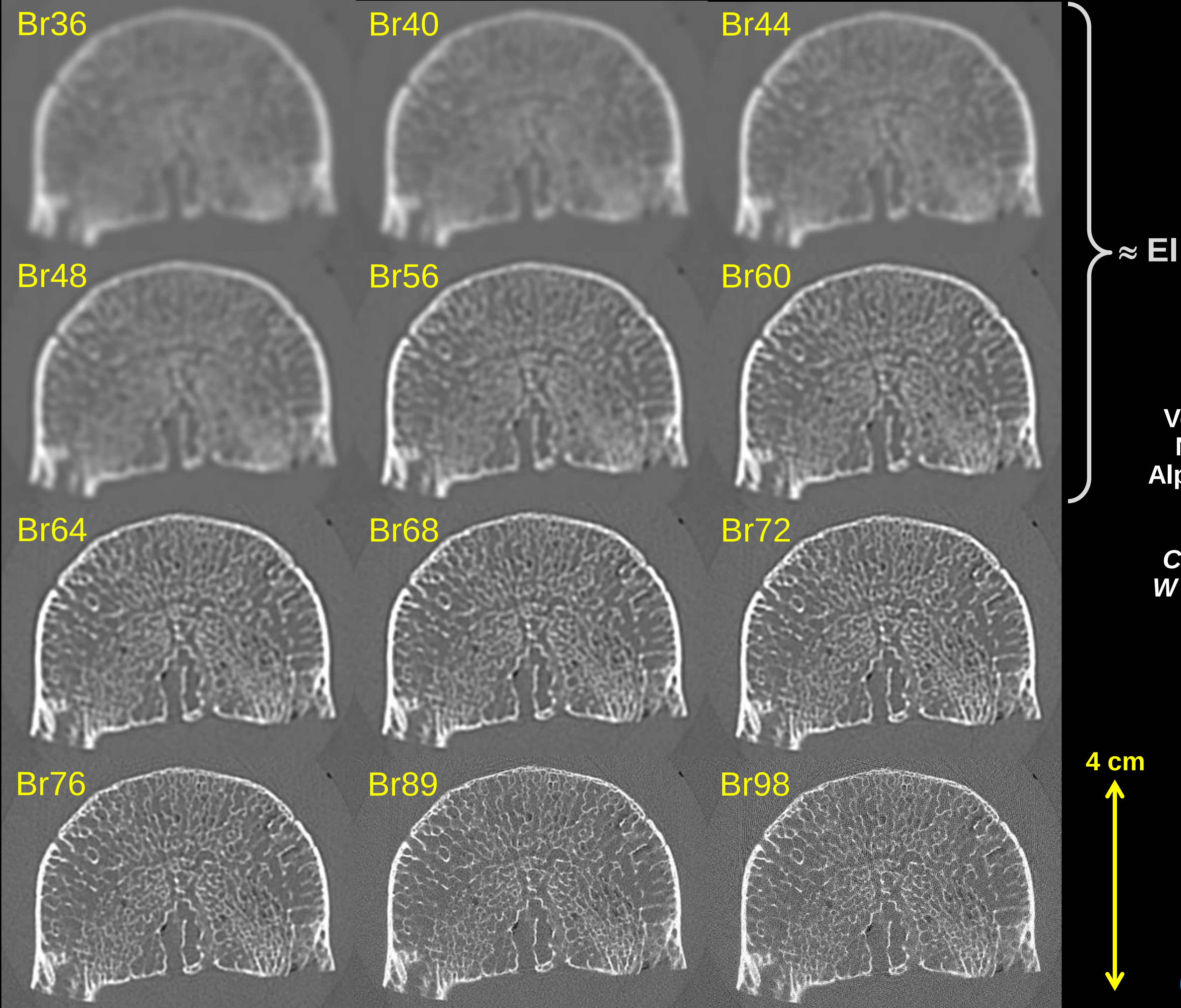

Vertebra at Naeotom Alpha in UHR mode.

***C* = 500 HU**
***W* = 3000 HU**

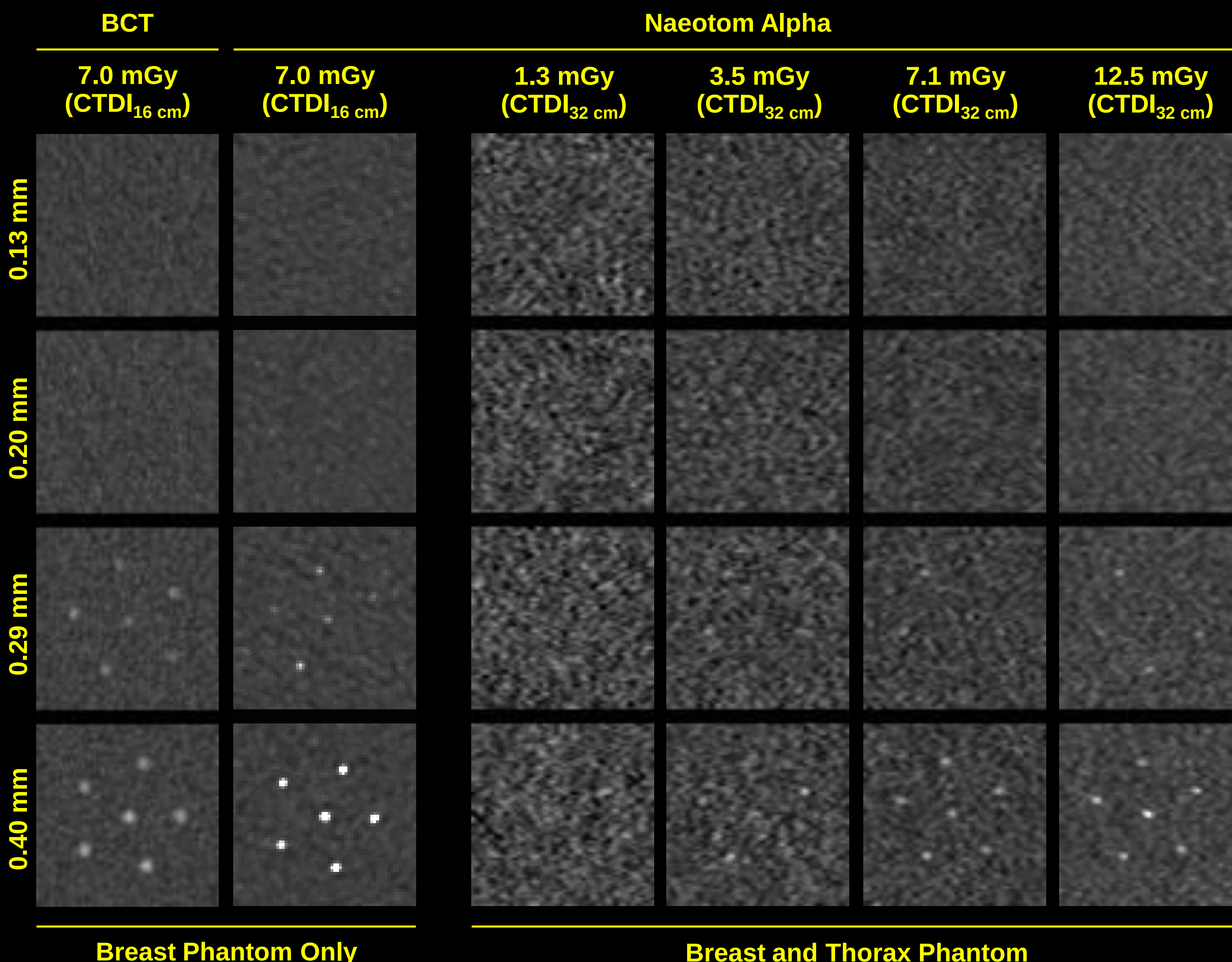

$CTDI_{16\ cm} \approx 2.1\ CTDI_{32\ cm}$

0.6 mm MIP, *C* = 300 HU, *W* = 1500 HU

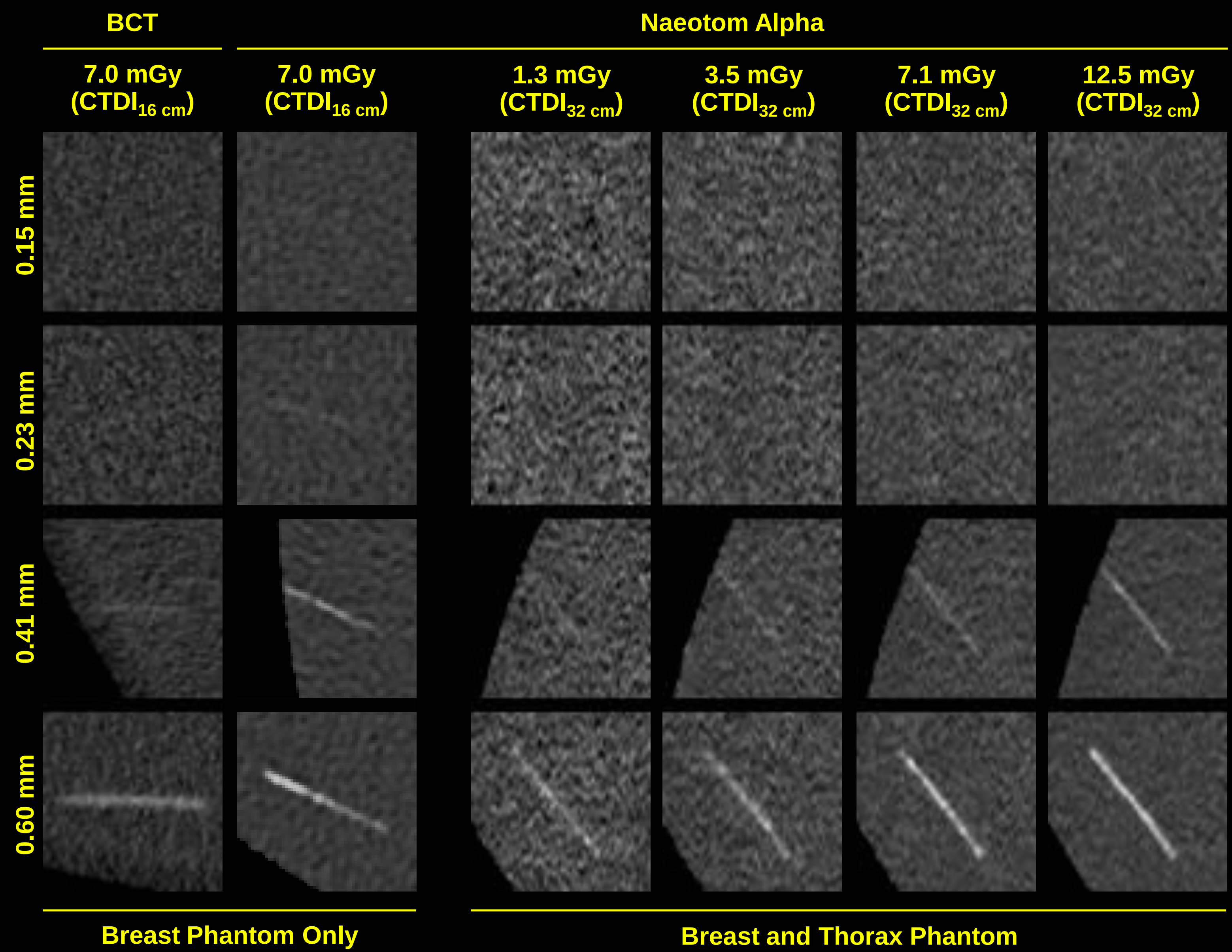

$CTDI_{16\ cm} \approx 2.1\ CTDI_{32\ cm}$

0.6 mm MIP, *C* = 300 HU, *W* = 1500 HU

dkfz.

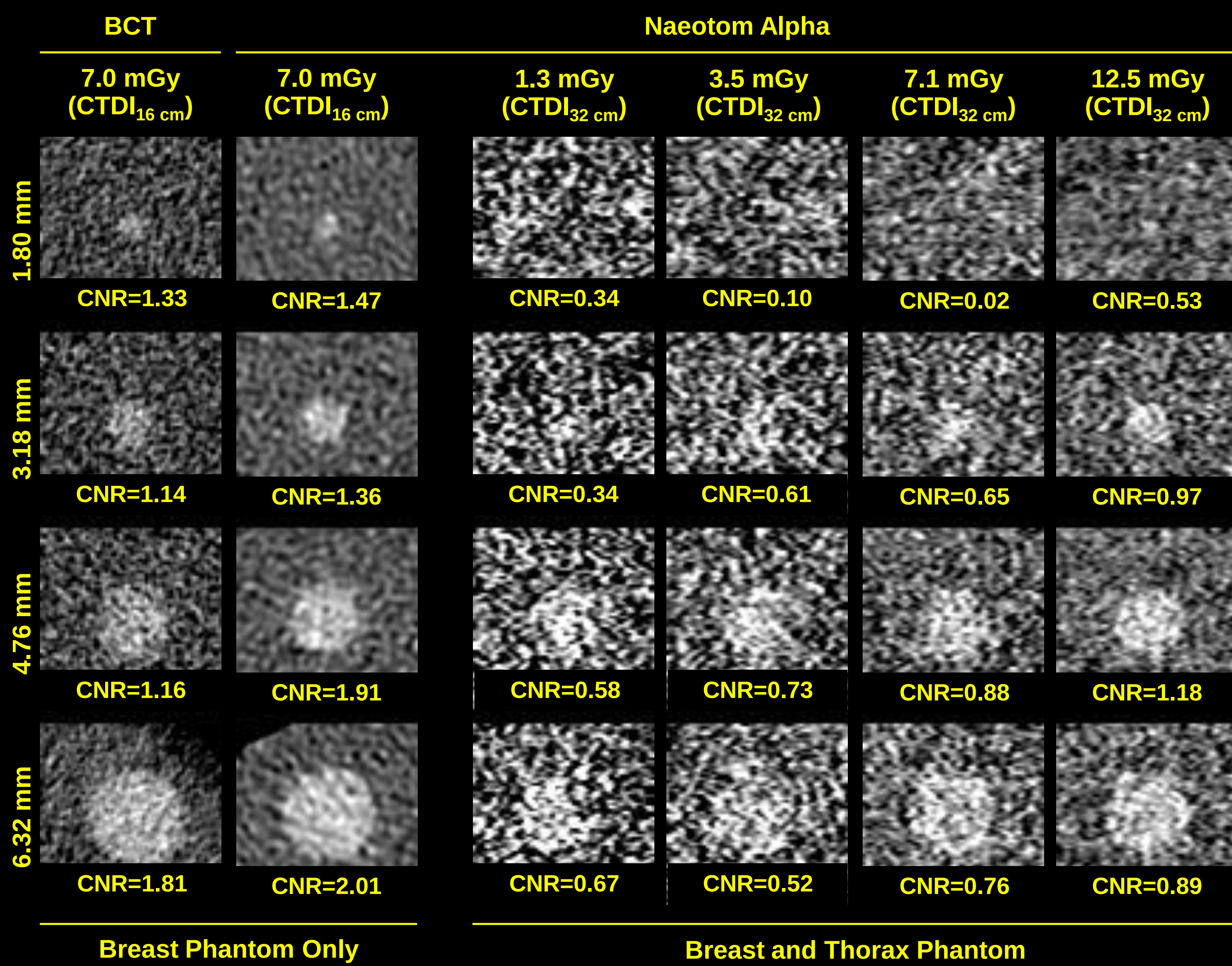

$CTDI_{16\ cm} \approx 2.1\ CTDI_{32\ cm}$

C = -50 HU, *W* = 400 HU

Advantages of Photon Counting CT

- No reflective gaps between detector pixels
  - Higher geometrical efficiency
  - Less dose
- No electronic noise
  - Less dose for infants
  - Less noise for obese patients
- Counting
  - Swank factor = 1 = maximal
  - “Iodine effect“ due to higher weights on low energies
- Energy bin weighting
  - Lower dose/noise
  - Improved iodine CNR
- Smaller pixels (to avoid pileup)
  - Higher spatial resolution
  - “Small pixel effect” i.e. lower dose/noise at conventional resolution
- Spectral information on demand
  - Dual Energy CT (DECT)
  - Multi Energy CT (MECT)

Dark Image of Photon Counter Shows Background Radiation

18 frames, 5 min integration time per frame

Energy Integrating (Dexela) | Photon Counting (Dectris Santis)

Events per Frame

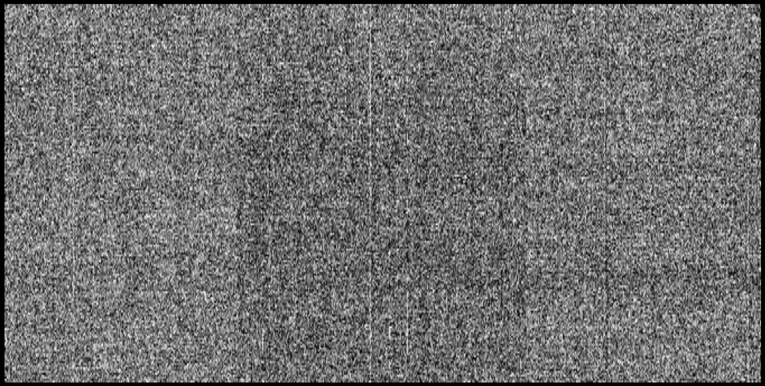

C/W = 0 a.u./70 a.u.

C/W = 1 cnts/2 cnts

Accumulated Signal

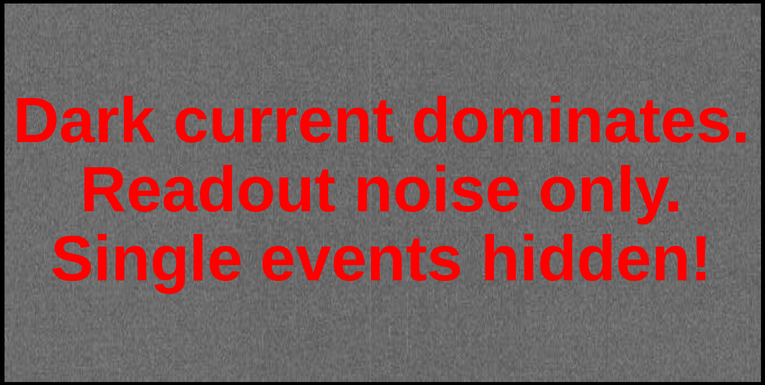

C/W = 30 a.u./450 a.u.

No dark current.
No readout noise.
Single events visible!

C/W = 3 cnts/8 cnts

Energy Integrating
(Detected Spectra at 100 kV and 140 kV)

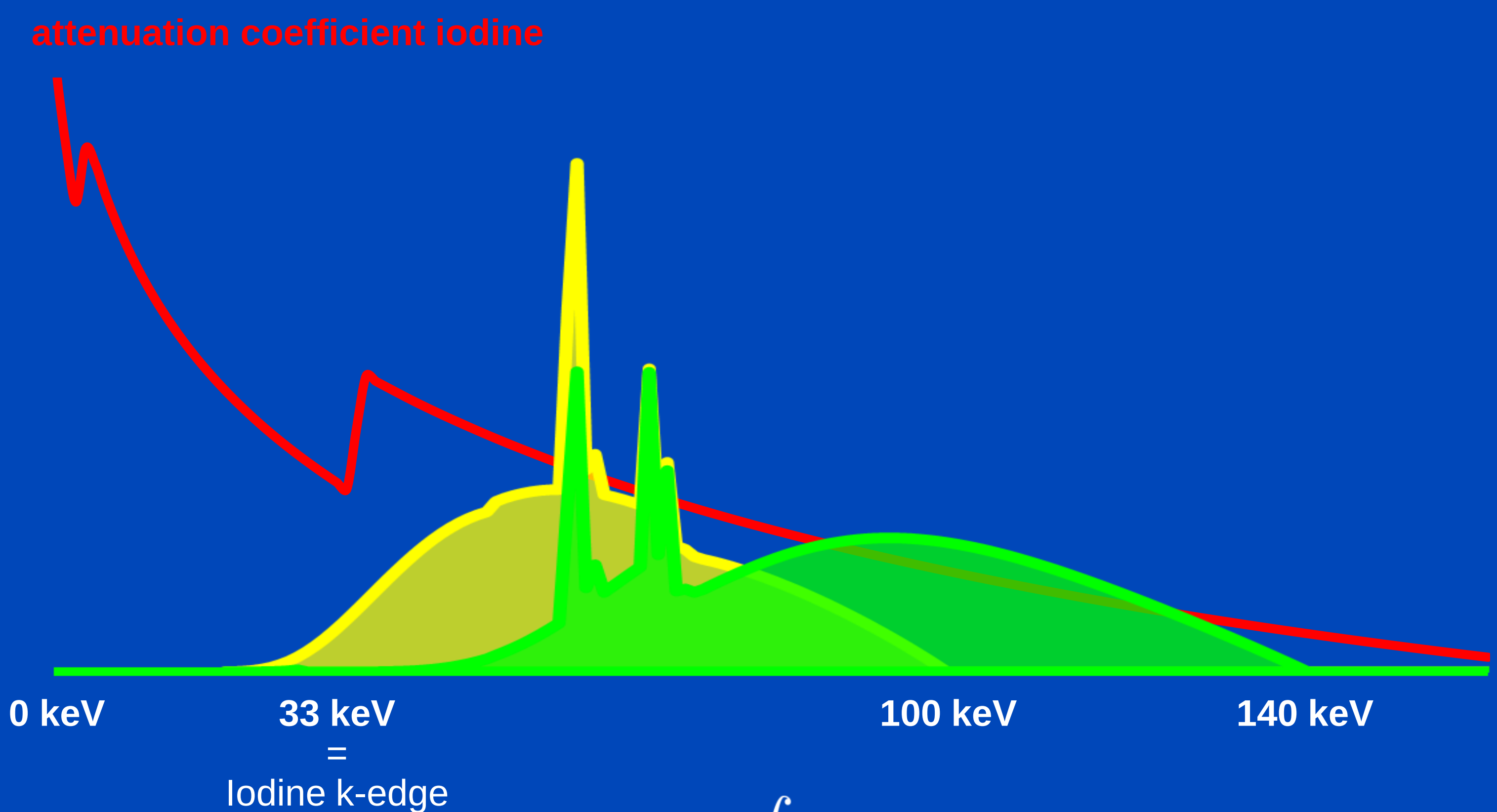

$$\mathrm{Signal}_{\mathrm{EI}} = \int dE\, E\; N(E)$$

100 kV and 140 kV EI spectra as seen after having passed 32 cm of water.

Photon Counting
(Detected Spectra at 100 kV and 140 kV)

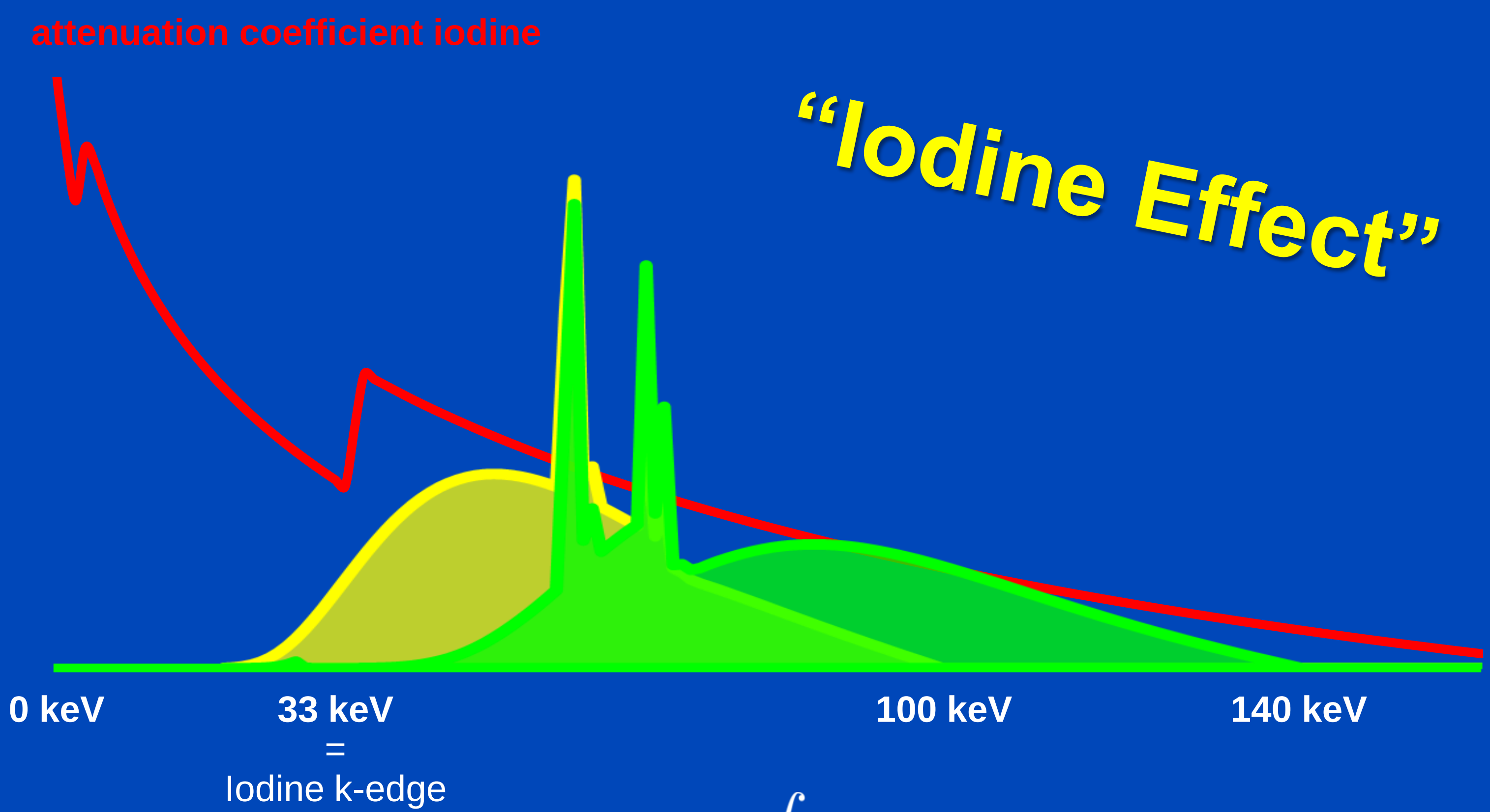

$$\mathrm{Signal}_{\mathrm{PC}} = \int dE\, 1\ N(E)$$

100 kV and 140 kV PC spectra (one bin) as seen after having passed 32 cm of water.

Expected Value and Variance

- **Transmitted number of photons *N*:**

$$N(E) = N_0(E)e^{-p\psi(E)}$$

- **Poisson distribution:** $\mathrm{E}N(E) = \mathrm{Var}N(E)$
- **Detected signal *S* with sensitivity *s*(*E*):**

$$S = \int dE\, s(E)N(E)$$

- **Expected value and variance of the signal *S*:**

$$\mathrm{E}S = \int dE\, s(E)\mathrm{E}N(E) \text{ and } \mathrm{Var}S = \int dE\, s^2(E)\mathrm{E}N(E)$$

- **Detector sensitivity: PC** $s(E) = 1$**, but EI** $s(E) \propto E$ **!**

Optimal Swank Factor?

- What is the sensitivity $s(E)$ that maximizes

$$\mathrm{SNR} = \frac{\mathrm{E}S}{\sqrt{\mathrm{Var}S}} \text{ ?}$$

- Formulate this as minimizing Var S for E S given:

$$\int dE \Big(s^2(E) + \lambda s(E)\Big)\, \mathrm{E}I(E)$$

- Variational calculus shows that the minimum occurs at $2\,s(E) + \lambda = 0$ which implies

$$s(E) = const.$$

- Thus, the optimal Swank factor can be achieved with a detector of constant sensitivity, e.g. with a PC detector.

Swank Factor

- The Swank factor measures the relative SNR^2, and thus the relative dose efficiency between photon counting (PC) and energy integrating (EI).
- PC always has the highest SNR.

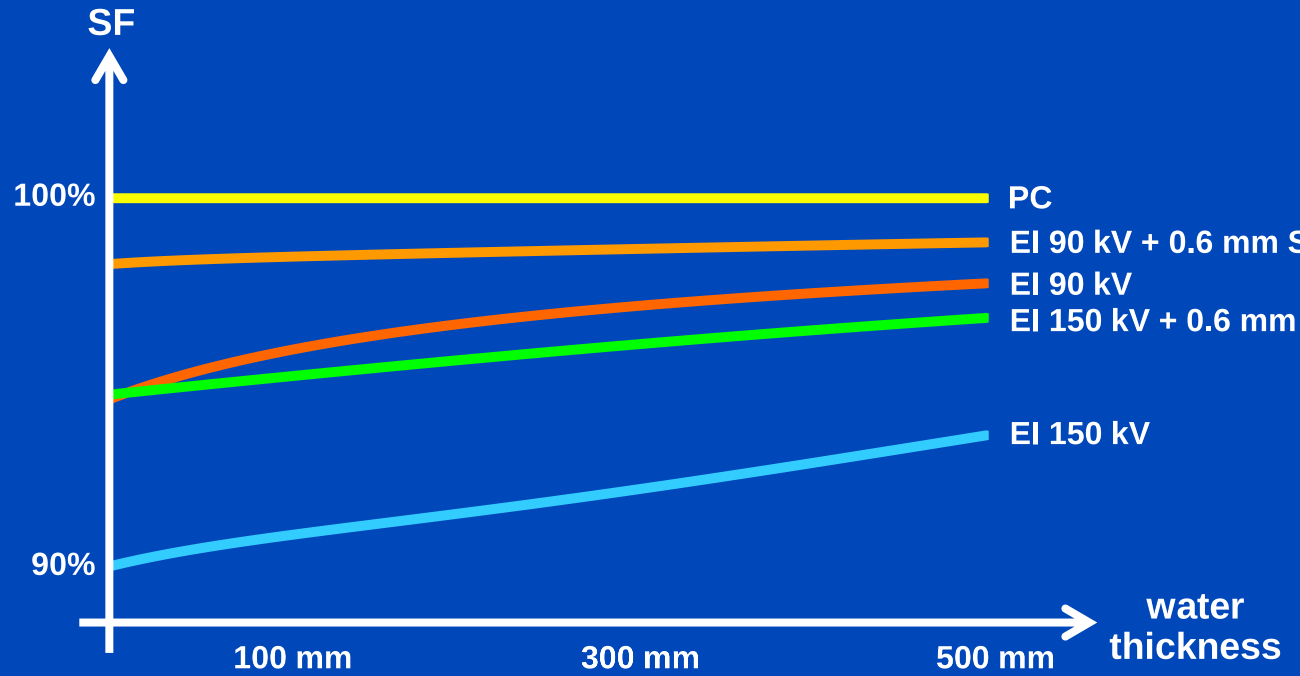

$$\mathrm{SF} = \frac{\mathrm{SNR}_{\mathrm{EI}}^2}{\mathrm{SNR}_{\mathrm{PC}}^2} = \frac{\left(\int dE\, E N(E)\right)^2}{\left(\int dE\, N(E)\right)\left(\int dE\, E^2 N(E)\right)} \leq 1$$

due to Schwarz‘ inequality

Photon Counting used to Maximize CNR

- With PC, energy bin sinograms can be weighted individually, i.e. by a weighted summation.
- To optimize the CNR the optimal bin weighting factor w_b is given by (weighting after log):

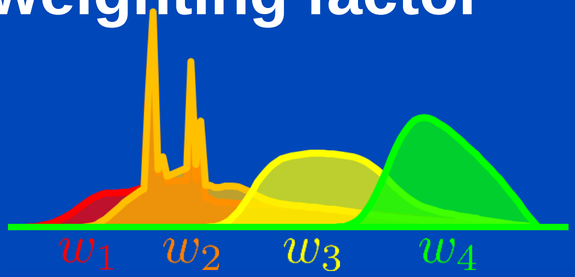

$$w_b \propto \frac{C_b}{V_b}$$

- The resulting CNR is

$$\mathrm{CNR}^2 = \frac{\left(\sum_b w_b C_b\right)^2}{\sum_b w_b^2 V_b}$$

- At the optimum this evaluates to

$$\mathrm{CNR}^2 = \sum_{b=1}^{B} \mathrm{CNR}_b^2$$

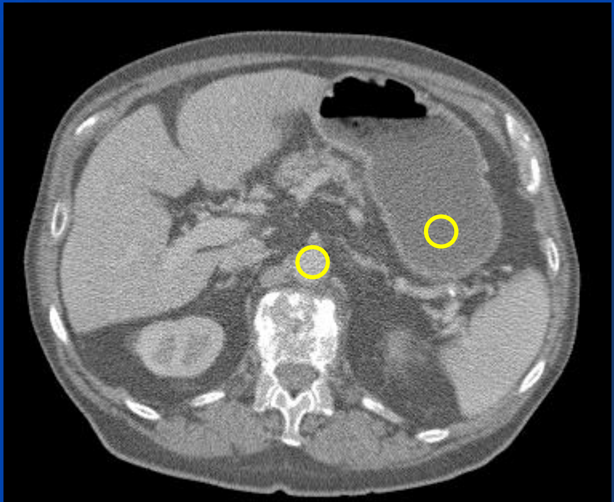

The two ROIs are used to measure the CNR.

Faby, Kachelrieß et al., MedPhys 42(7):4349-4366, July 2015.

dkfz.

Energy Integrating vs. Photon Counting
with 1 bin from 20 to 140 keV

Energy Integrating

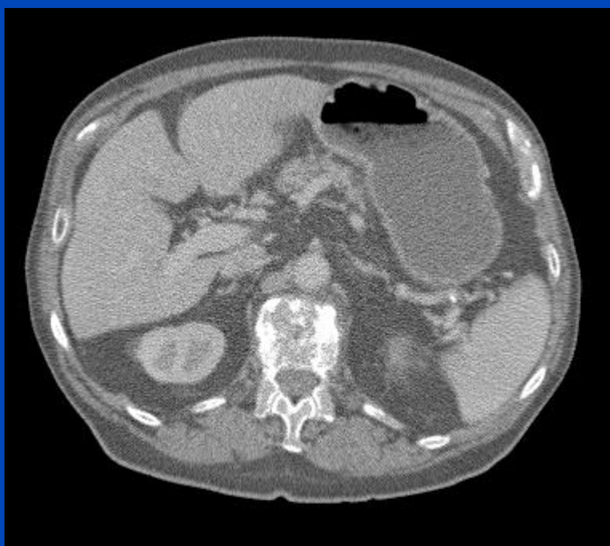

CNR = 2.11

PC minus EI

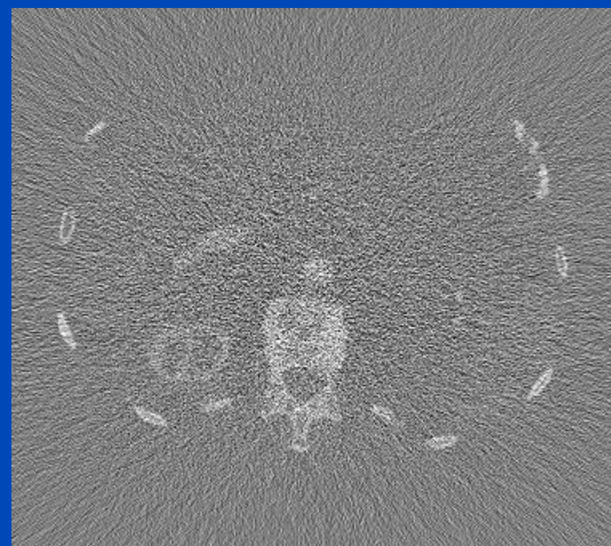

Photon Counting

CNR = 2.95

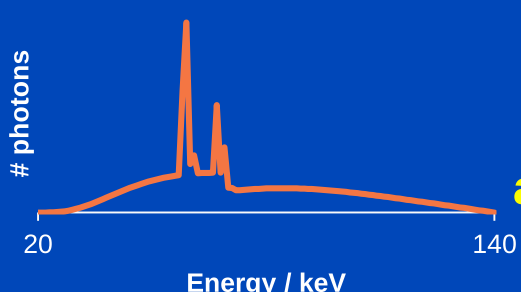

40% CNR improvement or 49% dose reduction achievable due to improved Swank factor and more weight on low energies (iodine contrast benefits).

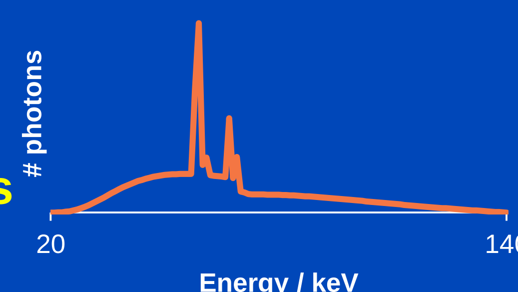

Faby, Kachelrieß et al., MedPhys 42(7):4349-4366, July 2015.
Images: *C* = 0 HU, *W* = 700 HU. Difference image: *C* = 0 HU, *W* = 350 HU. Bins start at 20 keV.

Energy Integrating vs. Photon Counting
with 4 bins from 20 to 140 keV

Energy Integrating

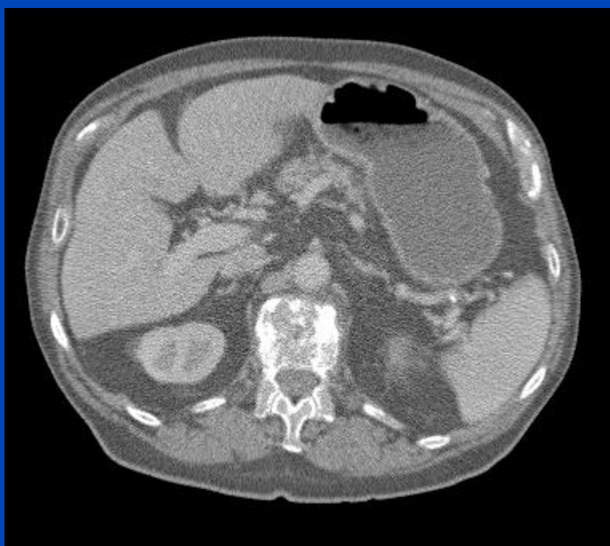

CNR = 2.11

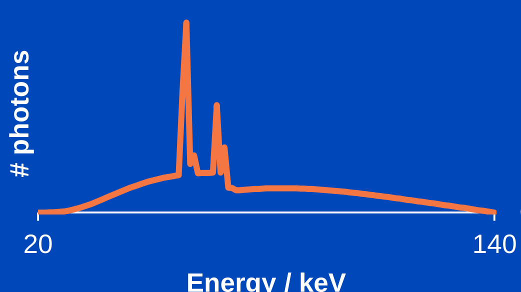

PC minus EI

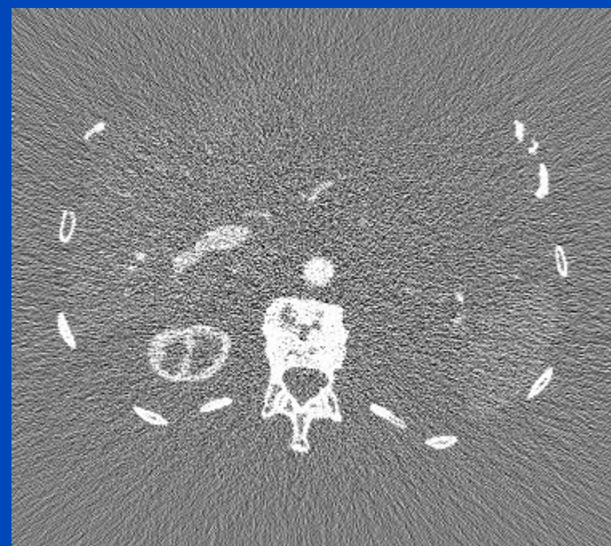

99% CNR improvement or 75% dose reduction achievable due to improved Swank factor and optimized energy weighting.

Photon Counting

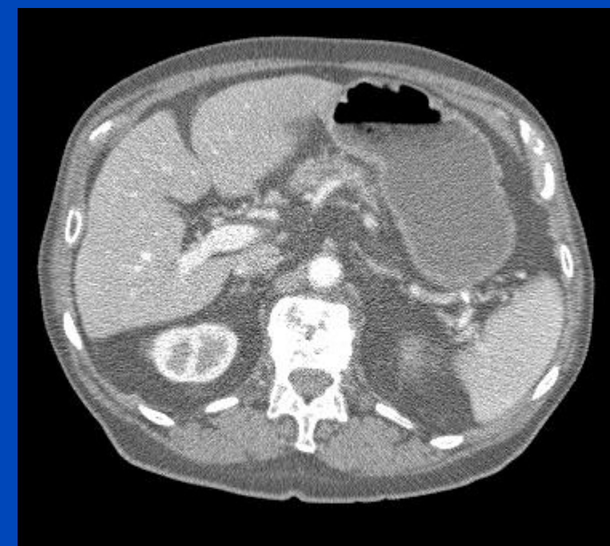

CNR = 4.19

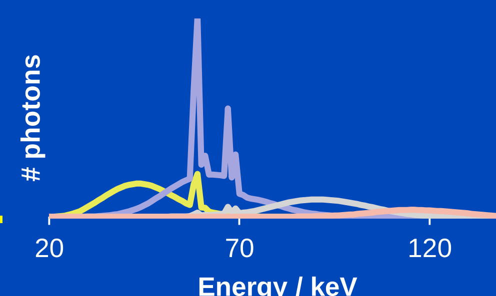

Faby, Kachelrieß et al., MedPhys 42(7):4349-4366, July 2015.
Images: *C* = 0 HU, *W* = 700 HU. Difference image: *C* = 0 HU, *W* = 350 HU. Bins start at 20 keV.

Iodine CNRD Assessment

- Images are acquired at different tube voltages:
  - 80 kV at 4.40 mGy ($CTDI_{vol\ 32\ cm}$) using 200 mAs_{eff}
  - 100 kV at 9.20 mGy ($CTDI_{vol\ 32\ cm}$) using 200 mAs_{eff}
  - 120 kV at 15.03 mGy ($CTDI_{vol\ 32\ cm}$) using 200 mAs_{eff}
  - 140 kV at 21.76 mGy ($CTDI_{vol\ 32\ cm}$) using 200 mAs_{eff}
- Pitch in all acquisitions was 0.6.
- Collimation for EI (32×0.6 mm) and PC (32×0.5 mm) was matched as close as possible, i.e. geometric efficiency is 80% vs. 82%
- Reconstruction is performed with matched spatial resolution using a D40f kernel onto a grid with a voxel spacing of 0.54 mm and a slice thickness of 1.2 mm.
- The thresholds were fixed at 20 keV and 50 keV, resulting in two bins: [20 keV, 50 keV] and [50 keV, *eU*].

Iodine CNRD Assessment

Reconstruction Examples @ 80 kV

Small (200 × 300 mm)

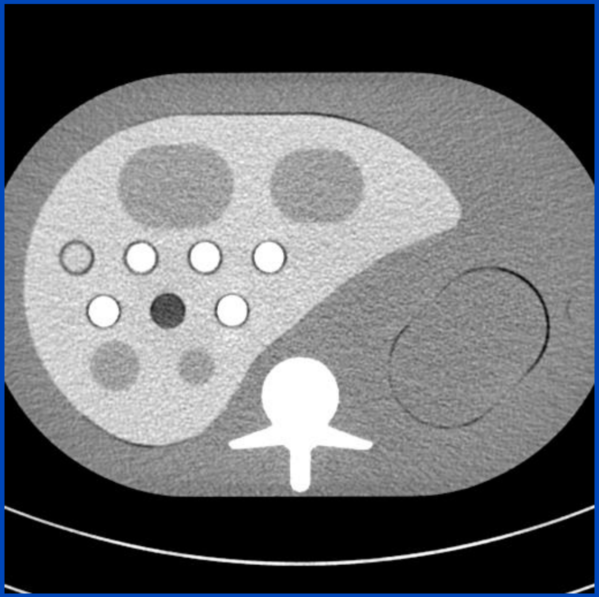

Medium (250 × 350 mm)

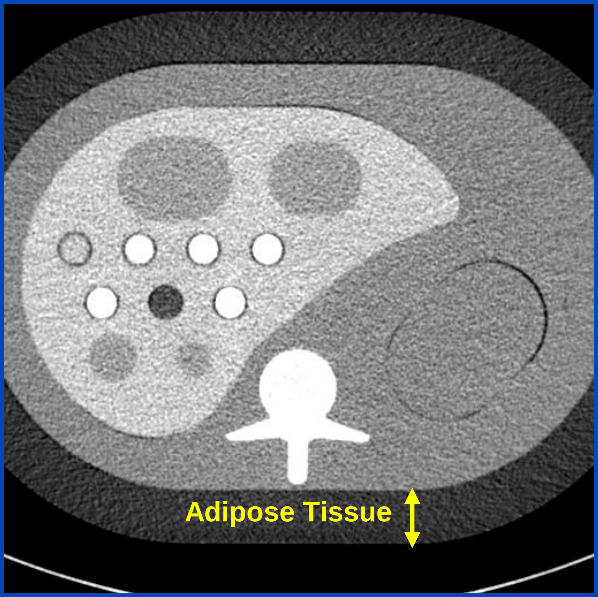

Large (300 × 400 mm)

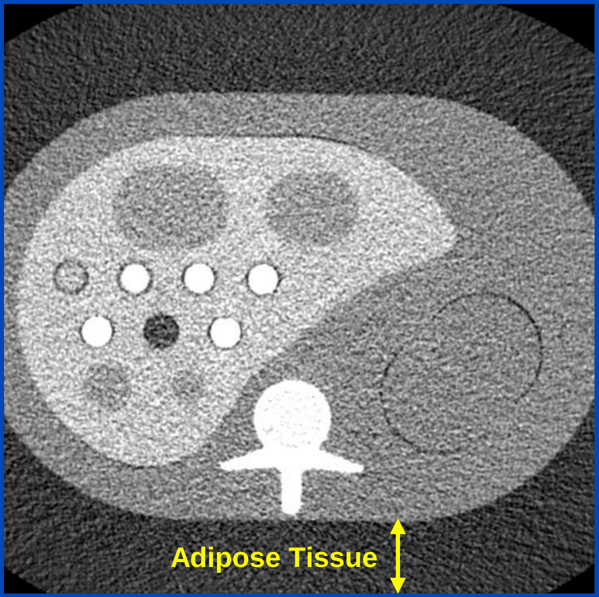

C = 0 HU, *W* = 400 HU

Iodine CNRD Assessment

Regions of Interest

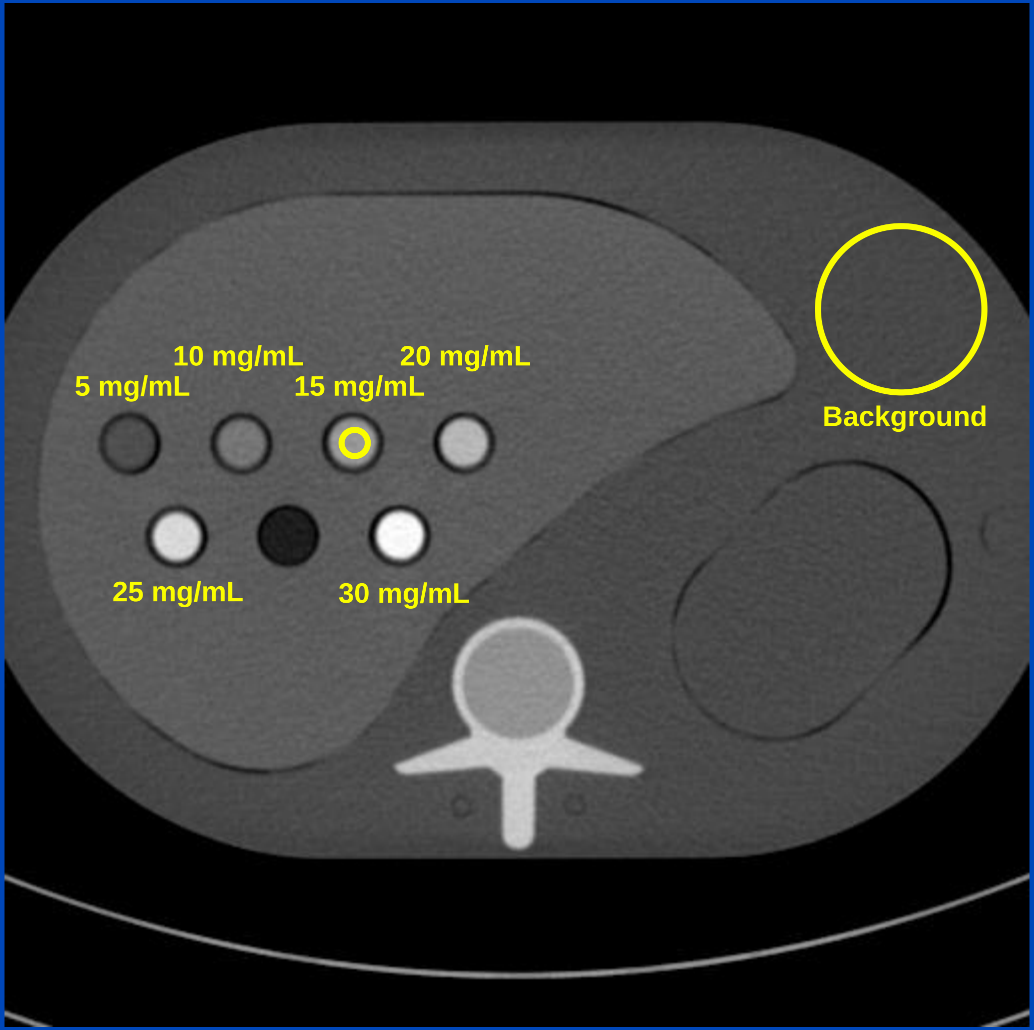

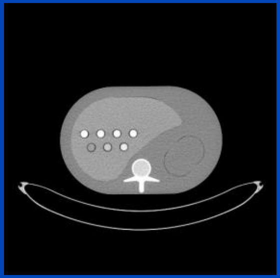

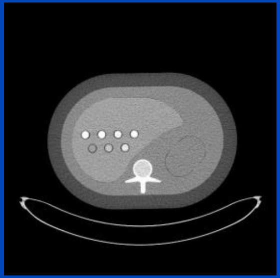

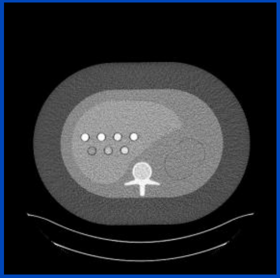

C = 180 HU, W = 600 HU

PC with 1 Bin vs. EI

Potential Dose Reduction

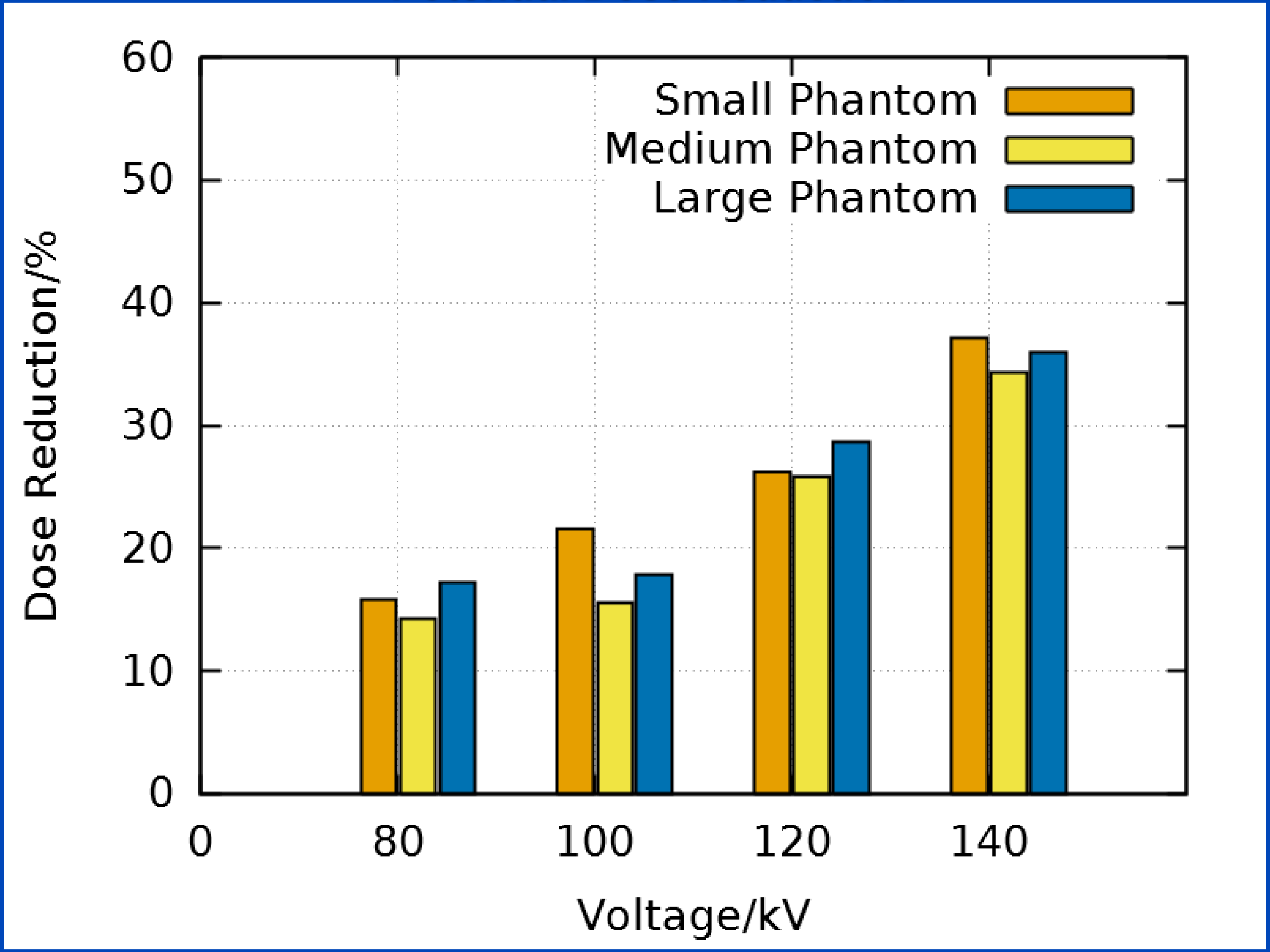

PC with 2 Bins vs. EI

Potential Dose Reduction

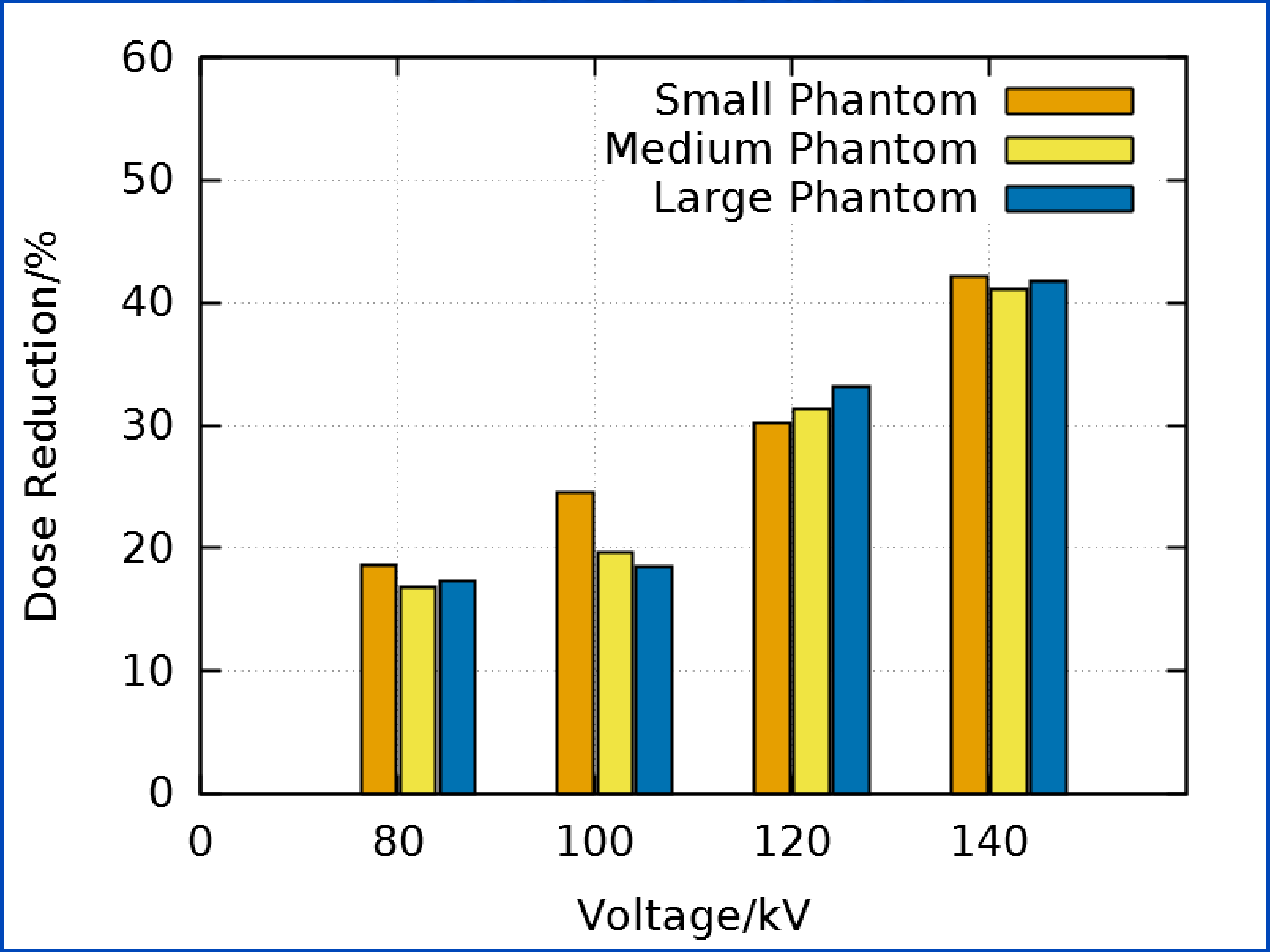

Pulse Pile-Up: Low Flux Rate

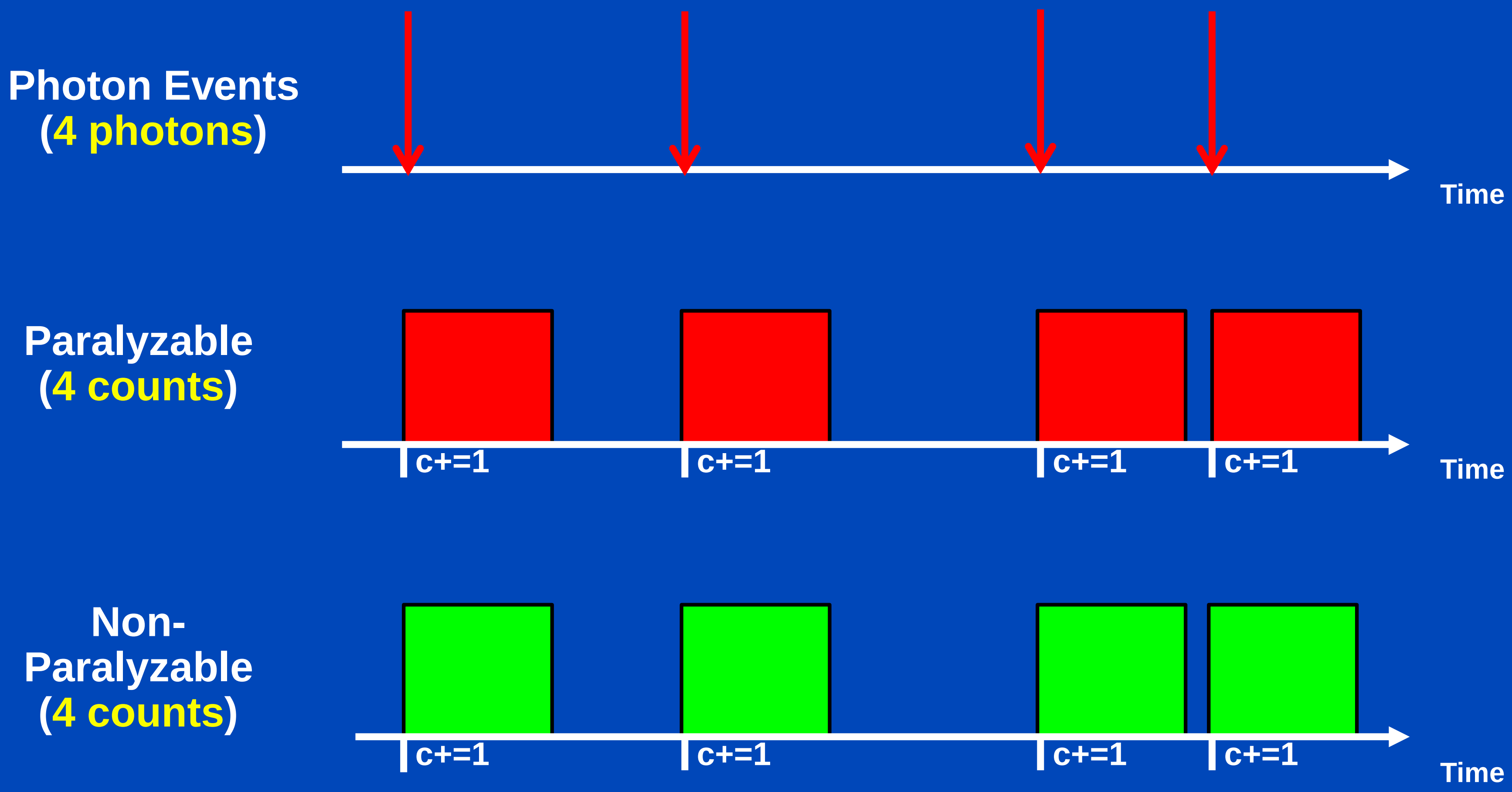

Boxes illustrate deadtime

Pulse Pile-Up: Medium Flux Rate

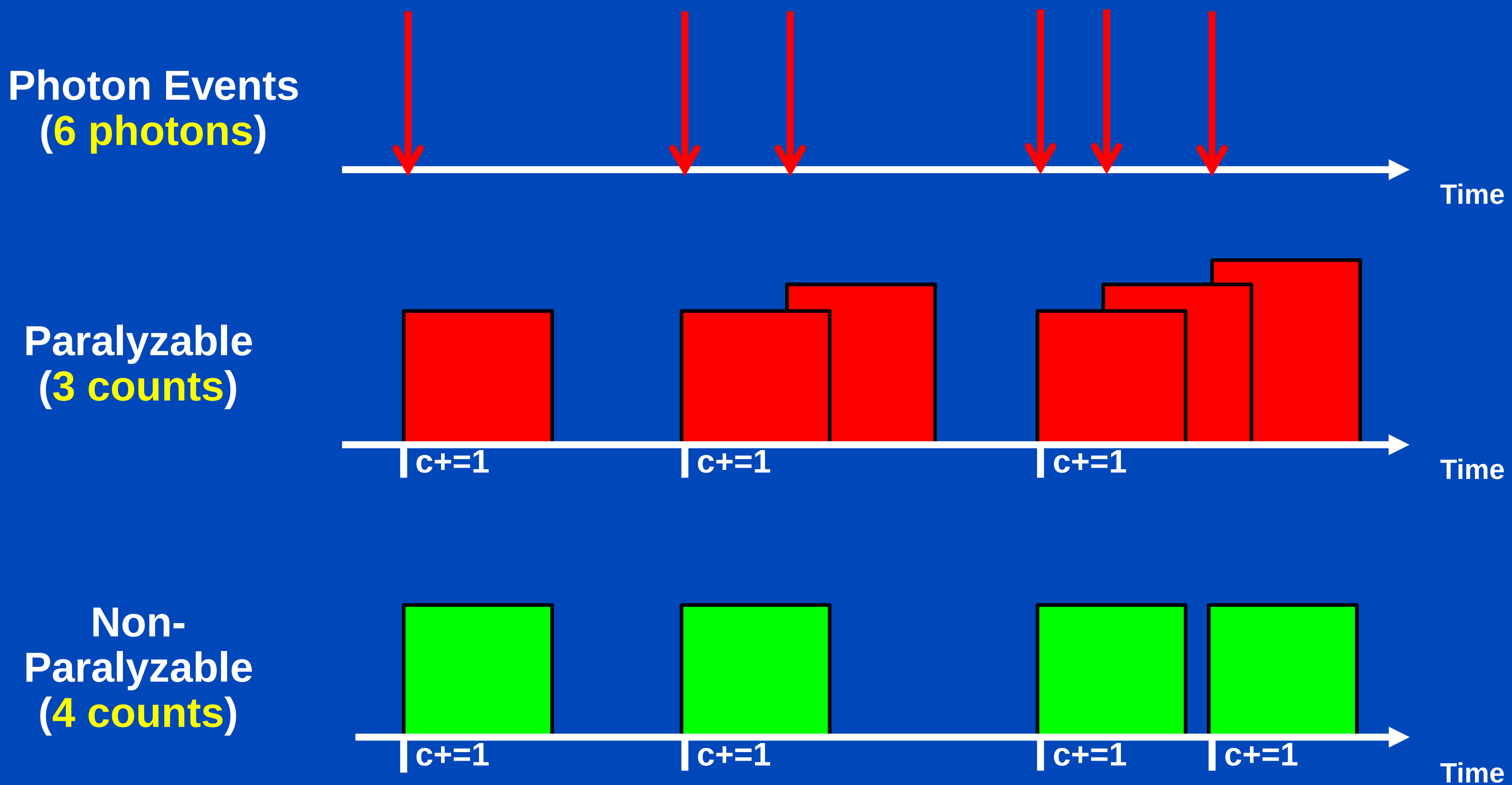

Boxes illustrate deadtime

Pulse Pile-Up: High Flux Rate

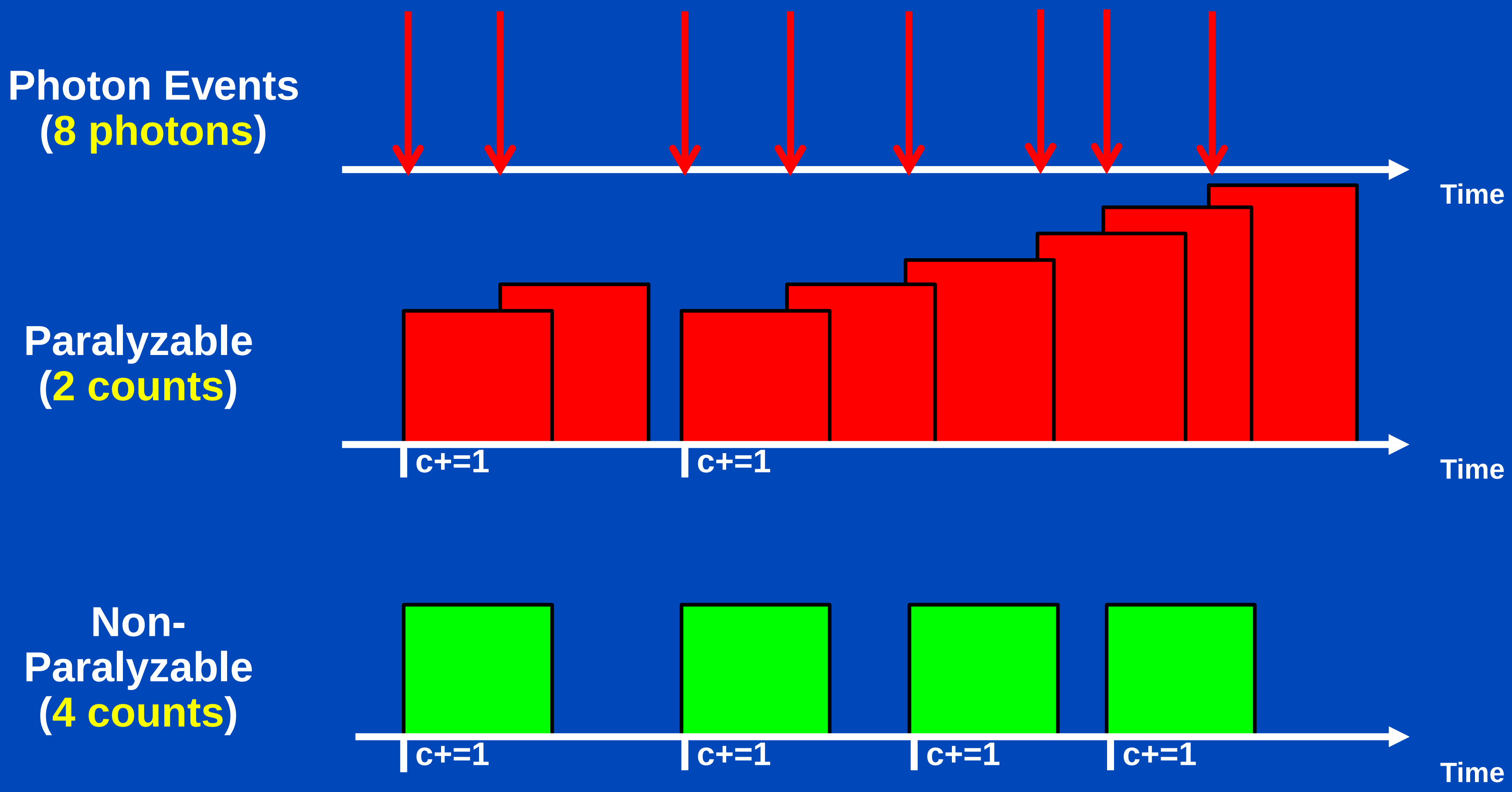

Boxes illustrate deadtime

Pulse Pile-Up: Recorded Counts

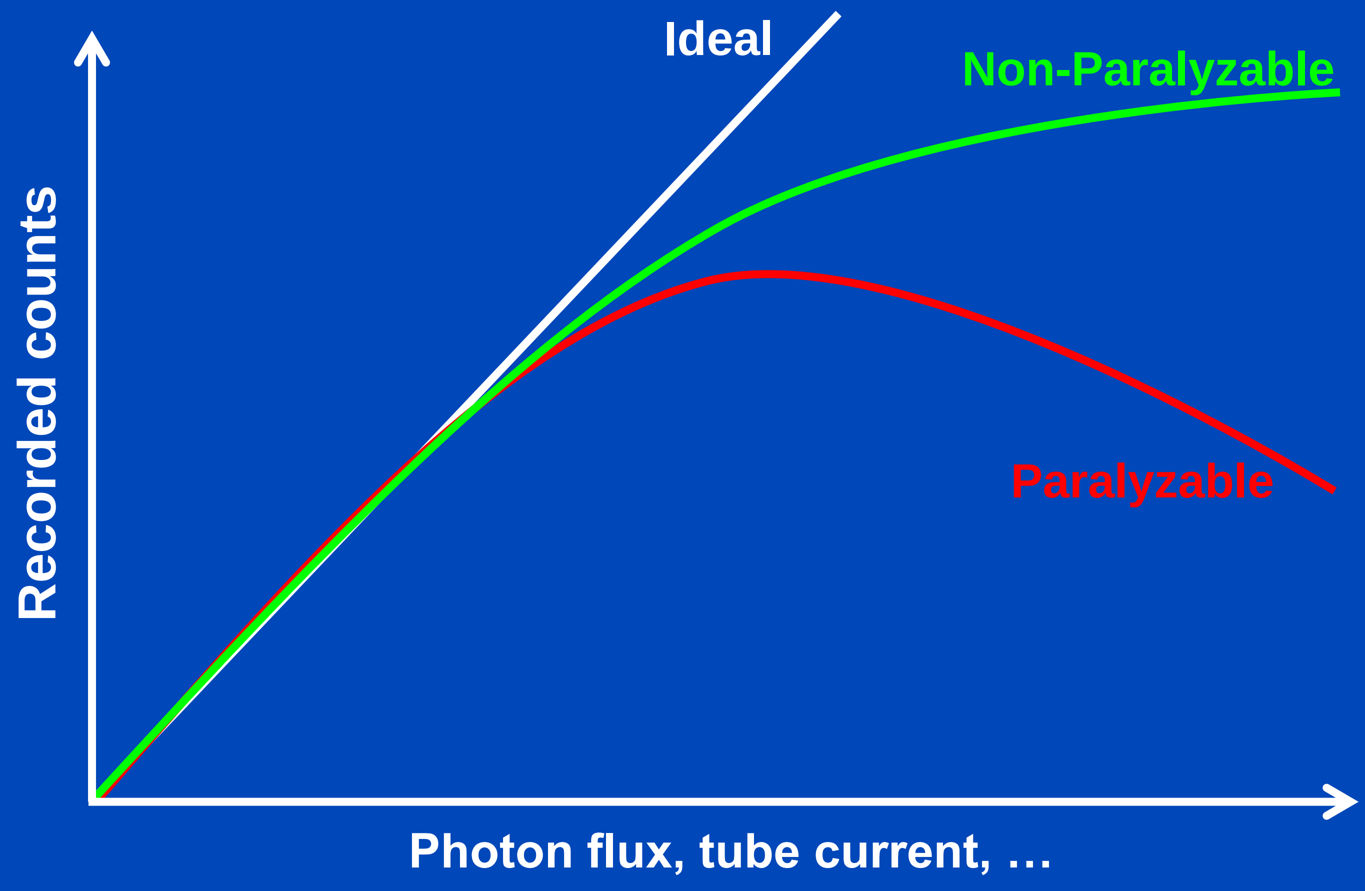

Spatial Resolution

- Small electrodes are necessary to avoid pile-up.
- High bias voltages (around 300 V) limit charge diffusion and thus blurring in the non-structured semiconductor layer.
- Thus, higher spatial resolution is achievable.

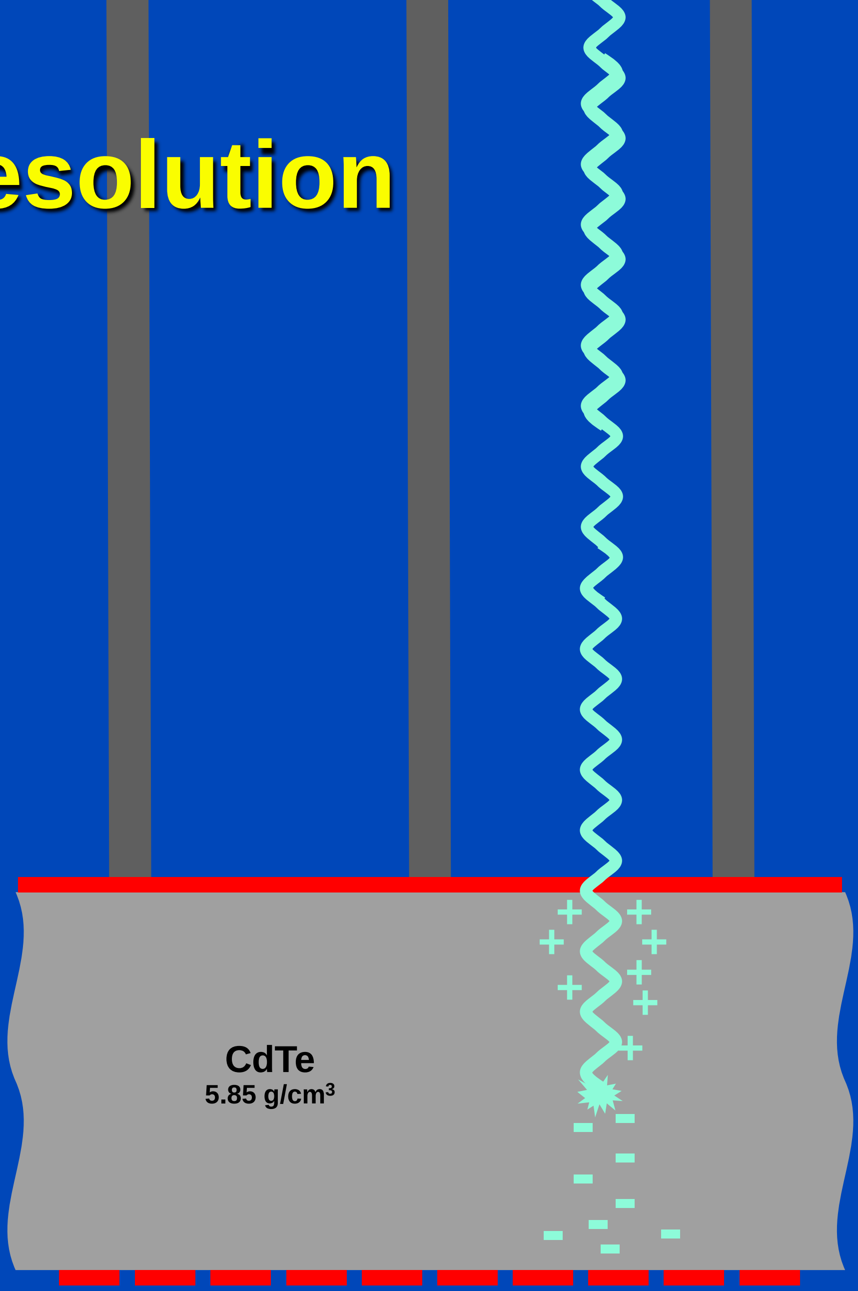

Dental Imaging

Somatom CounT

Conventional CT | **Ultra-High Resolution Photon-Counting CT** | **Anatomical Structures**

Conventional CT image (left, sharp B70f kernel, pixel size 0.27 mm, slice thickness 0.60 mm, 50 mGy $CTDI_{16cm}$) of a tooth in the maxilla. Acquisition using a ultra-high resolution photon-counting CT system (middle, ultra-high resolution U70f kernel, pixel size 0.13 mm, slice thickness 0.15 mm) of the same tooth. Labelled anatomical structures (right). (C = 2500 HU, W = 4500 HU) (ZD: zone of demineralization, ZP: zone of bacterial penetration, M: maxilla, MS: maxillary sinus, E: enamel, D: dentine, P: pulp cavity, G: gingiva, PS: periodontal space, DR: death tracts, ZS: zone of sclerosis)

Dental Imaging

Somatom CounT

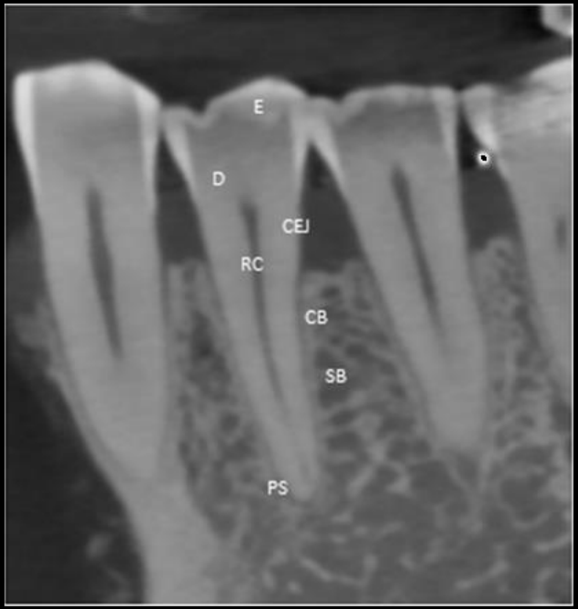

DVT
8 mGy, 102 kV

PCCT
8.5 mGy, 120 kV

PCCT
38 mGy, 120 kV

E: enamel, CEJ: cemento-enamel-junction, RC: root canal, CB: cortical bone, SB: spongious bone, PS: peridontal space

DVT: Veraview X800, Morita, Japan, PCCT: Somatom CounT, Siemens, Germany

Dose values are 16 cm CTDI values.

Slice positions between DVT and PCCT do not match exactly.

Collaboration with Dr. Maurice Rütters, Section of Periodontology, Department of Operative Dentistry, University Hospital Heidelberg.

To Bin or not to Bin?
(the continuous view)

This nice phrase was coined by Norbert Pelc.

- We have $\mathrm{PSF}(x) = s(x) * a(x)$ and $\mathrm{MTF}(u) = S(u)A(u)$.
- From Rayleigh‘s theorem we find noise is

$$\sigma^2 = \int dx\, a^2(x) = \int du\, A^2(u) = \int du\, \frac{\mathrm{MTF}^2(u)}{S^2(u)}$$

- Compare Small (A) with l pixels:

Avoid binning, if possible!

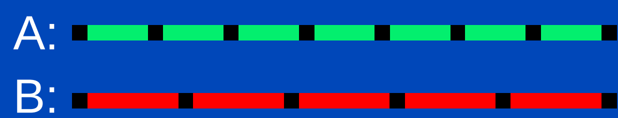

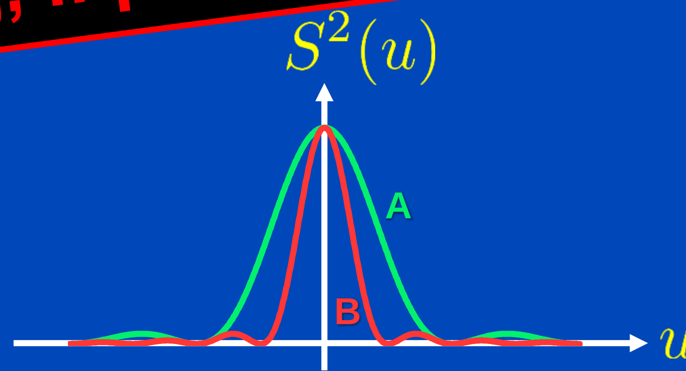

- We have $S_\mathrm{A}(u) > S_\mathrm{B}(u)$ and thus $\sigma_\mathrm{A}^2 < \sigma_\mathrm{B}^2$.
- This means that a desired PSF/MTF is often best achieved with smaller detectors.

Kachelrieß, Kalender. Med. Phys. 32(5):1321-1334, May 2005
Baek, Pineda, and Pelc. PMB 58:1433-1446, 2013

The "Small Pixel Effect"

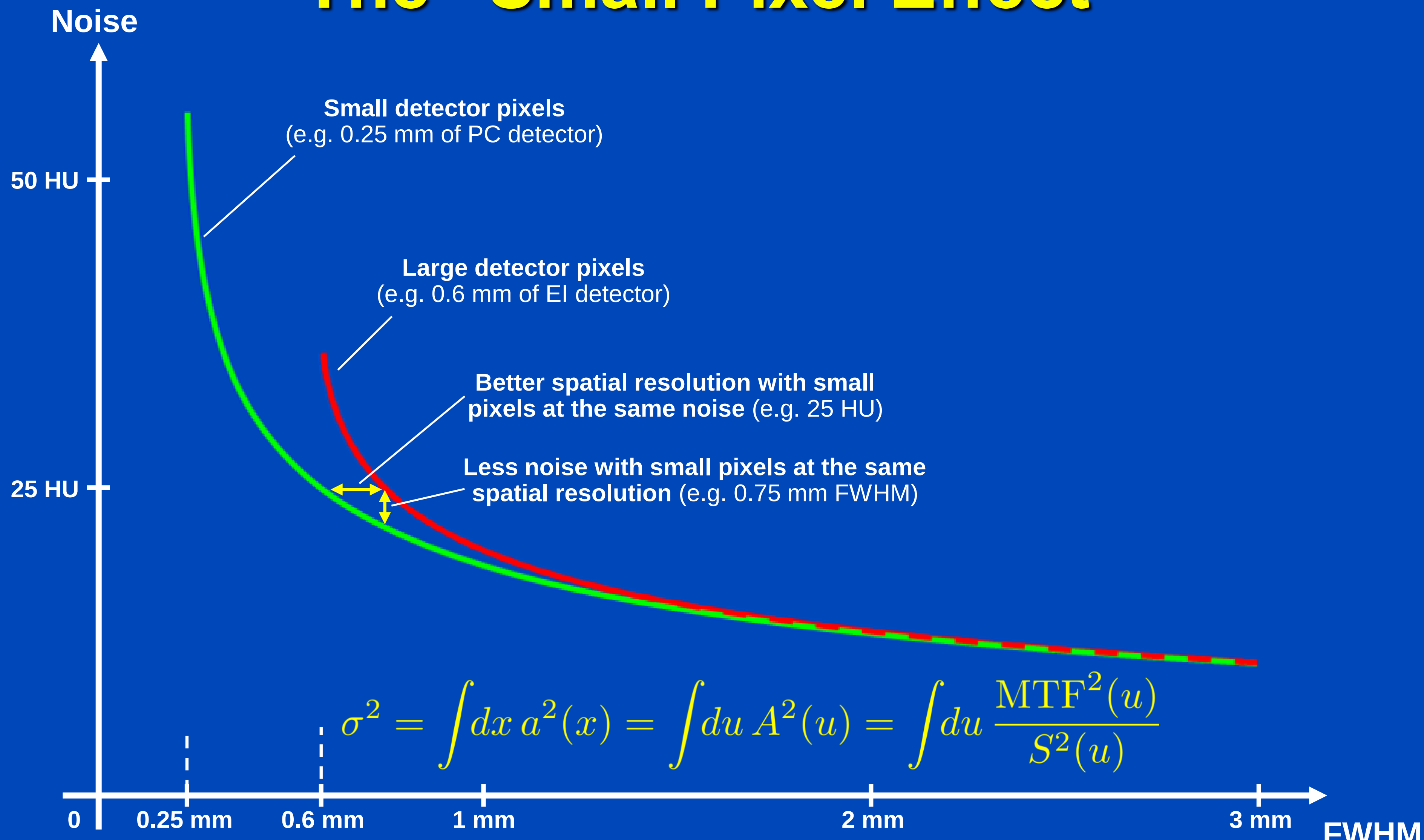

$$\sigma^2 = \int dx\, a^2(x) = \int du\, A^2(u) = \int du\, \frac{\mathrm{MTF}^2(u)}{S^2(u)}$$

Small Pixel Effect at Naeotom Alpha

Medium Phantom, 4 mGy $CTDI_{32}$

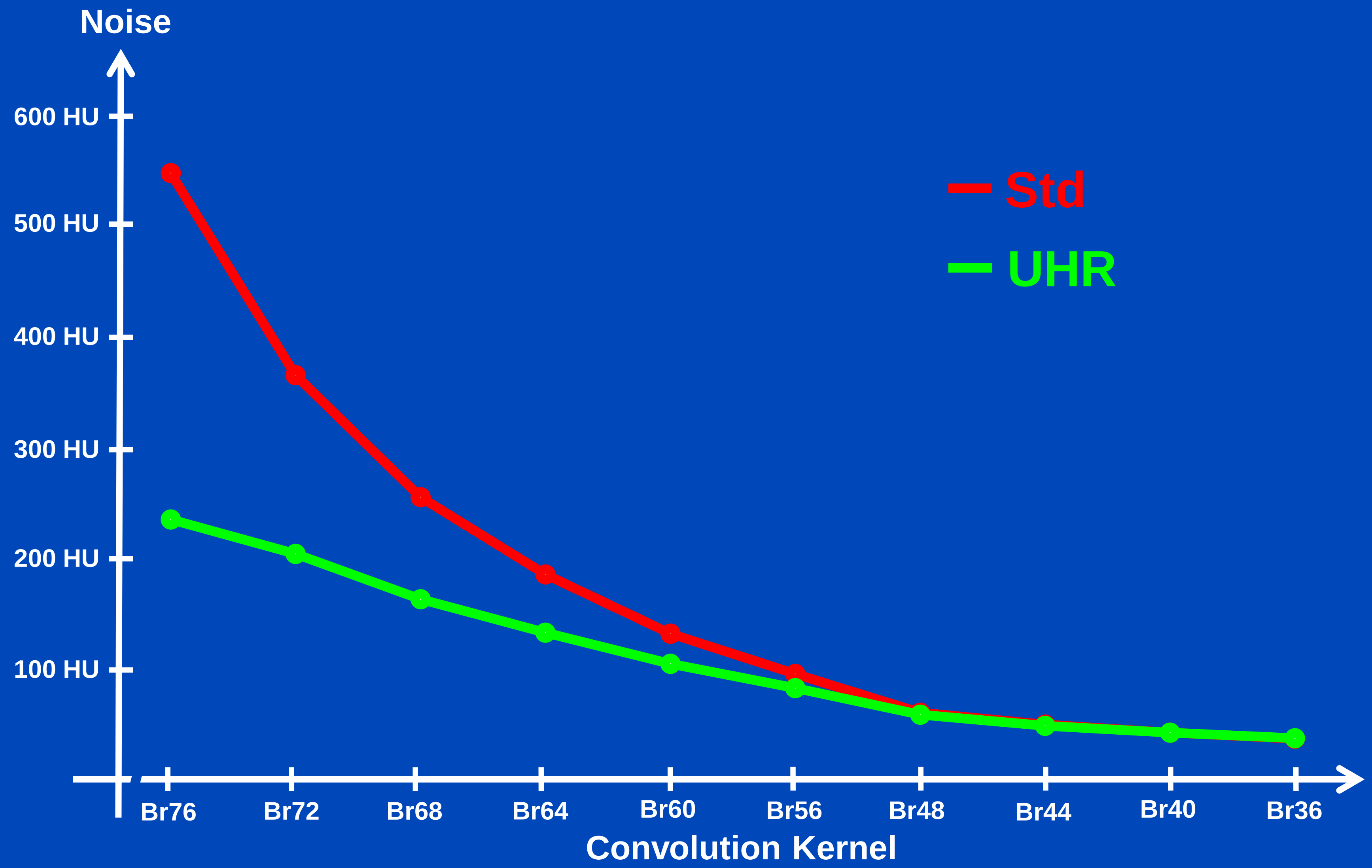

To disable the longitudinal small pixel effect, we reconstructed rather thick slices (1 mm thickness).

To Bin or not to Bin?

(the discrete view, LI)

- Let detector B be the 2-binned version of detector A:

$$B_{2n} = \frac{1}{2}(A_{2n} + A_{2n+1}) \qquad \mathrm{Var}\,B = \frac{1}{2}\mathrm{Var}\,A$$

- Assume LI to be used to find in-between pixel values. Wlog we may then consider B to be upsampled with mid-point interpolati… …r A:

$$\hat{B} \ldots \ldots)$$

- To ol… …etector we n…

$$a = \frac{1}{2}\left(1,\ 1\right) * \frac{1}{4}\left(1,\ 2,\ 1\right) = \frac{1}{8}\left(1,\ 3,\ 3,\ 1\right)$$

- Noise propagation yields 20% more noise (variance) for the binned detector:

$$\mathrm{Var}\,\hat{A} = \frac{20}{64}\mathrm{Var}\,A = \frac{5}{16}\mathrm{Var}\,A$$

$$\mathrm{Var}\,\hat{B} = \frac{3}{8}\,\mathrm{Var}\,A = \frac{6}{5}\,\mathrm{Var}\,\hat{A} = 1.2\,\mathrm{Var}\,\hat{A}$$

20% more noise variance may be compensated by 20% more x-ray dose. Any alternative? Yes:

Avoid binning, if possible!

In 2D binning implies 44% more noise variance or dose. Again, the answer is: „not to bin“.

All images reconstructed with 1024^2 matrix and 0.15 mm slice increment.
C = 1000 HU
W = 3500 HU

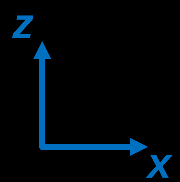

Data courtesy of the Institute of Forensic Medicine of the University of Heidelberg and of the Division of Radiology of the German Cancer Research Center (DKFZ)

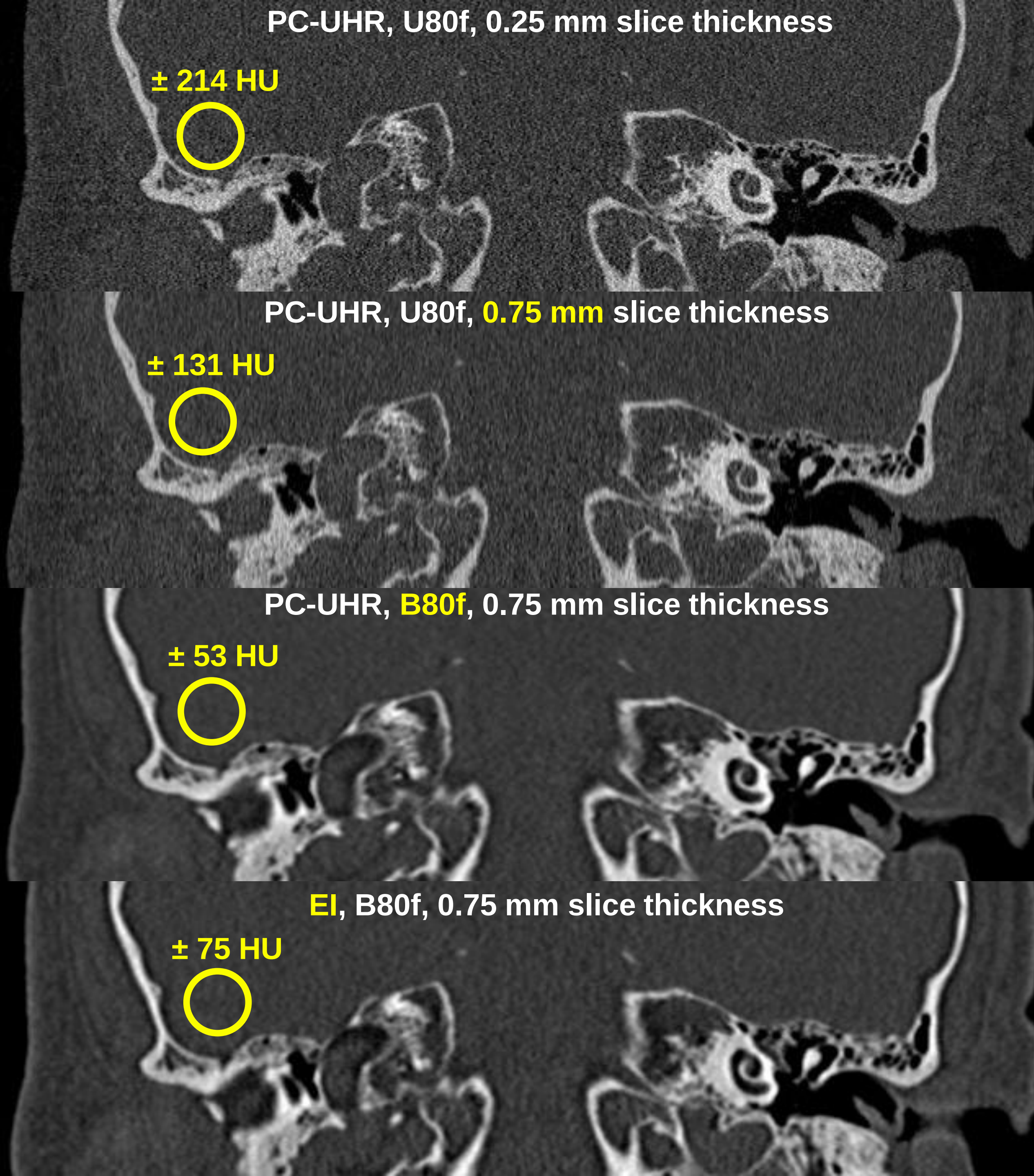

10% MTF: 19.1 lp/cm
10% MTF:17.2 lp/cm
xy FWHM: 0.48 mm
z FWHM: 0.40 mm
$CTDI_{vol}$: 16.0 mGy

10% MTF: 19.1 lp/cm
10% MTF:17.2 lp/cm
xy FWHM: 0.48 mm
z FWHM: 0.67 mm
$CTDI_{vol}$: 16.0 mGy

10% MTF: 9.3 lp/cm
10% MTF:10.5 lp/cm
xy FWHM: 0.71 mm
z FWHM: 0.67 mm
$CTDI_{vol}$: 16.0 mGy

10% MTF: 9.3 lp/cm
10% MTF:10.5 lp/cm
xy FWHM: 0.71 mm
z FWHM: 0.67 mm
$CTDI_{vol}$: 16.0 mGy

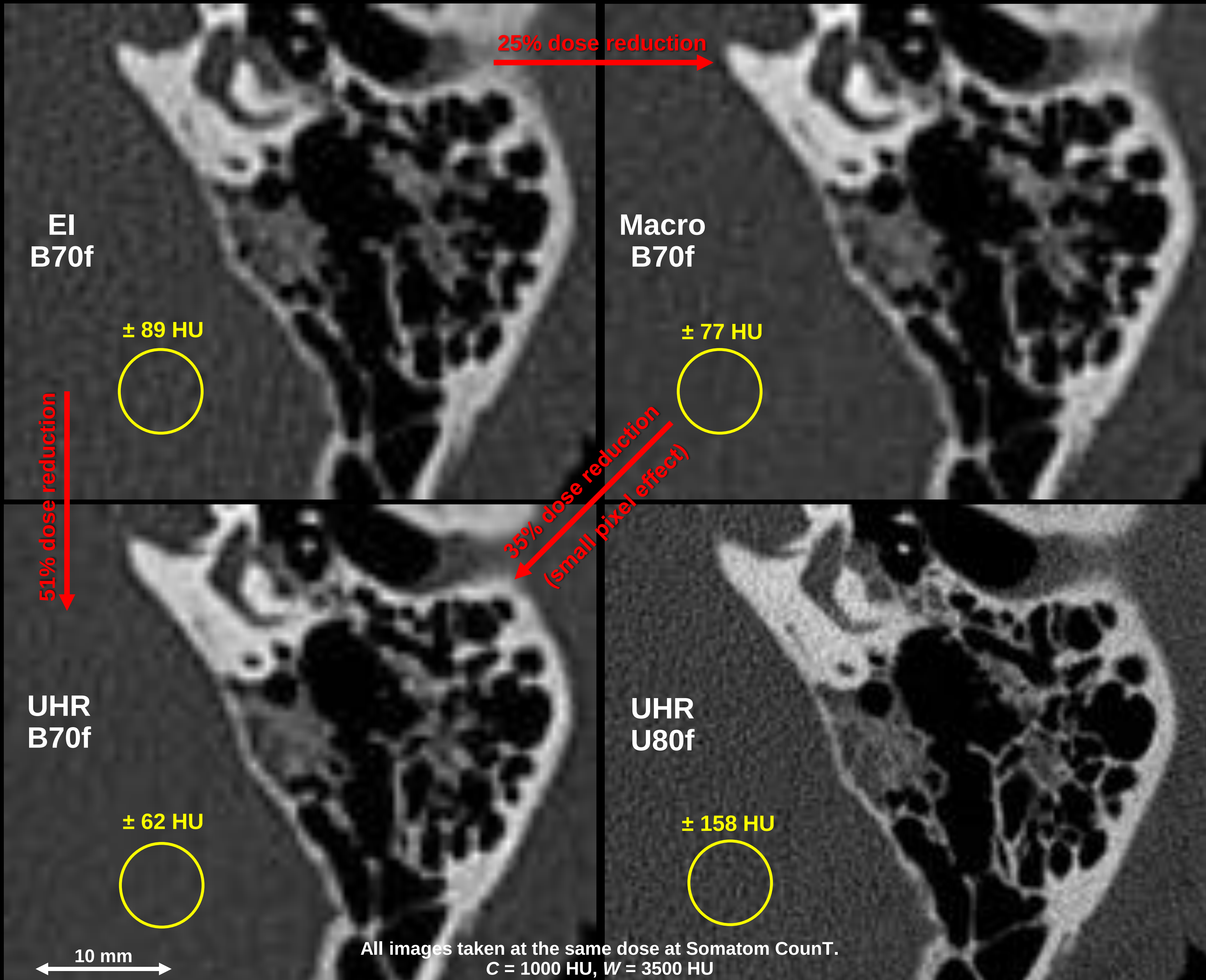

All images taken at the same dose at Somatom CounT.
C = 1000 HU, W = 3500 HU

Acquisitions at same noise

EI, B70f

UHR, B70f

C = 1000 HU
W = 3500 HU

Acquisition with EI:
- **Tube voltage of 120 kV**
- **Tube current of 350 mAs**
- **Resulting dose of $\mathrm{CTDI}_{\mathrm{vol\ 32\ cm}}$ = 26.4 mGy**

Acquisition with UHR:
- **Tube voltage of 120 kV**
- **Tube current of 200 mAs**
- **Resulting dose of $\mathrm{CTDI}_{\mathrm{vol\ 32\ cm}}$ = 16.1 mGy**

This is a 39% reduction of dose!

L. Klein, C. Amato, S. Heinze, M. Uhrig, H.-P. Schlemmer, M. Kachelrieß, and S. Sawall. **Effects of Detector Sampling on Noise Reduction in a Clinical Photon Counting Whole-Body CT**. Investigative Radiology, vol. 55(2):111-119, February 2020.

Energy Integrating Detector (B70f)

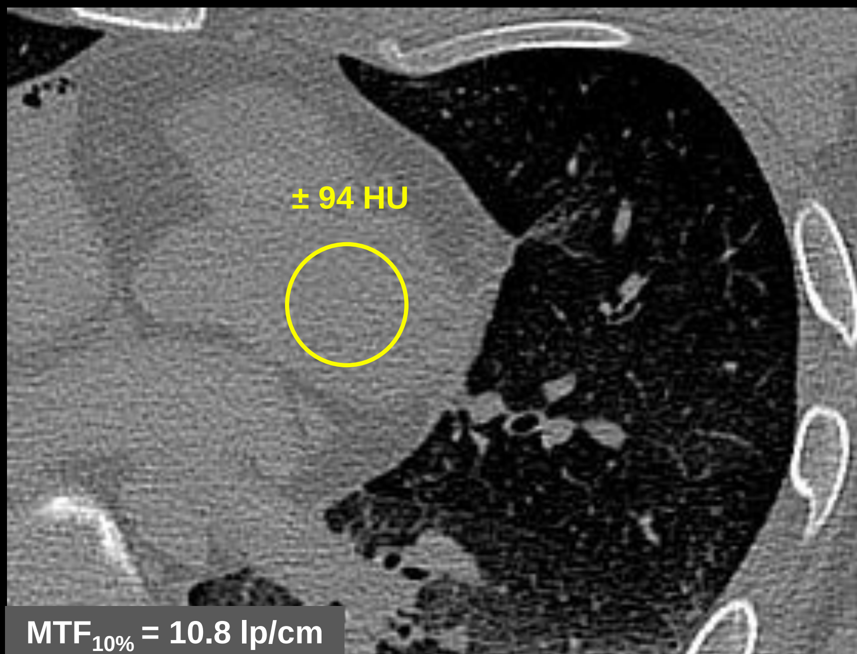

Photon Counting Detector (B70f)

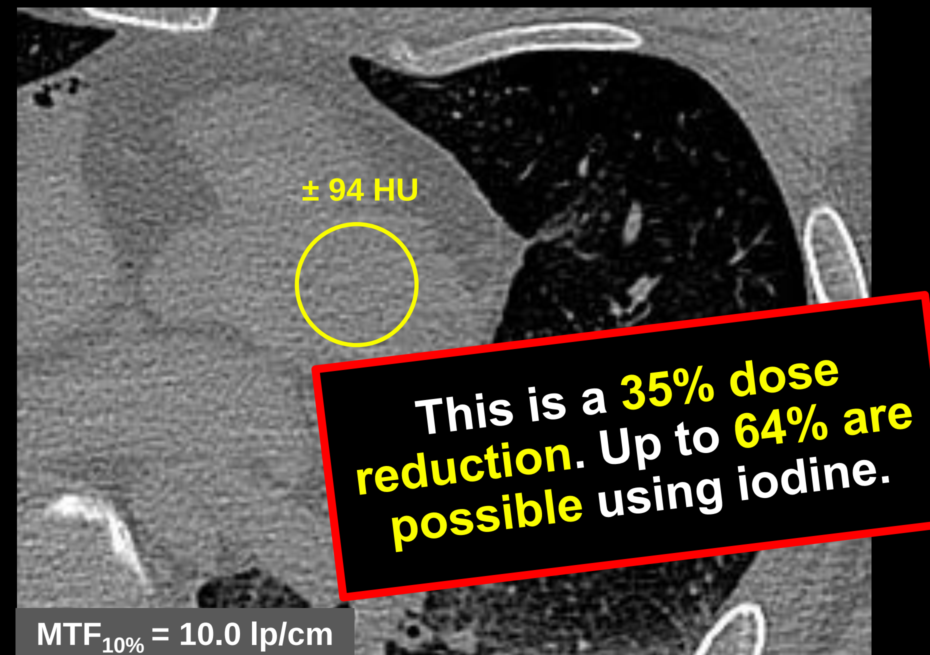

Acquisition with EI:
- **Tube voltage of 120 kV**
- **Tube current of 300 mAs**
- **Resulting dose of $\mathrm{CTDI}_{\mathrm{vol}\ 32\ \mathrm{cm}}$ = 22.6 mGy**

Acquisition with UHR:
- **Tube voltage of 120 kV**
- **Tube current of 180 mAs**
- **Resulting dose of $\mathrm{CTDI}_{\mathrm{vol}\ 32\ \mathrm{cm}}$ = 14.6 mGy**

C = 50 HU, W = 1500 HU

X-Ray Dose Reduction of B70f

PC vs. PC
("small pixel effect only")

UHR vs. Macro	80 kV	100 kV	120 kV	140 kV
S	**23%** ± 12%	**34%** ± 10%	**35%** ± 11%	**25%** ± 10%
M	**32%** ± 10%	**32%** ± 8%	**35%** ± 8%	**34%** ± 9%
L	**35%** ± 10%	**29%** ± 15%	**27%** ± 9%	**31%** ± 11%

PC vs. EI
("small pixel effect" and "iodine effect")

UHR vs. EI	80 kV	100 kV	120 kV	140 kV
S	**33%** ± 9%	**52%** ± 5%	**57%** ± 7%	**57%** ± 6%
M	**41%** ± 8%	**47%** ± 7%	**60%** ± 6%	**62%** ± 4%
L	**48%** ± 8%	**43%** ± 10%	**54%** ± 6%	**63%** ± 5%

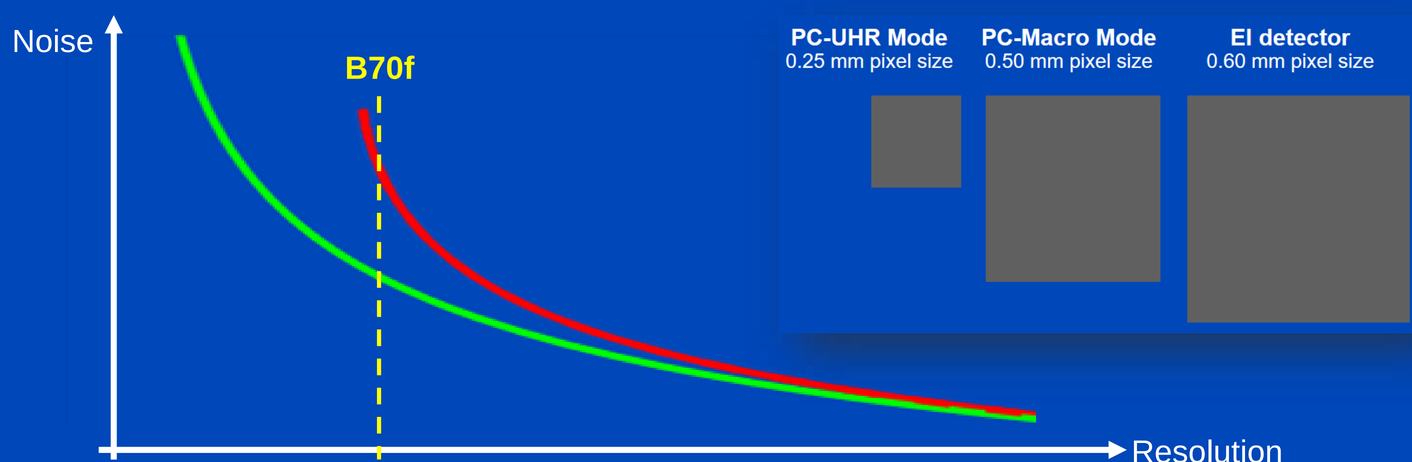

Klein, Kachelrieß, Sawall et al. Invest. Radiol. 55(2), Feb 2020

X-Ray Dose Reduction of D40f

PC vs. PC (“small pixel effect only”)

UHR vs. Macro	80 kV	100 kV	120 kV	140 kV
S	**5%** ± 16%	**12%** ± 17%	**17%** ± 17%	**9%** ± 15%
M	**11%** ± 14%	**9%** ± 12%	**16%** ± 16%	**13%** ± 13%
L	**11%** ± 14%	**6%** ± 17%	**6%** ± 17%	**4%** ± 17%

PC vs. EI (“small pixel effect” and “iodine effect”)

UHR vs. EI	80 kV	100 kV	120 kV	140 kV
S	**10%** ± 11%	**28%** ± 11%	**36%** ± 12%	**38%** ± 12%
M	**15%** ± 12%	**23%** ± 12%	**40%** ± 10%	**43%** ± 9%
L	**24%** ± 14%	**17%** ± 11%	**33%** ± 12%	**43%** ± 9%

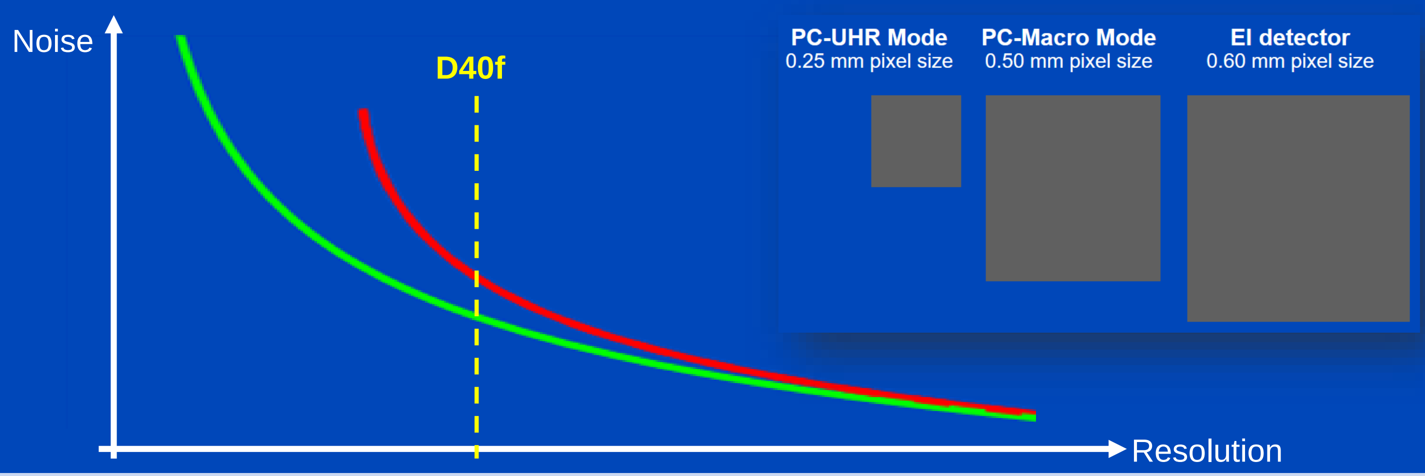

Klein, Kachelrieß, Sawall et al. Invest. Radiol. 55(2), Feb 2020

Drawbacks of UHR?

Power of Vectron X-Ray tube in Naeotom Alpha

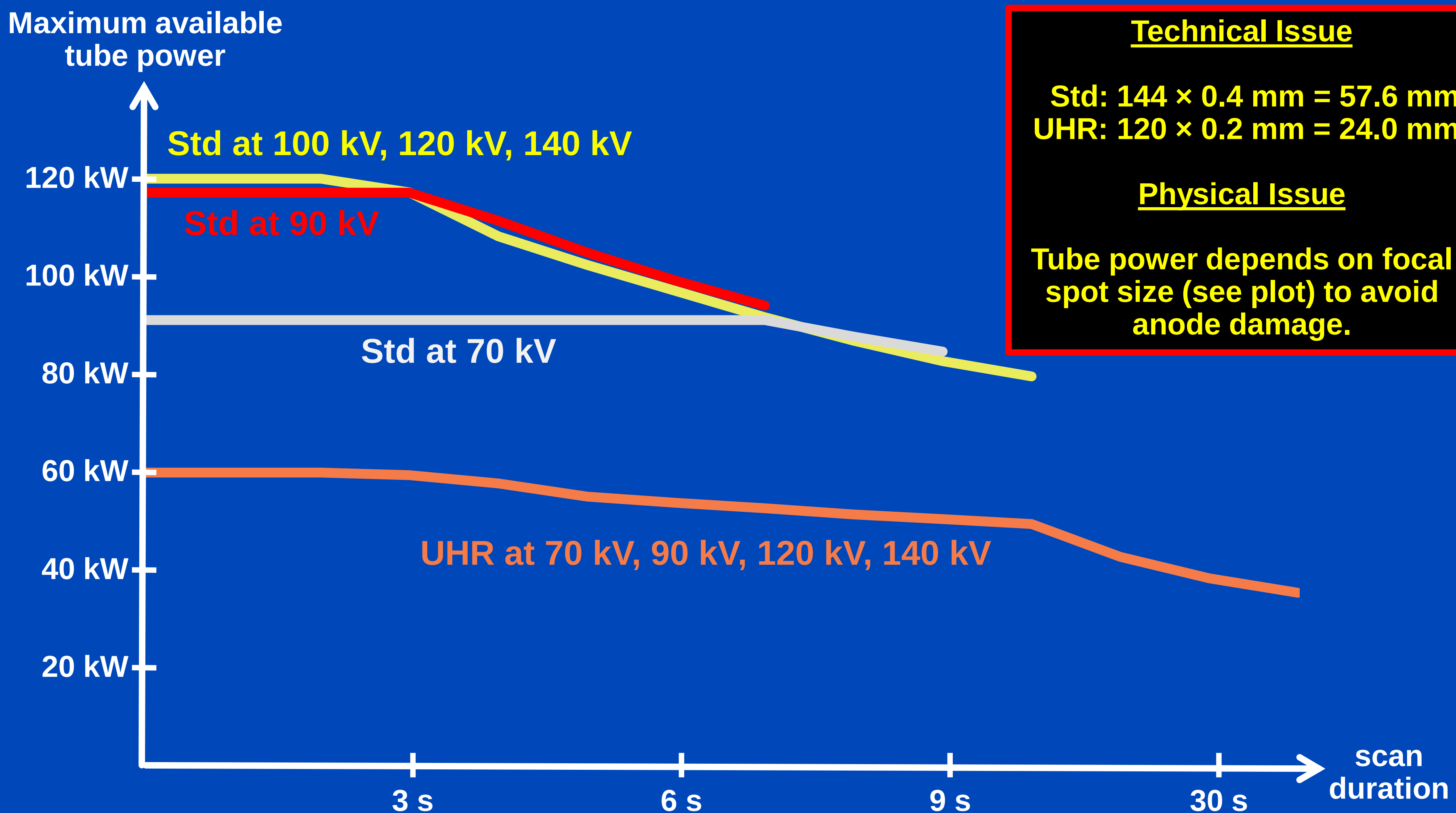

Technical Issue

Std: 144 × 0.4 mm = 57.6 mm
UHR: 120 × 0.2 mm = 24.0 mm

Physical Issue

Tube power depends on focal spot size (see plot) to avoid anode damage.

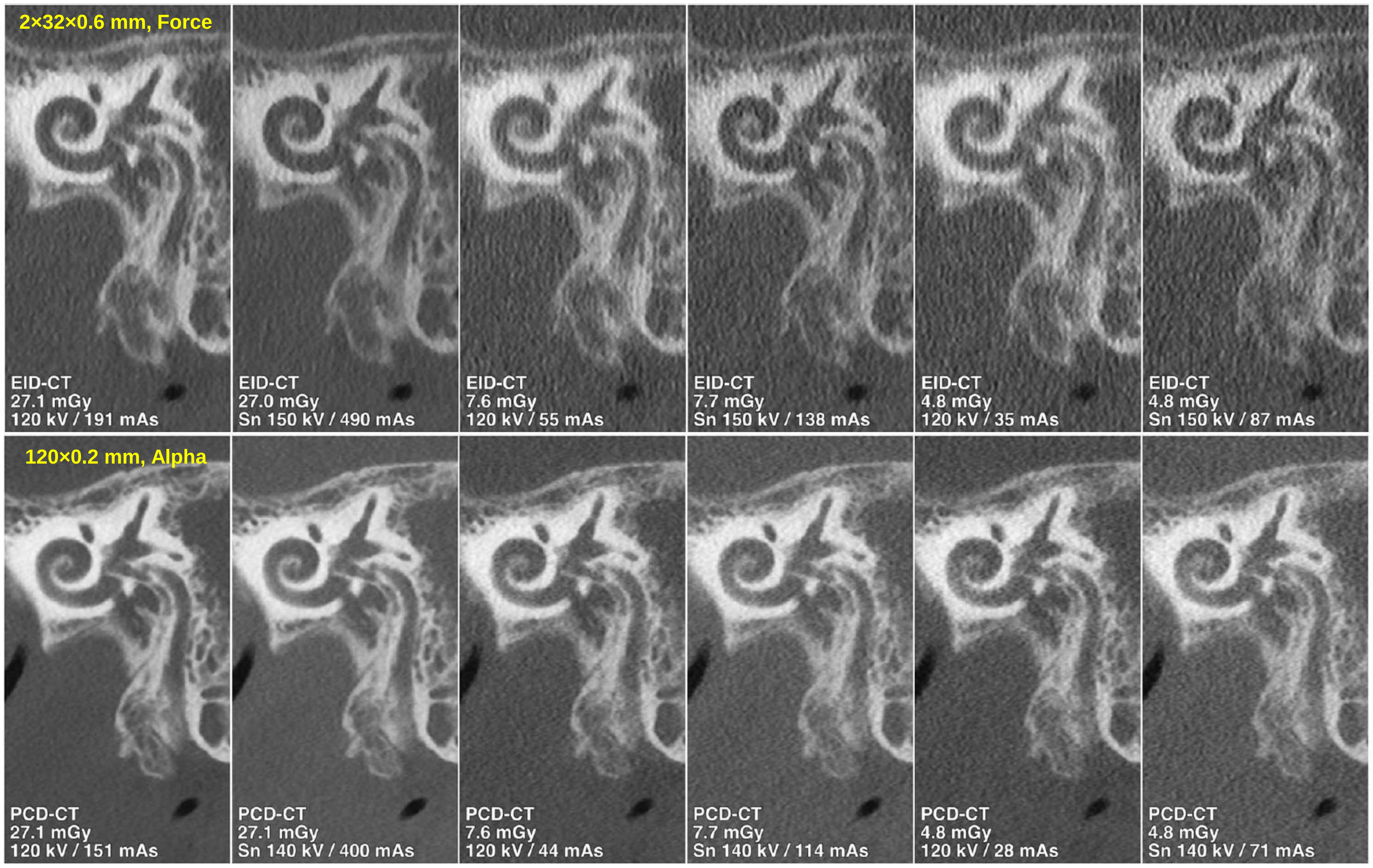

Matched MTF (Force: Ur77, ρ_{10} = 22.0 lp/cm, ρ_{50} = 16.5 lp/cm. Alpha: Hr76, ρ_{10} = 21.0 lp/cm, ρ_{50} = 16.5 lp/cm) iterative reconstruction with Admire or QIR, level 3 at 0.4 mm slice thickness, 0.2 mm slice increment, 512×512 reconstruction matrix with 50 mm size.

Grunz et al. Spectral shaping via tin prefiltration in ultra-high-resolution photon-counting and energy-integrating detector CT of the temporal bone. Invest. Radiol. 57(12), 2022

Alpha UHR used for Coronary CTA

Slice thickness: 0.2 mm

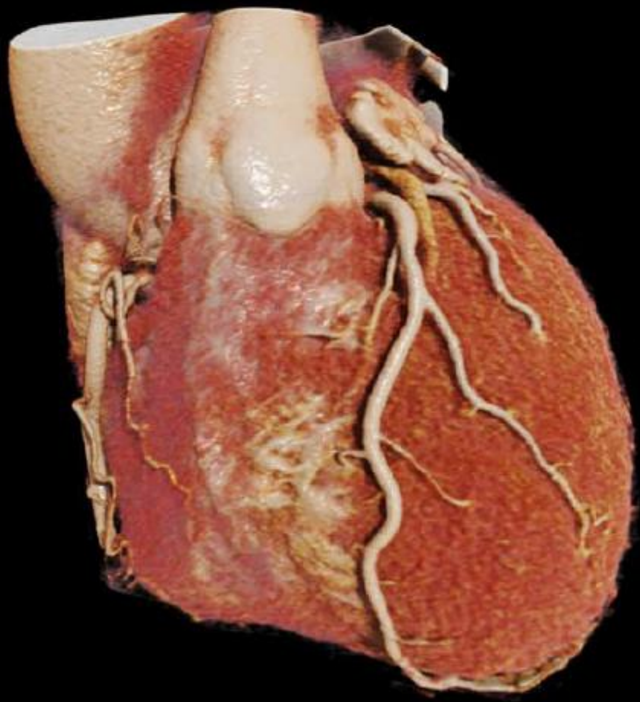

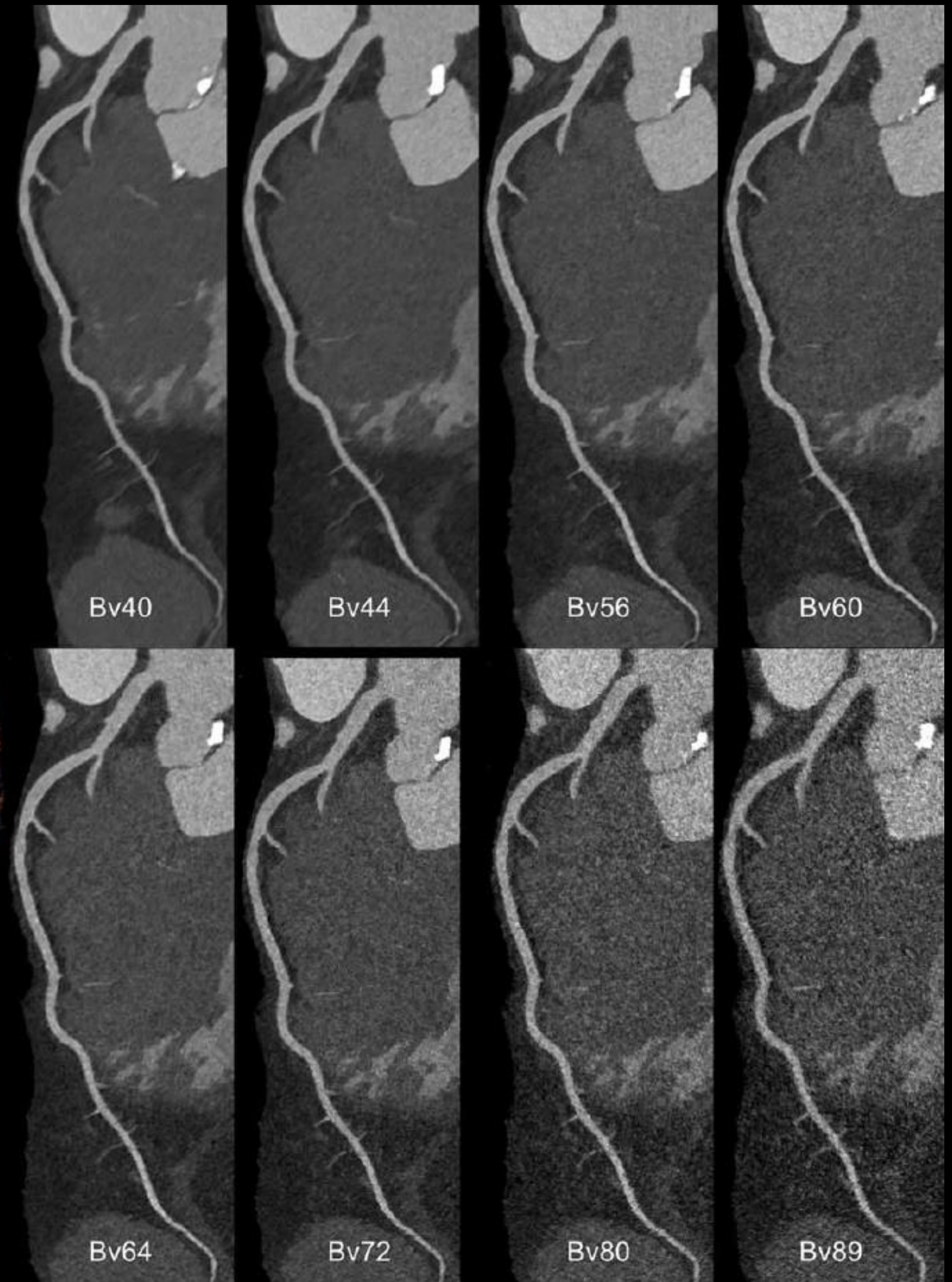

Mergen et al. Ultra-high-resolution coronary CT angiography with photon-counting detector CT. Invest. Radiol. 57(12), 2022

More than Dual Energy?

- Ways to remove the spectral overlap?
- Lower noise, less dose?
- Improve contrast-to-noise ratio at unit dose?
- Distinguish more than three materials?

$$\mu(E) = \cancel{\eta(E)} + \tau(E) + \sigma(E) + \cancel{\kappa(E)}$$

Rayleigh Photo Compton Pair

$$\tau(E) \propto \rho \frac{Z^3}{E^3}$$

$$\sigma(E) \propto \rho \frac{Z}{A} f(E)$$

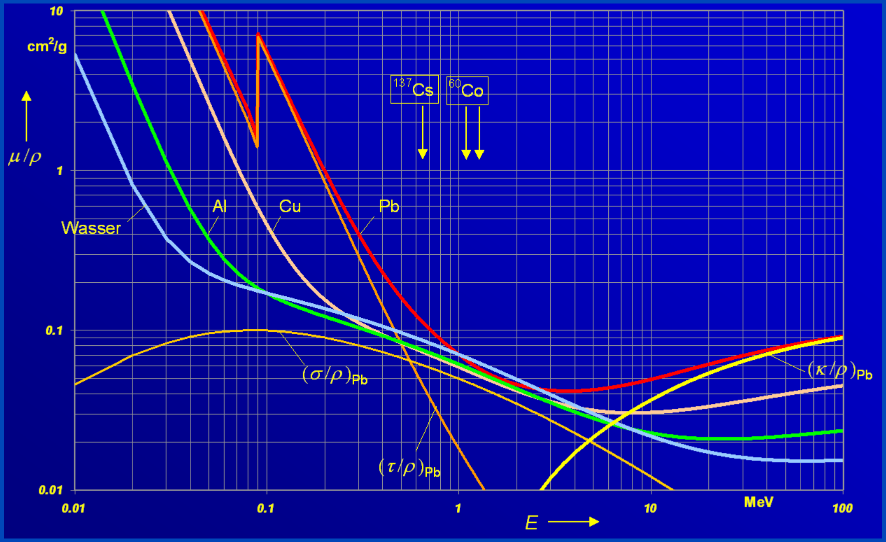

K-Edges: More than Dual Energy CT?

$$\mu(\boldsymbol{r}, E) = f_1(\boldsymbol{r})\psi_1(E) + f_2(\boldsymbol{r})\psi_2(E) + \cancel{f_3(\boldsymbol{r})\psi_3(E)} + \ldots$$

Apart from special applications, e.g.
Iodine k-edge imaging of the breast

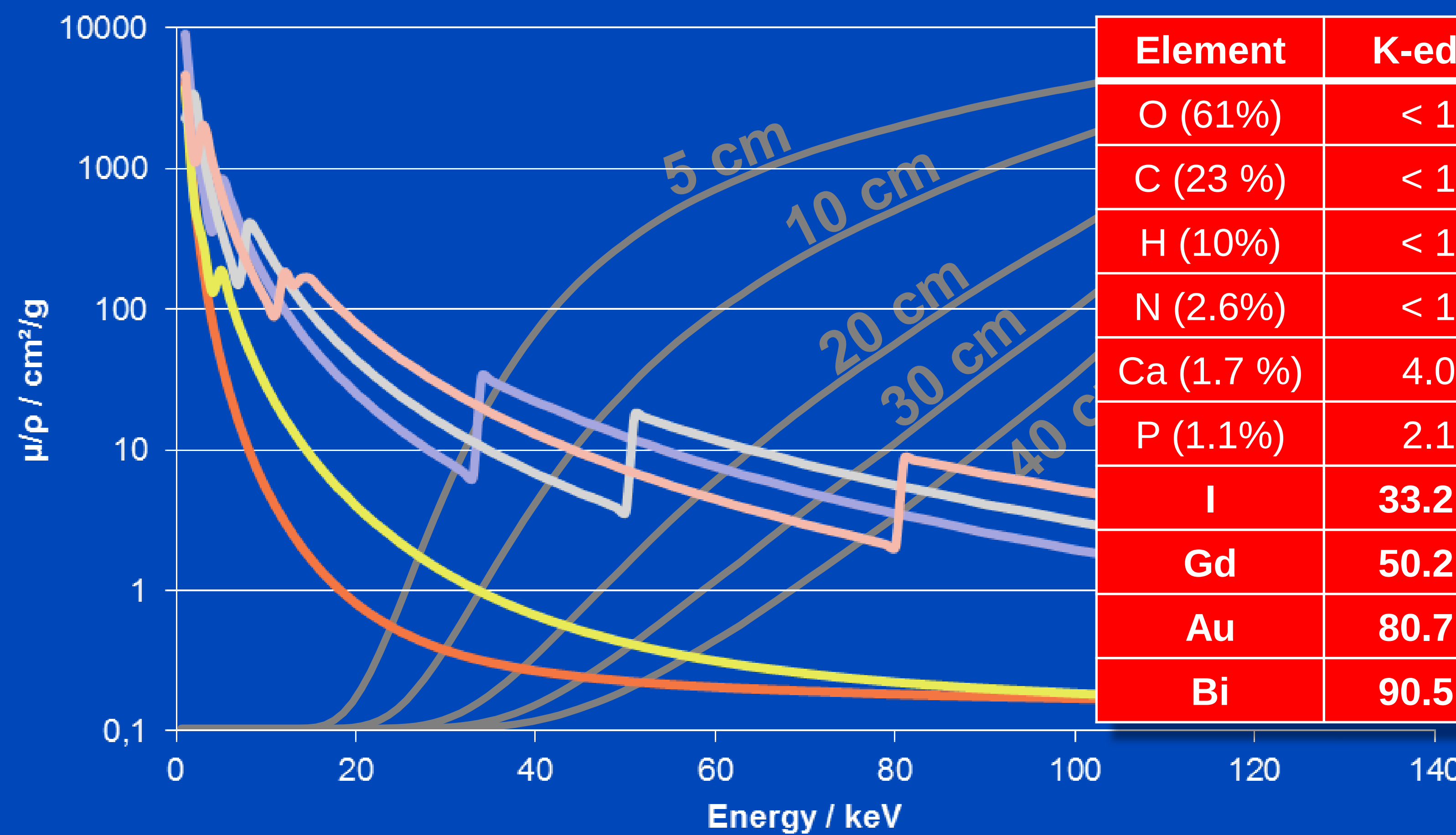

Element	K-edge
O (61%)	< 1 keV
C (23 %)	< 1 keV
H (10%)	< 1 keV
N (2.6%)	< 1 keV
Ca (1.7 %)	4.0 keV
P (1.1%)	2.1 keV
I	**33.2 keV**
Gd	**50.2 keV**
Au	**80.7 keV**
Bi	**90.5 keV**

Gray curves: 120 kV water transmission on a non-logarithmic ordinate individually normalized to 1 at 140 keV.

MECT

Ca-Gd-I Decomposition

Chess pattern mode
140 kV, 20/35/50/65 keV
***C* = 0 HU, *W* = 1200 HU**

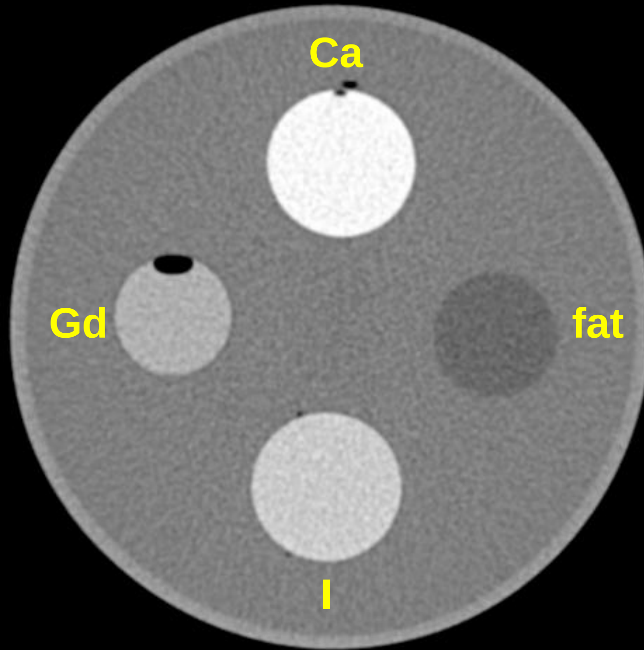

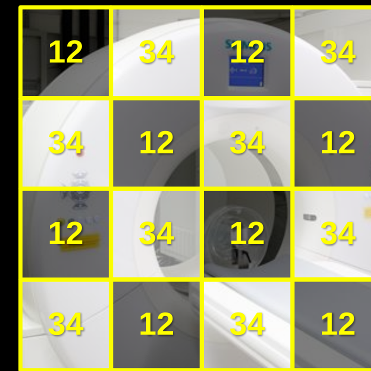

Calcium image

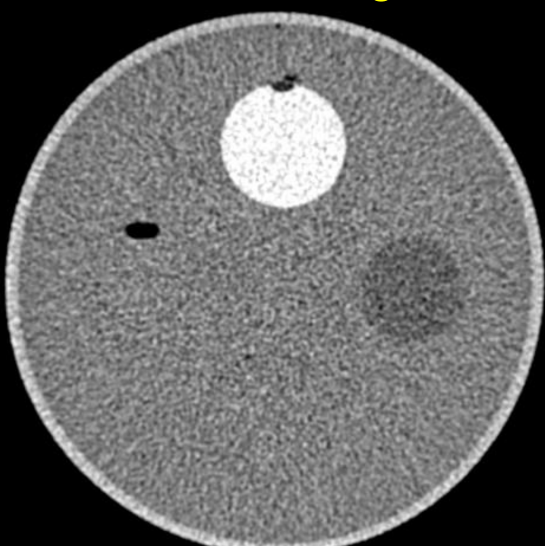

Gadolinium image

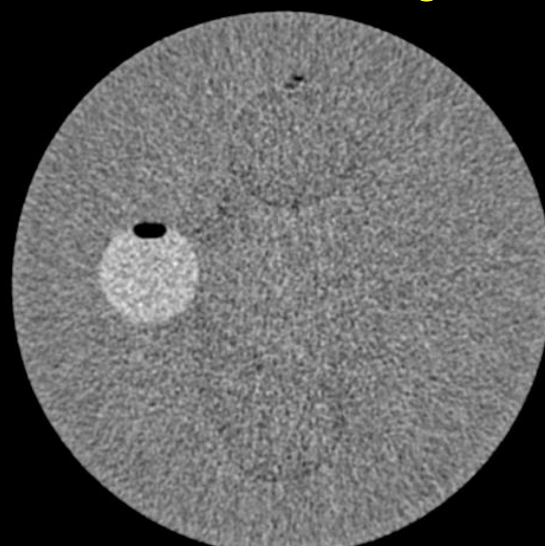

Iodine image

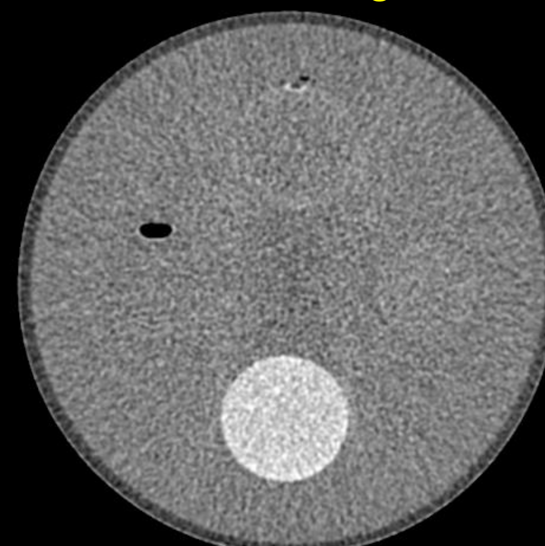

Courtesy of Siemens Healthcare

Potential Advantages of PCCT

- Everything retrospectively on demand
  - Spatial resolution
  - Spectral information
  - Virtual tube voltage setting
- Higher spatial resolution due to
  - smaller pixels
  - lower cross-talk between pixels
- Lower dose/noise due to
  - energy bin weighting
  - no electronic noise
  - Swank factor = 1
  - smaller pixels
- Spectral information on demand
  - single energy
  - dual energy
  - multiple energy
  - virtual monochromatic
  - K-edge imaging
  - …

Potential clinical impact

Which Hardware Technology is Best?

Results – Different DECT Techniques

DS 100 kV / Sn 140 kV | TVS 80 kV / 140 kV | Sandwich 140 kV | Split detector 120 kV

VNC

Iodine

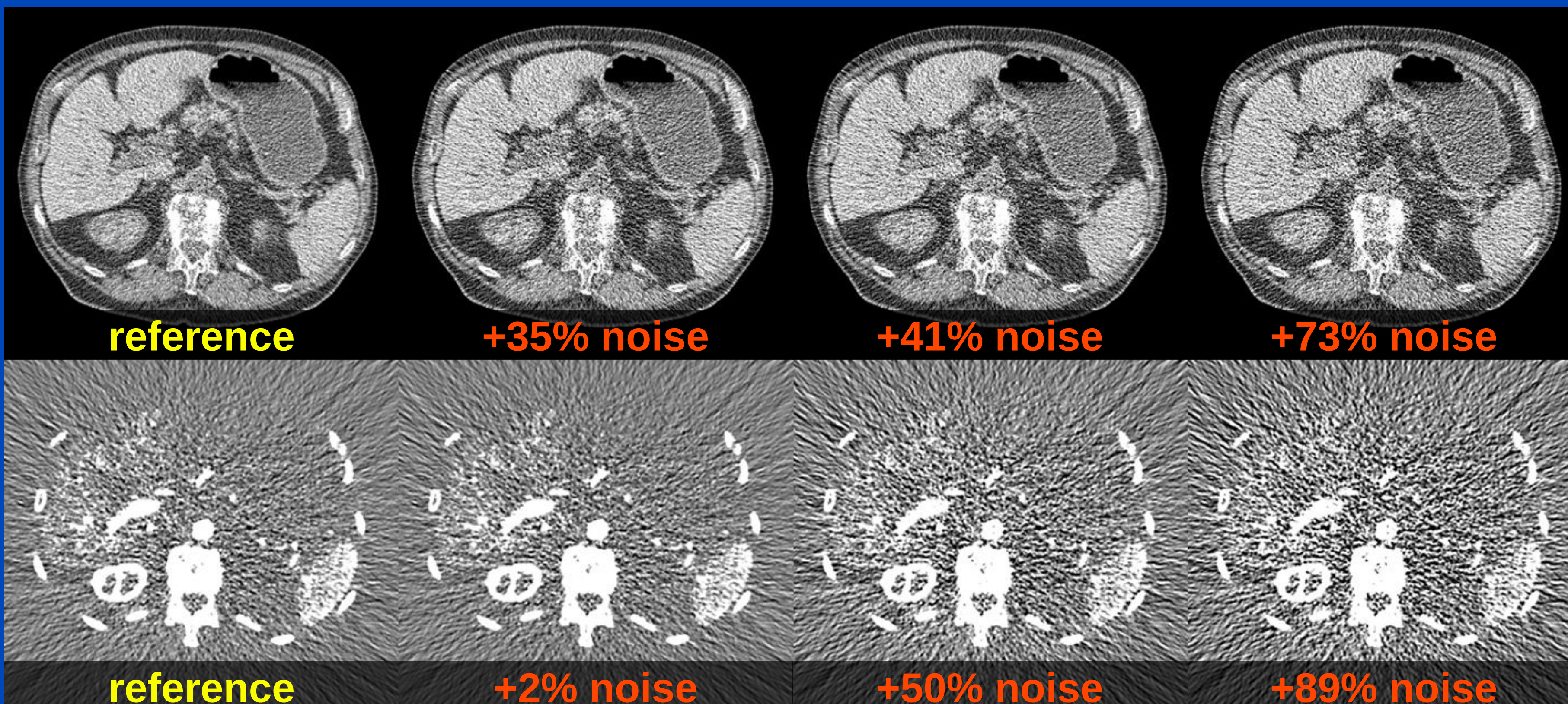

Faby and Kachelrieß, MedPhys 42(7):4349-4366, July 2015.

Water: *C* = 0 HU / *W* = 400 HU
Iodine: *C* = 0 mg/mL / *W* = 6 mg/mL

Results – PC (Realistic PC Model)

DS 100 kV / Sn 140 kV | PC 2 bins | PC 4 bins | PC 8 bins

VNC

Iodine

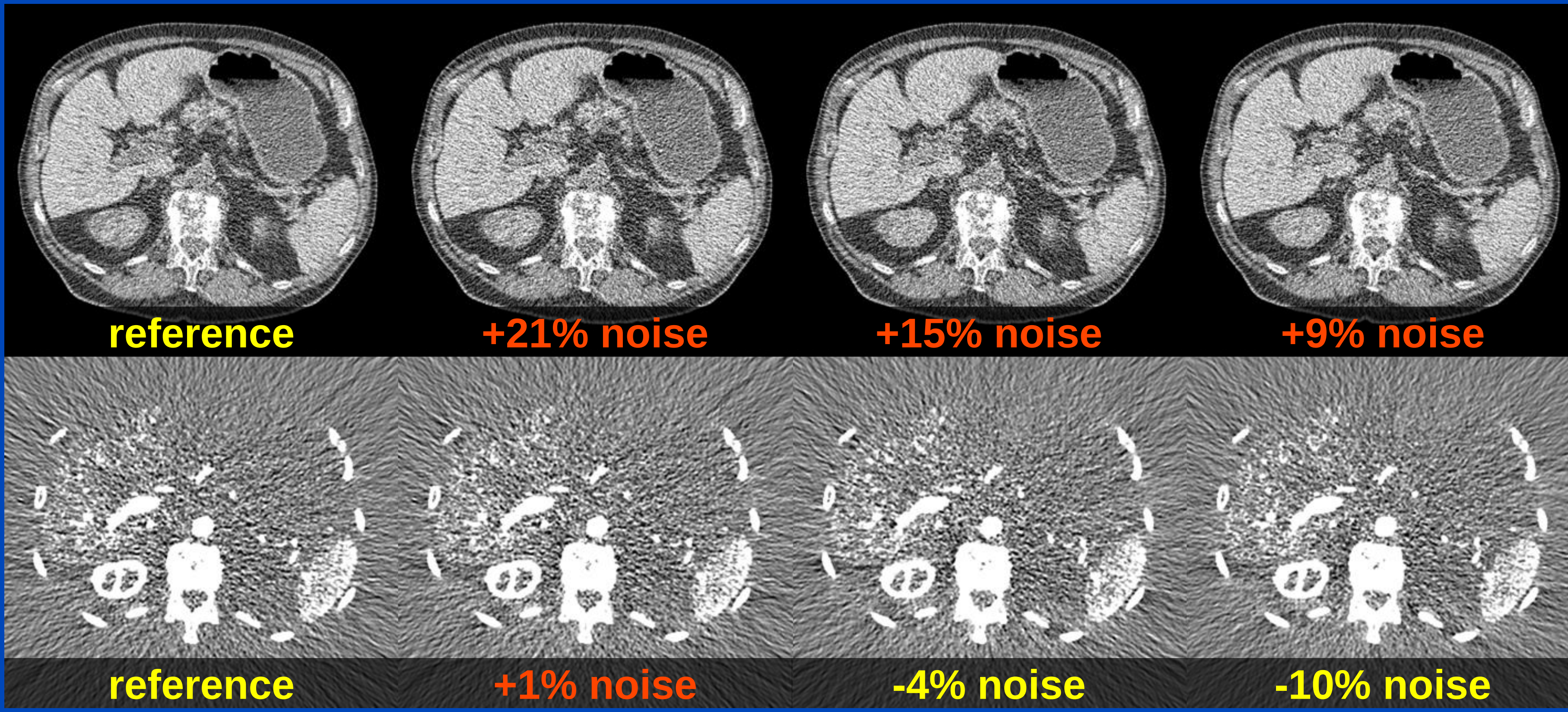

Water: *C* = 0 HU / *W* = 400 HU
Iodine: *C* = 0 mg/mL / *W* = 6 mg/mL

Results – PC/PC (Realistic PC Model)

PC 100 kV / PC Sn 140 kV

DS 100 kV / Sn 140 kV	DS PC 1 bin	DS PC 2 bins	DS PC 4 bins

VNC

Iodine

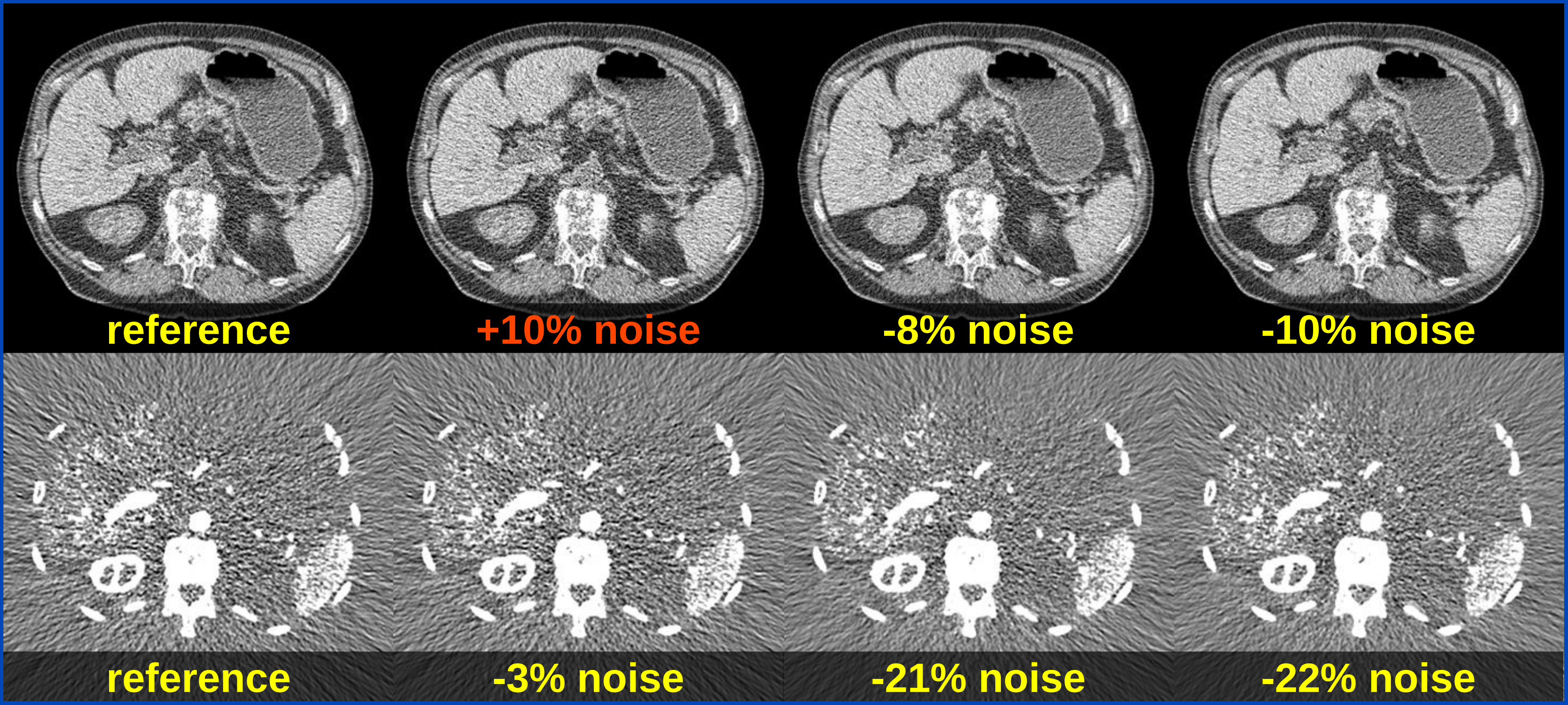

80 kV / 140 kV

Used in
- Siemens‘ 1st generation DSCT

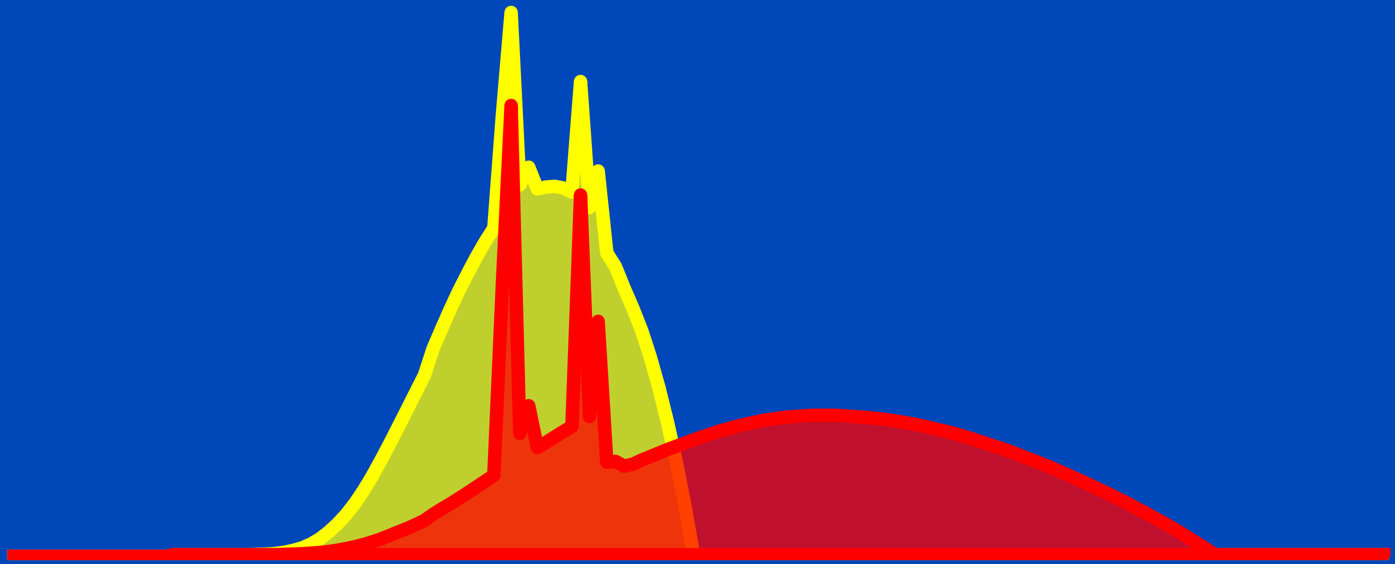

DSCT spectra as seen with one bin after having passed a 32 cm water layer.

80 kV / 140 kV $Sn_{0.4\ mm}$

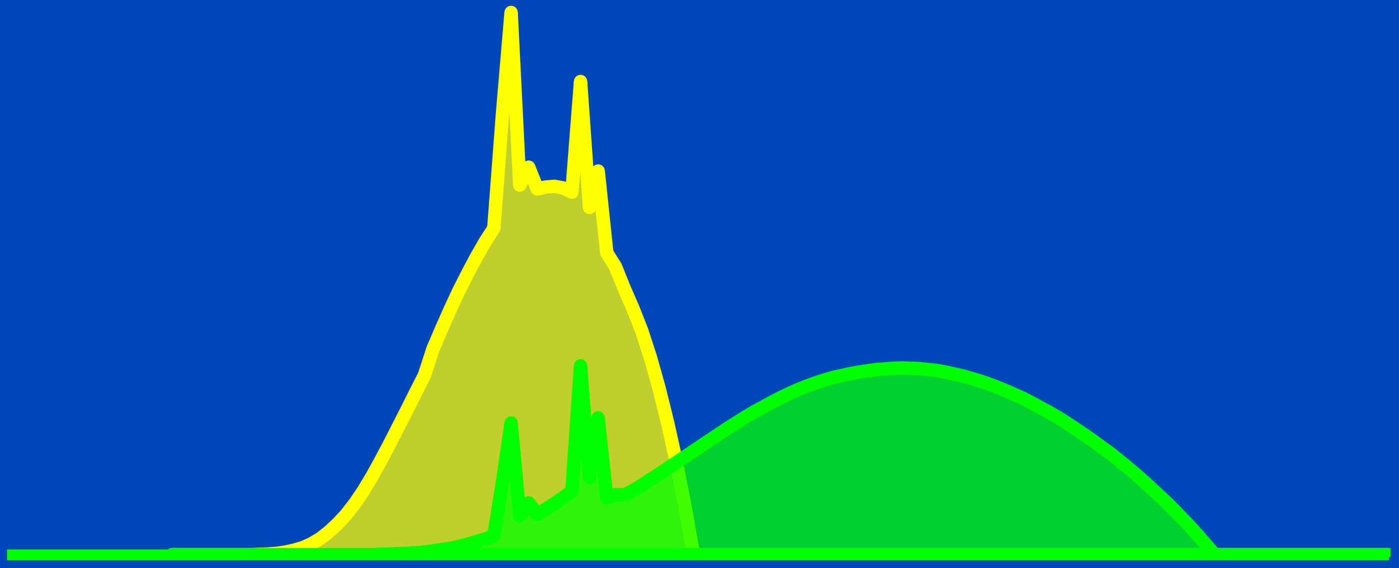

Used in
- Siemens‘ 2nd generation DSCT

DSCT spectra as seen with one bin after having passed a 32 cm water layer.

90 kV / 150 kV $Sn_{0.6\ mm}$

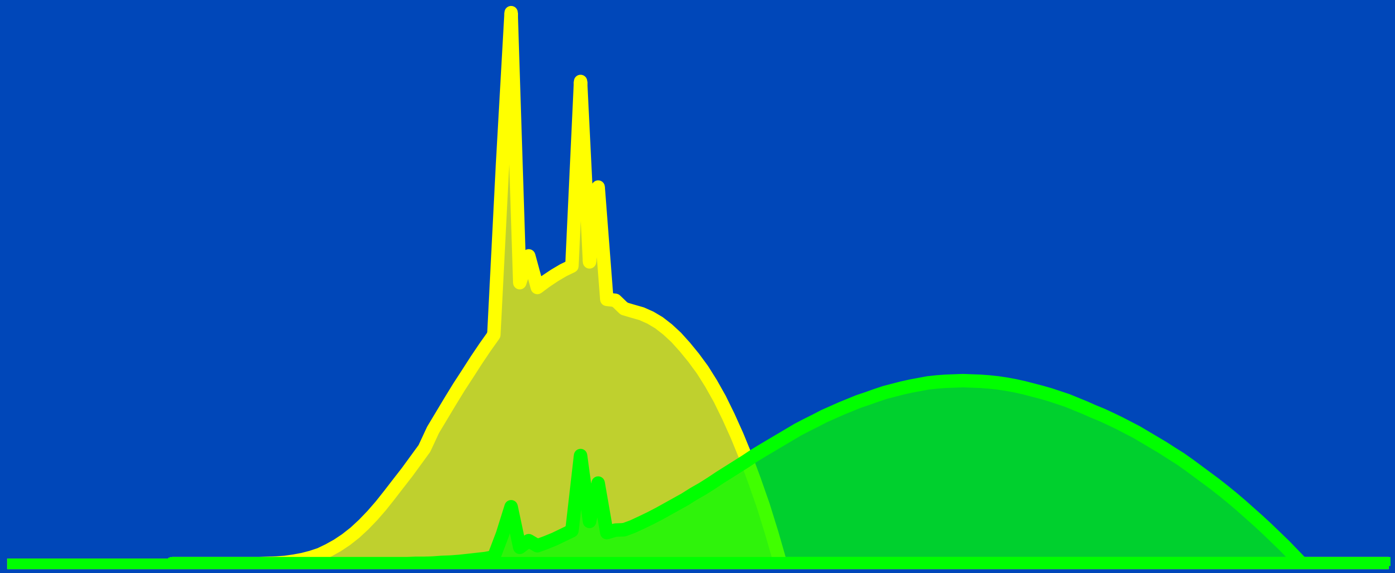

Used in
- Siemens‘ 3rd generation DSCT

DSCT spectra as seen with one bin after having passed a 32 cm water layer.

90 kV / 150 kV $Sn_{0.6\ mm}$

Used in
- Siemens' 3rd generation DSCT

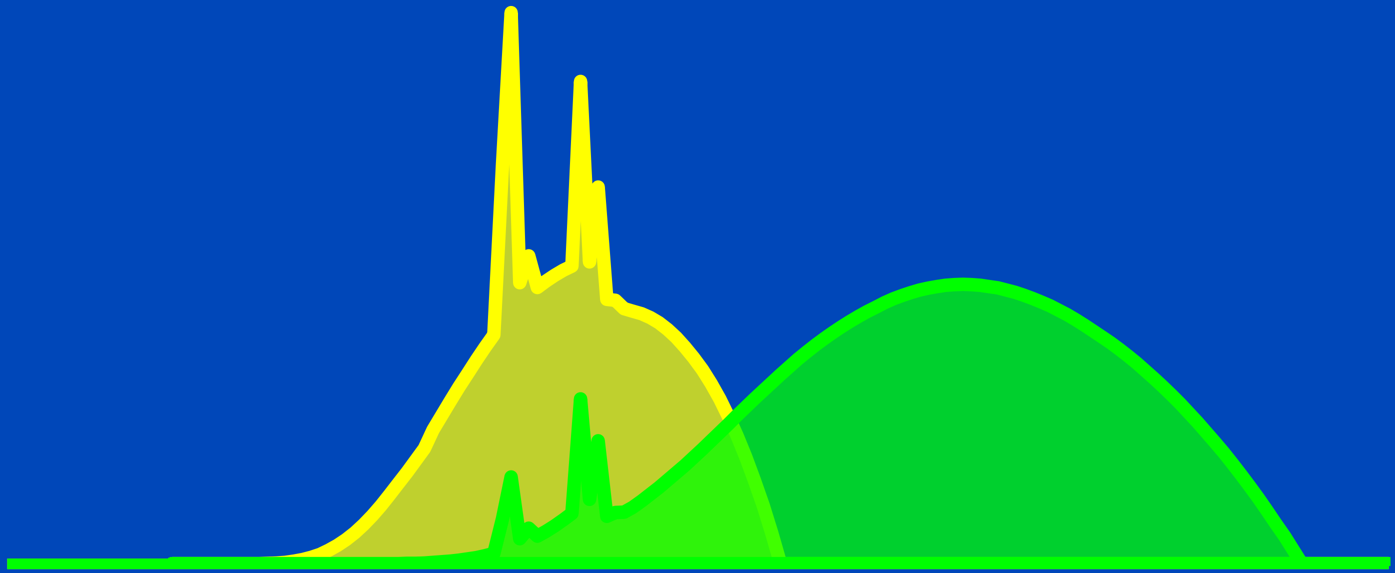

DSCT spectra as seen with one bin after having passed a 32 cm water layer.

90 kV / 150 kV $Sn_{0.6\ mm}$

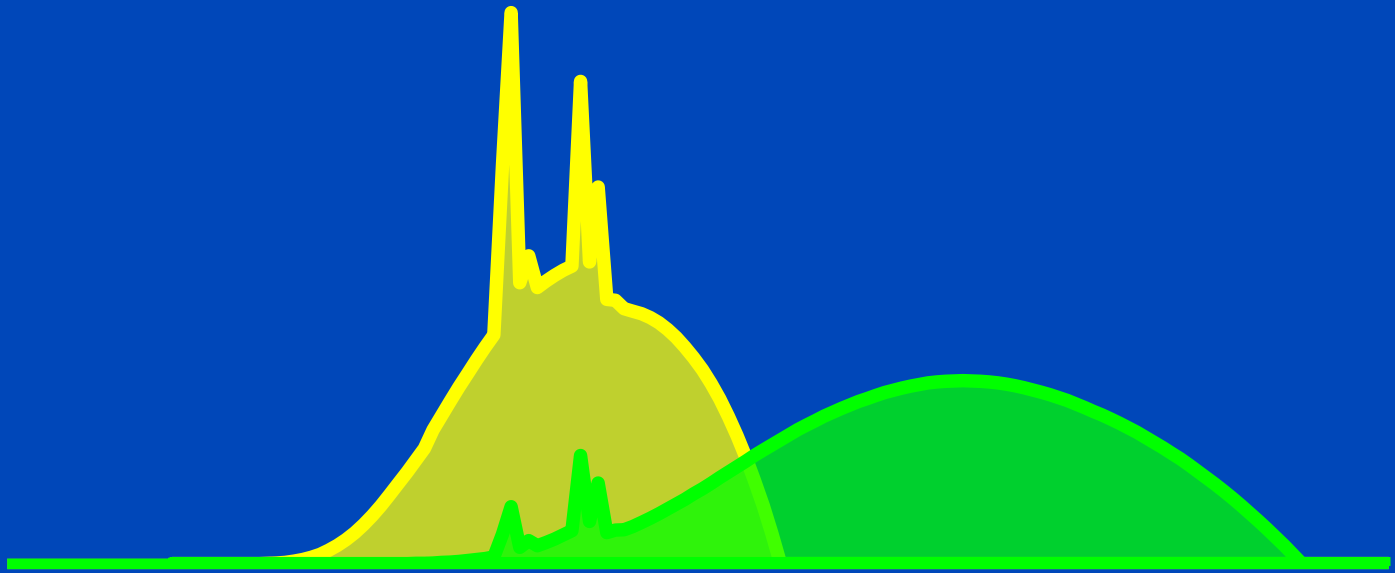

Used in
- Siemens‘ 3rd generation DSCT

DSCT spectra as seen with one bin after having passed a 32 cm water layer.

90 kV / 150 kV $Sn_{0.6\ mm}$

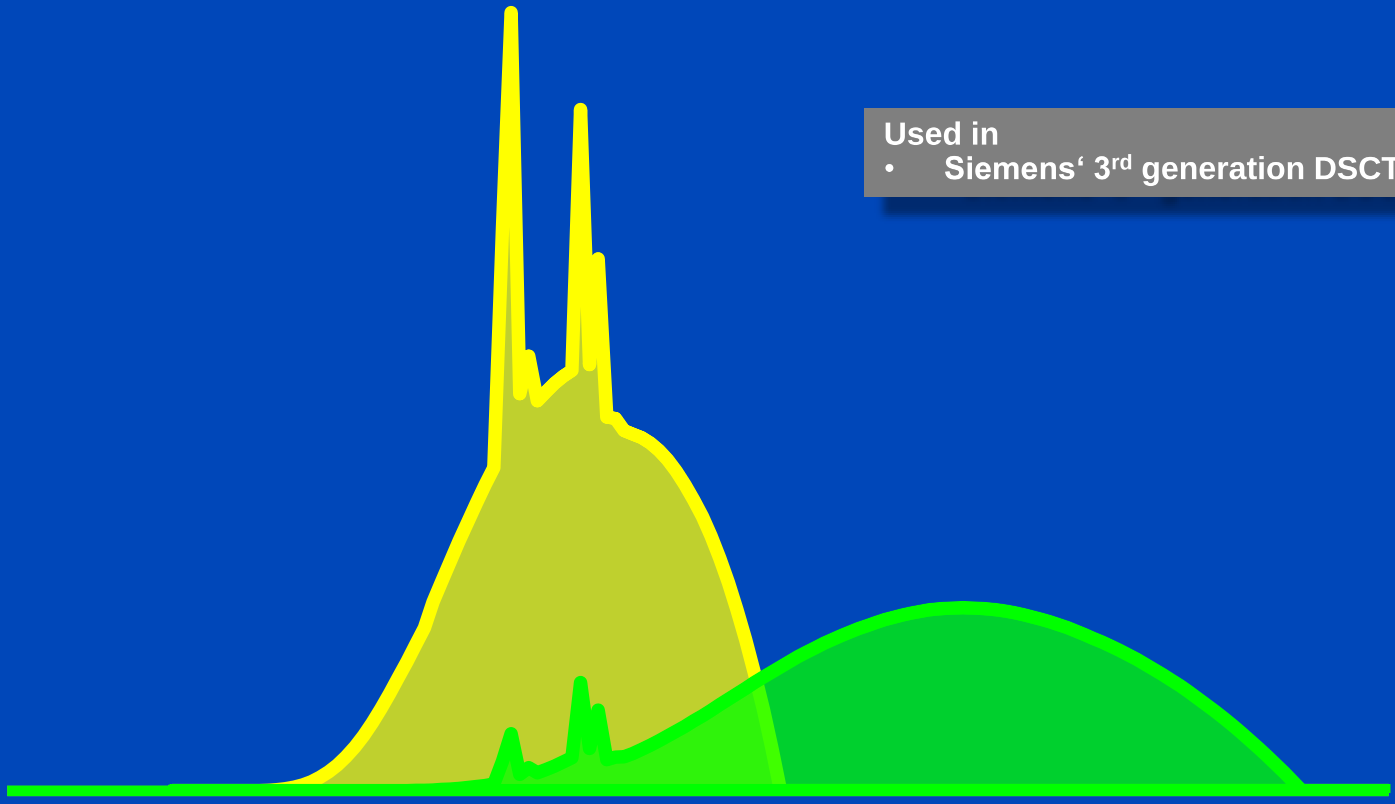

Used in
- **Siemens‘ 3rd generation DSCT**

DSCT spectra as seen with one bin after having passed a 32 cm water layer.

Conclusions

- PCCT offers several advantages: low dose, high spatial resolution, spectral information on demand.
- Thereby, it outperforms all EI CT systems by far.
- PCCT further outperforms all DECT implementations other than dual source CT (DSCT).
  - Fast tube voltage switching, sandwich detectors, or split filter DECT implementations are inferior compared with PCCT.
  - DSCT, cannot be outperformed by single source PCCT. The reason is that DSCT marginalizes the spectral overlap by using a selective prefilter on the high kV tube.
  - To outperform DSCT in terms of spectral performance it is necessary to have a DS-PCCT system with a prefilter on the high kV tube.

Thank you!

Job opportunities through DKFZ's international Fellowship programs (marc.kachelriess@dkfz.de).
Parts of the reconstruction software were provided by RayConStruct® GmbH, Nürnberg, Germany.